Supporting Information

Phototoxicity of Hydroxymethyl-BODIPYs: Are Photocages That Innocent?

Kirill M. Kuznetsov,[a] Pierre Mesdom,[a] Kallol Purkait,[a] Olivier Blacque,[b] Arthur H. Winter,[c]* Kevin Cariou,[a]* and Gilles Gasser[a]*

[a] Chimie ParisTech, PSL University, CNRS, Institute of Chemistry for Life and Health Sciences, Laboratory for Inorganic Chemical Biology, 75005 Paris, France.

[b] Department of Chemistry, University of Zurich, Winterthurerstrasse 190, 8057 Zurich, Switzerland.

[c] Department of Chemistry, Iowa State University, Ames, 50014 Iowa, United States.

ORCID Numbers:

Kirill Kuznetsov: 0000-0003-1322-5973

Pierre Mesdom: 0000-0003-1069-2138

Kallol Purkait: 0000-0002-7177-8034

Olivier Blacque: 0000-0001-9857-4042

Arthur Winter: 0000-0003-2421-5578

Kevin Cariou: 0000-0002-5854-9632

Gilles Gasser: 0000-0002-4244-5097

Experimental Section

Materials.

Starting materials for the chemical synthesis were purchased from TCI chemicals (boron trifluoride – ether complex, piperidine, methylmagnesium bromide, N-bromosuccinimide, tris(2,2'-bipyridyl)ruthenium(II) chloride hexahydrate), Thermofisher (pyridine, MitoTracker™, M22426, LysoTracker™ Deep Red), Sigma-Aldrich (solvents, phosphorus(V) oxychloride, protoporphyrin IX), BLDpharm (N,N-diisopropylethylamine, 2,4-dimethyl-1H-pyrrole, acetoxyacetylchloride, 4-methoxybenzaldehyde, sodium hydroxide), and Fluorochem (sodium hydroxide, solvents). Deuterated solvents were acquired from Eurisotop to perform NMR experiments.

Instrumentation and methods (NMR, HRMS, CHN, IR, HPLC, X-ray).

Nuclear magnetic resonance (NMR) spectra (^{1}H, ^{1}H-^{1}H COSY, ^{19}F, ^{13}C) were recorded on a Bruker 400 MHz NMR spectrometer at 25°C, and the chemical shift (δ) values are reported in parts per million (ppm). The residual solvent peak was used as an internal standard.[1] The standard abbreviations were used: *J* – coupling constants (Hz), s – singlet, d – doublet, t – triplet, and m – multiplet. Electrospray ionization-mass spectrometry (ESI-HRMS) experiments were measured using a Thermo Scientific (Thermo Fisher Scientific) LTQ-Orbitrap XL instrumentation in positive mode. Analytical HPLC included: 2×Agilent G1361 1260 Prep Pump system (Agilent Technologies) with an Agilent G7115A 1260 DAD WR detector that was equipped with an Agilent Pursuit XRs 5C18 column (100 Å, C18 5 µm 250 × 4.6 mm). HPLC pure solvents used are methanol with the addition of 0.1% formic acid (solvent A) and water with the addition of 0.1 % formic acid (solvent B). The water for HPLC analysis was purified using a Barnstead™ Pacific TII Water Purification System. To calculate the retention ratio (R_t), the following equation was used: $R_t = t_r/t_0$, where t_r is the retention time of the analyte, t_0 is the total time of the experiment. For Fourier-transform infrared spectroscopy (FT-IR) analysis, the samples were examined in pressed KBr tablets. Infrared spectroscopic measurements were carried out on a Thermo Fisher Nicolet IS 20 spectrometer combined with a Garrick Bogomolets instrument. Elemental microanalysis was performed using a Thermo Flash 2000 elemental analyzer. Single crystal X-ray diffraction data were collected at 160.0(1) K on a Rigaku OD Synergy/Hypix diffractometer using the Cu Kα radiation (λ = 1.54184 Å) from a dual-wavelength X-ray source and an Oxford Instruments Cryojet XL cooler. The selected suitable single crystal was mounted using polybutene oil on a flexible loop fixed on a goniometer head and immediately transferred to the diffractometer. Pre-experiment, data collection, data reduction, and analytical absorption correction[2] were performed with the program suite *CrysAlisPro*, version 1.171.43.136a, Rigaku Oxford Diffraction Ltd, Yarnton, Oxfordshire, England, 2024. Using *Olex2*,[3] the structure was solved with the *SHELXT*[4] small molecule structure solution program and refined with the *SHELXL* program package[4] by full-matrix least-squares minimization on F^2. *PLATON*[5] was used to validate the result of the X-ray analysis. For more details about the data collection and refinement parameters, see Tables S1-S8 below. The structure of **11** has been solved and refined successfully with no unusual features. All H-atoms were placed geometrically and refined isotropically using a riding model, with C—H = 0.95 Å (C-aromatic) and 0.98 Å (C-methyl) in association with Uiso(H) = 1.2Ueq(C-aromatic) or 1.5Ueq(C-methyl). CCDC-2454511 contains the supplementary crystallographic data for this paper. The data can be obtained free of charge from The Cambridge Crystallographic Data Centre

via www.ccdc.cam.ac.uk/structures. All the final compounds were stored in an amber glass vial at -20°C freezer.

Photophysical measurements.

To calculate excitation coefficients according to the Beer–Bouguer–Lambert law, UV-vis absorption spectra were measured in acetonitrile (HPLC pure) at room temperature with a concentration of about 10^{-5} M using a Cary 3500 UV-vis spectrophotometer. Excitation and emission spectra were measured on FluoroMax (Jobin-Yvon/Horiba) of samples with 10^{-3} M concentration in acetonitrile (HPLC pure) at 350 nm (excitation wavelength) in the quartz cuvette. Quantum yields were calculated according to the HORIBA Scientific protocol (A Guide to Recording Fluorescence Quantum Yields, Jobin Yvon).[6] The quantum yield of the control $[Ru(bpy)_3]Cl_2$ is considered to be 0.018 ± 0.002.[7,8] The data was processed using Origin 2021b.

Stability studies.

The stability of the compounds (5 μM) in 200 μL MeOH/DMSO (v/v, 1/1) was monitored at 37°C by absorption spectra changes using 96-well plates in triple utilizing Cytation 5 cell imaging Multi-Mode Reader instrument of BioTek Instruments. The same experiment was conducted in Dulbecco's Phosphate Buffered Saline , no calcium, no magnesium (Fischer Scientific, Cat. No. 12559069). As well, absorption was monitored for the same solution utilizing a Cary 3500 UV-vis spectrophotometer at indicated time intervals. The size of nanoparticles formed by the compounds was determined by dynamic light scattering (DLS) on a Malvern ZetaSizer Nano ZS of samples with 10^{-5} M concentration. The data was processed using Origin 2021b.

ROS generation evaluation in solution.

The superoxide trap (dihydrorhodamine 123, DHR 123, 10 mM) was dissolved in 200 μL solution in DMSO/MeOH (v/v, 1/1) or PBS to reach a concentration of 10 μM in 200 μL. The concentration of the test compounds **4**, **5**, **6**, **7**, and **11** was 5 μM, and 0.25 μM for compounds **2** and **3**. The emission spectra changes were monitored using a Cytation 5 cell imaging Multi-Mode Reader instrument of BioTek Instruments (λ_{ex} = 488 nm, λ_{em} = 520 nm). The samples were irradiated with LUMOS-BIO photoreactor (Atlas Photonics) in 96-well plates using 645 nm irradiation (**4**, **5**, **6**, **7**, **11**, 9.00 J/cm^2) or 510 nm (**2**, **3**, 2.44 J/cm^2). After an indicated period, the fluorescence intensity was monitored. The analysis was conducted using Origin 2021b.

The singlet oxygen trap (9,10-anthracenediyl-bis(methylene)dimalonic acid, ABMDMA, 10 mM) was dissolved in a 200 μL solution of 5 μM of the probe in DMSO/MeOH (v/v, 1/1) or PBS to reach a concentration of 10 μM of the trap. The samples were irradiated with LUMOS-BIO photoreactor (Atlas Photonics) in 96-well plates using 645 nm irradiation (9.00 J/cm^2) or 510 nm (2.44 J/cm^2), and the generation was monitored as an absorbance at 400 nm in triplicate for the indicated time on Cytation 5 cell imaging Multi-Mode Reader instrument of BioTek Instruments.[9] A separate study of the changes in the absorption spectra of probes in triplicate with the same concentration was carried out to account for the effect of their change in absorbance at 400 nm wavelength. The analysis was conducted using Origin 2021b.

Photobleaching studies.

Compounds were dissolved in non-deuterated (absorbance) or deuterated (NMR) MeOH/DMSO (1 mg/mL and 10^{-5} M, v/v, 1/1) and were irradiated using 510 nm (10 min for

2, **3**) or 645 nm (1 hour for **4**, **5**, **6**, **7**, **11**) excitation wavelength in a LUMOS-BIO photoreactor (Atlas Photonics). The spectral changes were monitored using the Cytation 5 cell imaging Multi-Mode Reader instrument of BioTek Instruments. The NMR spectra changes were monitored for 24 hours without irradiation and after 1 hour of irradiation at 25°C.

Aggregation studies.

Sample compounds were analyzed in 3 mL PBS solution (20 μM). The samples were irradiated using 510 (10 min for **2**, **3**) or 645 nm (1 hour for **4**, **5**, **6**, **7**, **11**) in 96-well plates using LUMOS-BIO photoreactor (Atlas Photonics) at 37 °C. The dark sample was kept at 37 °C for 1 hour. The size of the aggregates was estimated by dynamic light scattering (DLS) on a Malvern ZetaSizer Nano ZS (11 scans, 10 seconds each) in triplicate.

Cell lines and cell culture.

Human retinal pigment epithelial-1 (RPE-1) cells were cultured in complete Dulbecco's Modified Eagle Medium/F-12 Nutrient Mixture (Fischer Scientific, Cat. No. 11514436) with 10% fetal bovine serum (FBS), penicillin, and streptomycin (100 $U \cdot mL^{-1}$). Adenocarcinomic human alveolar basal epithelial cells (A549) were grown F-12K medium (Fischer Scientific, Cat. No. 21127022) with 10% fetal bovine serum (FBS, Fischer Scientific, Cat. No. 11573397), penicillin (100 $U \cdot mL^{-1}$), streptomycin (100 $U \cdot mL^{-1}$, Fischer Scientific, Cat. No. 11548876). Cells were grown in normoxic conditions, the cell lines were maintained in the presence of ca. 15% O_2, 5% CO_2, and 70% humid atmosphere at 37 °C in a Forma™ Steri-Cycle™ i160 CO2 Incubator, Thermo Scientific. The Gibco™ Trypsin-EDTA (0.25%), phenol red (Fischer Scientific, Cat. No. 11560626), and Gibco™ PBS, no calcium, no magnesium (Fischer Scientific, Cat. No. 12559069) were used for trypsinization.

Confocal microscopy.

Cells A549 were seeded at a 10,000 cells/well density in 8-well plates (IBIDI treat micro plates, 250 μL/well) and incubated for 24 hours at 37 °C, 5% CO_2. Then, 250 μL of 80 μM solution of the compound was added to reach 40 μM overall concentration. After 4 hours of incubation, the medium was replaced, washed 3 times with PBS, and 400 μL medium without phenol red was added. The confocal images were recorded on an SP8 confocal microscope (Leica Microsystems, Nanterre, France) equipped with a 63X/1.40 oil objective at room temperature. The compounds were excited at 405 nm (average laser intensity, collected at 420-472 nm), 488 nm (low laser intensity, collected at 488-552 nm), 552 nm (low laser intensity, collected at 600-650 nm), 638 nm (average laser intensity, collected at 650-700 nm). The images were recorded using LAZ X Office 1.4.7.

Phototoxicity.

Cells A549 and RPE1 were seeded at 2,000 cells/well density in 96-well plates (100 μL/well) and incubated for 72 hours at 37 °C, 5% CO_2. The medium was replaced by test compound dilutions in fresh medium (100 μL/well), and cells were incubated at 37 °C, 5% CO_2 for 4 hours. Following the protocol, the medium was replaced with 100 μL of fresh medium before irradiation. Plates were then irradiated at 510 nm (2.44 J/cm^2) or 645 nm for 1 h (9.00 J/cm^2) using a LUMOS-BIO photoreactor (Atlas Photonics). As a control, a plate was kept in the dark for the same amount of time (1 hour) at 37°C, 0% CO_2. Cells were then incubated to reach 48 hours after the addition of the compounds at 37 °C, 5% CO_2. The medium was replaced with 100 μL of fresh medium containing resazurin (0.2 mg/mL). After 4 hours of incubation at 37 °C, 5% CO_2, plates were read using a SpectraMaxM2 Microplate Reader

(λ_{exc} = 540 nm, λ_{read} = 590 nm). Fluorescence data were normalized, and data were fitted using Origin 2021b, and IC_{50} was calculated.

ROS generation evaluation *in vitro*.

To estimate ROS generation *in vitro* A549 cells were seeded at 10,000 cells/well density in 96-well plates (100 µL/well) and incubated for 24 hours at 37 °C, 5% CO_2. The medium was replaced by a test compound (5 µM) in fresh medium (100 µL/well), and cells were incubated at 37 °C, 5% CO_2 for 4 hours. The medium was replaced by 100 µL of fresh medium with the addition of the trap dichlorofluorescein (20 µM). Dichlorodihydrofluorescein (DCFH) is easily oxidized intracellularly to fluorescent dichlorofluorescein (DCF). Plates were then incubated for 30 min in the dark and irradiated at 510 nm or 645 nm for 10 min (2.44 J/cm^2) or 1 hour (9.00 J/cm^2), respectively, using a LUMOS-BIO photoreactor (Atlas Photonics). The emission was monitored using a SpectraMaxM2 Microplate Reader (λ_{exc} = 485 nm, λ_{read} = 520 nm). DCFH trap (20 µM), $Ru(bpy)_3Cl_2 \cdot 6H_2O$, PPIX, and hydrogen peroxide (800 µM) were used as controls.

The study to evaluate the rate of phototransformations with DCFH trap was conducted in DMSO/MeOH (v/v, 1/1) using LUMOS-BIO photoreactor (Atlas Photonics) with 645 nm (9.00 J/cm^2) irradiation wavelength for 30 min at 25 °C. DCFH, **5**, and **7** were taken from the stock solution to reach the concentration 1.6 mg/mL, 1.0 mg/mL, 1.0 mg/mL.

Synthesis description

(5,5-difluoro-1,3,7,9-tetramethyl-5H-4l4,5l4-dipyrrolo[1,2-c:2',1'-f][1,3,2]diazaborinin-10-yl)methyl acetate (1, BODIPYOH).

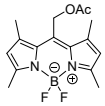

The compound was prepared using a previously described procedure (24 % yield), R_f (DCM) = 0.43.[10]

(5,5-difluoro-1,3,7,9-tetramethyl-5H-4l4,5l4-dipyrrolo[1,2-c:2',1'-f][1,3,2]diazaborinin-10-yl)methanol (2, BODIPYOH).

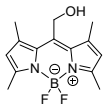

The compound was prepared using a previously described procedure (58 % yield), R_f (DCM) = 0.30.[11]

^{1}H NMR (400 MHz, $CDCl_3$) δ = 6.09 (s, 2H), 4.91 (s, 2H), 2.55 – 2.48 (m, 12H) ppm.

^{13}C NMR (101 MHz, $CDCl_3$) δ = 155.6, 141.0, 139.1, 132.3, 121.8, 55.0, 15.3, 14.4 ppm.

^{19}F NMR (376 MHz, $CDCl_3$) δ = 146.5 ppm.

HRMS (ESI+) calc. for $[M+H]^+$ ($C_{14}H_{18}BF_2N_2O^+$): 279.1475, found 279.1472.

IR 3804, 3692, 3557, 3109, 2959, 2929, 2868, 2822, 2777, 2733, 2670, 2509, 2397, 2346, 2252, 2091, 2014, 1984, 1851, 1746, 1695, 1557, 1531, 1515, 1475, 1443, 1403, 1370, 1305, 1254, 1205, 1163, 1125, 1079, 1037, 985, 841, 822, 752, 724, 668, 631 cm^{-1}.

CHN Anal. calc. for $C_{14}H_{17}BF_2N_2O$ (%): C, 60.46; H, 6.16; N, 10.07. Found: C, 60.29; H, 6.29; N, 10.09.

(1,3,5,5,7,9-hexamethyl-5H-4l4,5l4-dipyrrolo[1,2-c:2',1'-f][1,3,2]diazaborinin-10-yl)methanol (3, BODIPYMeOH).

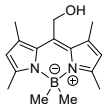

The compound was synthesized according to a previously described procedure (38 % yield), R_f (DCM) = 0.27.[11]

^{1}H NMR (400 MHz, $CDCl_3$) δ = 6.08 (s, 2H), 4.96 (s, 2H), 2.52 (s, 6H), 2.46 (s, 6H), 0.18 (s, 6H) ppm.

^{13}C NMR (101 MHz, $CDCl_3$) δ = 153.0, 138.4, 137.1, 130.7, 122.7, 56.5, 16.7, 16.1, 9.3 ppm.

HRMS (ESI+) calc. for $[M+H]^+$ ($C_{16}H_{24}BN_2O^+$): 271.1976, found 271.1981.

IR 3230, 2950, 2901, 2836, 2735, 2672, 2532, 2341, 2070, 1823, 1566, 1548, 1520, 1452, 1415, 1363, 1307, 1216, 1179, 1149, 1109, 1060, 1034, 988, 950, 836, 812, 759, 668, 633 cm^{-1}.

CHN Anal. calc. for $C_{16}H_{23}BN_2O\cdot(H_2O)_{1/6}$ (%): C, 70.35; H, 8.61; N, 10.25. Found: C, 70.55; H, 8.60; N, 10.24.

(5,5-difluoro-3,7-bis((E)-4-methoxystyryl)-1,9-dimethyl-5H-4l4,5l4-dipyrrolo[1,2-c:2',1'-f][1,3,2]diazaborinin-10-yl)methyl acetate (4, BODIPYmodOAc).

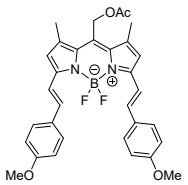

The compound was synthesized according to a previously described procedure (Quant.), R_f (DCM) = 0.70, R_t = 0.20 (HPLC conditions).[10]

^{1}H NMR (400 MHz, $CDCl_3$) δ = 7.62 – 7.54 (m, 6H), 7.22 (d, 2H), 6.93 (d, $^3J_{H\text{-}H}$ =8.8 Hz, 4H), 6.72 (s, 2H), 5.30 (s, 2H), 3.86 (s, 6H), 2.42 (s, 6H), 2.15 (s, 3H) ppm.

^{13}C NMR (101 MHz, CDCl3) δ = 170.8, 160.7, 153.5, 140.1, 136.7, 134.7, 129.6, 129.4, 118.8, 117.3, 114.5, 58.3, 55.5, 20.9, 16.0 ppm.

^{19}F NMR (376 MHz, CDCl3) δ = 138.5 ppm.

HRMS (ESI+) calc. for $[M]^+$ ($C_{32}H_{31}BF_2N_2O_4^+$): 556.2345, found 556.2349.; calc. for $[M+Na]^+$ ($C_{32}H_{31}BF_2N_2O_4Na^+$): 579.2243, found 579.2246.

IR 3629, 3557, 3207, 3078, 3015, 2997, 2976, 2934, 2910, 2838, 2763, 2563, 2341, 2285, 2047, 1739, 1597, 1548, 1461, 1436, 1394, 1375, 1296, 1251, 1223, 1200, 1123, 1025, 992, 957, 922, 890, 864, 820, 726 cm^{-1}.

CHN Anal. calc. for $C_{32}H_{31}BF_2N_2O_4\cdot(H_2O)_{1/2}$ (%): C, 68.10; H, 5.54; N, 4.96. Found: C, 68.13; H, 5.74; N, 5.17.

(5,5-difluoro-3,7-bis((E)-4-methoxystyryl)-1,9-dimethyl-5H-4l4,5l4-dipyrrolo[1,2-c:2',1'-f][1,3,2]diazaborinin-10-yl)methanol (5, BODIPYmodOH).

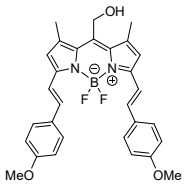

The compound was synthesized according to a previously described procedure (54 % yield), R_f (DCM) = 0.40, R_t = 0.18 (HPLC conditions).[10]

^{1}H NMR (400 MHz, $CDCl_3$) δ = 7.58 (m, 6H), 7.21 (d, $^3J_{H\text{-}H}$ = 16 Hz, 2H), 6.93 (d, $^3J_{H\text{-}H}$ = 8.8 Hz, 4H), 6.72 (s, 2H), 4.95 (s, 2H), 3.86 (s, 6H), 2.57 (s, 6H) ppm.

^{13}C NMR (101 MHz, DMSO) δ = 160.3, 151.9, 140.9, 137.1, 136.3, 133.7, 128.9, 128.8, 118.4, 116.1, 114.7, 55.3, 54.1, 15.4 ppm.

^{19}F NMR (376 MHz, $CDCl_3$) δ =138.4 ppm.

HRMS (ESI+) calc. for $[M]^+$ ($C_{30}H_{29}BF_2N_2O_3^+$): 514.2239, found 514.224; calc. for $[M+Na]^+$ ($C_{30}H_{29}BF_2N_2O_3Na^+$): 537.2137, found 537.2141.

IR 3557, 3183, 1337, 3099, 3074, 3025, 2934, 2908, 2836, 2759, 2563, 2502, 2343, 2038, 1881, 1811, 1767, 1599, 1548, 1524, 1506, 1492, 1464, 1443, 1391, 1366, 1310, 1296, 1258, 1211, 1195, 1165, 1121, 1079, 1023, 999, 948, 929, 890, 857, 813, 796, 726, 682, 656 cm^{-1}.

CHN Anal. calc. for $C_{30}H_{29}BF_2N_2O_3\cdot(H_2O)_{1/3}$ (%): C, 69.20; H, 5.81; N, 5.38. Found: C, 69.22; H, 5.57; N, 5.60.

5,5-difluoro-10-(hydroxymethyl)-3,7-bis((E)-4-methoxystyryl)-1,9-dimethyl-5H-4l4,5l4-dipyrrolo[1,2-c:2',1'-f][1,3,2]diazaborinine-2-carbaldehyde (6, BODIPYmodOHCHO)

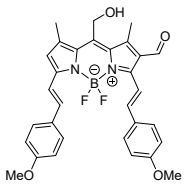

The compound was synthesized according to a previously described procedure.[10.1021/jo901407h] Dry DMF (38 eq, 7.6 eq, 588 µL) and $POCl_3$ (32 eq, 6.4 eq, 598 µL) were cooled down to 0°C and mixed for 10 min under a nitrogen atmosphere. After being warmed to room temperature, it was stirred for an additional 30 min. To this reaction mixture, **5** (1 eq, 0.2 mmol, 104 mg) was added in 1,2-dichloroethane (3 mL), and stirred for an additional 2 hours. Then the mixture was poured into saturated aqueous $NaHCO_3$ (20 mL) under ice-cold conditions. After being warmed to room temperature, the mixture was stirred for 30 min. The organic layers were combined, dried over anhydrous $MgSO_4$, and evaporated in vacuo. The crude product was further purified using column chromatography (silica gel, cyclohexane/DCM) (78 % yield), R_f (DCM) = 0.00, R_t = 0.27 (HPLC conditions).[10]
^{1}H NMR (400 MHz, $CDCl_3$) δ = 10.14 (s, 1H), 7.65 – 7.53 (m, 6H), 7.42 (d, $^3J_{H-H}$ = 16.1 Hz, 1H), 7.07 (d, $^3J_{H-H}$ = 16.3 Hz, 1H), 6.95 (d, $^3J_{H-H}$ = 8.8 Hz, 4H), 6.89 (s, 1H), 4.93 (d, $^3J_{H-H}$ = 2.8 Hz, 2H), 3.87 (s, 6H), 2.94 (s, 3H), 2.67 (d, $^3J_{H-H}$ = 1.1 Hz, 3H) ppm.

^{13}C NMR (101 MHz, $CDCl_3$) δ = 187.7, 161.9, 160.8, 159.4, 154.3, 144.1, 142.1, 140.4, 138.8, 134.4, 130.9, 130.3, 129.4, 129.3, 128.7, 121.7, 116.3, 115.3, 114.7, 114.4, 55.6, 55.6, 37.7, 36.6, 16.5, 12.9 ppm.

IR 3307, 3181, 3069, 3011, 2964, 2931, 2838, 2761, 2556, 2521, 2437, 2341, 2287, 2045, 1947, 1669, 1599, 1548, 1515, 1492, 1454, 1422, 1370, 1321, 1305, 1272, 1207, 1177, 1093, 1065, 1034, 1109, 964, 932, 866, 829, 780, 724, 696, 649 cm^{-1}.

CHN Anal. calc. for $C_{33}H_{35}BN_2O_4 \cdot (CH_2Cl_2)_{1/3}$ (%): C, 64.59; H, 5.36; N, 4.81. Found: C, 64.69; H, 5.17; N, 4.11.

(3,7-bis((E)-4-methoxystyryl)-1,5,5,9-tetramethyl-5H-4l4,5l4-dipyrrolo[1,2-c:2',1'-f][1,3,2]diazaborinin-10-yl)methanol (7, BODIPYmodMeOH).

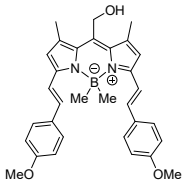

The compound was synthesized according to a previously described procedure (93 % yield), R_f (DCM) = 0.40, R_t = 0.31 (HPLC conditions).[10]
^{1}H NMR (400 MHz, $CDCl_3$) δ = 7.50 (d, $^3J_{H-H}$ = 8.7 Hz, 4H), 7.47 (d, $^3J_{H-H}$ = 16.2 Hz, 2H), 7.07 (d, $^3J_{H-H}$ = 16.2 Hz, 2H), 6.94 (d, $^3J_{H-H}$ = 8.7 Hz, 4H), 6.73 (s, 2H), 5.00 (s, 2H), 3.86 (s, 6H), 2.60 (s, 6H), 0.45 (s, 6H) ppm.

^{13}C NMR (101 MHz, DMSO-d_6) δ = 159.8, 149.3, 137.9, 137.2, 132.8, 132.6, 129.4, 128.2, 118.5, 118.0, 114.6, 55.3, 15.7 ppm.

IR 3431, 3088, 3018, 3001, 2950, 2931, 2899, 2938, 2747, 2677, 2556, 2346, 2259, 2229, 2063, 2019, 1811, 1603, 1562, 1510, 1489, 1468, 1417, 1389, 1368, 1314, 1291, 1256, 1214, 1174, 1149, 1097, 1027, 999, 957, 857, 813, 754, 736 cm^{-1}.

CHN Anal. calc. for $C_{32}H_{35}BN_2O_3 \cdot CH_2Cl_2$ (%): C, 67.01; H, 6.31; N, 4.74. Found: C, 67.00; H, 6.55; N, 4.69.

(2,8-dibromo-5,5-difluoro-1,3,7,9-tetramethyl-5H-4l4,5l4-dipyrrolo[1,2-c:2',1'-f][1,3,2]diazaborinin-10-yl)methyl acetate (8, BODIPYBrOAc).

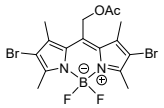

The compound was synthesized according to a previously described procedure (37 % yield), R_f (DCM) = 0.60.[11]

^{1}H NMR (400 MHz, $CDCl_3$) δ = 5.31 (s, 2H), 2.59 (s, 6H), 2.38 (s, 6H), 2.16 (s, 3H) ppm.

^{13}C NMR (101 MHz, $CDCl_3$) δ = 170.5, 155.3, 139.0, 133.9, 131.9, 77.2, 58.1, 53.6, 20.7, 14.9, 14.0 ppm.

(2,8-dibromo-5,5-difluoro-3,7-bis((E)-4-methoxystyryl)-1,9-dimethyl-5H-4l4,5l4-dipyrrolo[1,2-c:2',1'-f][1,3,2]diazaborinin-10-yl)methyl acetate (9, BODIPYBrmodOAc).

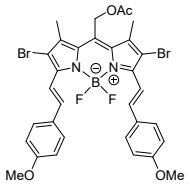

The compound was synthesized according to a previously described procedure.[10] Compound **8** (1 eq, 0.785 mmol, 375 mg) was dissolved in the mixture of 4-anisaldehyde (10 eq, 7.8 mmol, 1 mL) and piperidine (2 drops) at RT. The mixture was heated to 60°C in a vacuum for 1 hour. Then the reaction was stopped, and the crude was extracted on silica, purified by column chromatography (silica, cyclohexane:DCM, 4:1, to cyclohexane:DCM, 1:1) to obtain green powder (59 % yield), R_f (DCM) = 0.63.

^{1}H NMR (400 MHz, $CDCl_3$) δ = 8.14 (d, $^3J_{H\text{-}H}$ = 16.6 Hz, 2H), 7.61(d, $^3J_{H\text{-}H}$ = 8.6 Hz, 4H), 7.58 (d, $^3J_{H\text{-}H}$ = 16.2 Hz), 6.96 (d, $^3J_{H\text{-}H}$ = 8.6 Hz, 4H), 5.35 (s, 2H), 3.87 (s, 6H), 2.41 (s, 6H), 2.16 (s, 3H) ppm.

^{13}C NMR (101 MHz, $CDCl_3$) δ = 170.6, 161.1, 149.3, 140.0, 139.1, 133.8, 129.8, 129.6, 116.2, 114.5, 111.4, 58.5, 55.6, 20.8, 14.8 ppm.

^{19}F NMR (376 MHz, $CDCl_3$) δ = 138.89 ppm.

(2,8-dibromo-5,5-difluoro-3,7-bis((E)-4-methoxystyryl)-1,9-dimethyl-5H-4l4,5l4-dipyrrolo[1,2-c:2',1'-f][1,3,2]diazaborinin-10-yl)methanol (10, BODIPYBrmodOH).

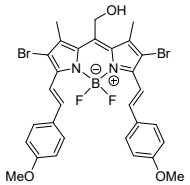

The compound was synthesized according to a previously described procedure.[10] Compound **9** (561 mg) was dissolved in the mixture of DCM (20 mL), MeOH (20 mL), and 0.1 M NaOH solution (4 mL). The reaction was left stirring for 2 hours. Then DCM and MeOH were evaporated at 40°C, and the aqueous residue was washed with EtOAc (3 x 20 mL), dried over Na_2SO_4, filtered, and the solvent was evaporated. Crude mixture was separated by column chromatography (silica, DCM:cyclohexane, 1:1, to DCM:MeOH, 1:0, to DCM:MeOH, 9:1) that resulted in green powder (1 % yield), R_f (DCM) = 0.32, R_t = 0.81 (HPLC conditions).

^{1}H NMR (400 MHz, $CDCl_3$) δ = 8.13 (d, $^3J_{H-H}$ = 16.6 Hz, 2H), 7.61 (d, $^3J_{H-H}$ = 8.6 Hz, 4H), 7.58 (d, $^3J_{H-H}$ = 16.6 Hz, 2H), 6.98 (d, $^3J_{H-H}$ = 8.8 Hz, 4H), 4.98 (s, 2H), 3.87 (s, 6H), 2.59 (s, 6H).

2,8-dibromo-5,5-difluoro-3,7-bis((E)-4-methoxystyryl)-1,9-dimethyl-5H-4l4,5l4-dipyrrolo[1,2-c:2',1'-f][1,3,2]diazaborinine-10-carbaldehyde (11, BODIPYBrmodCHO).

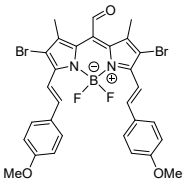

The compound was synthesized following the procedure described for compound **10** (49 % yield), R_f (DCM) = 0.80, R_t = 0.78 (HPLC conditions).
^{1}H NMR (400 MHz, $CDCl_3$) δ = 10.64 (s, 1H), 8.18 (d, $^3J_{H-H}$ = 16.6 Hz, 2H), 7.62 (d, $^3J_{H-H}$ = 8.7 Hz, 4H), 7.57 (d, $^3J_{H-H}$ = 16.4 Hz, 2H), 6.95 (d,$^3J_{H-H}$ = 8.7 Hz, 4H), 3.87 (s, 6H), 2.17 (s, 6H) ppm.

^{13}C NMR (101 MHz, $CDCl_3$) δ = 193.10, 161.37, 150.44, 140.33, 129.79, 129.68, 116.10, 114.60, 55.60, 29.85, 15.02 ppm.

^{19}F NMR (376 MHz, $CDCl_3$) δ = 138.83 ppm.

IR 3391, 3188, 3071, 3013, 2957, 2905, 2838, 2756, 2602, 2516, 2425, 2336, 2278, 2056, 2031, 1886, 1825, 1706, 1594, 1531, 1513, 1480, 1443, 1363, 1326, 1303, 1254, 1193, 1121, 1081, 1037, 999, 971, 829, 724, 661 cm^{-1}.

CHN Anal. calc. for $C_{30}H_{25}BBr_2F_2N_2O_3$ (%): C, 53.77; H, 3.76; N, 4.18. Found: C, 53.39; H, 3.38; N, 4.18.

NMR

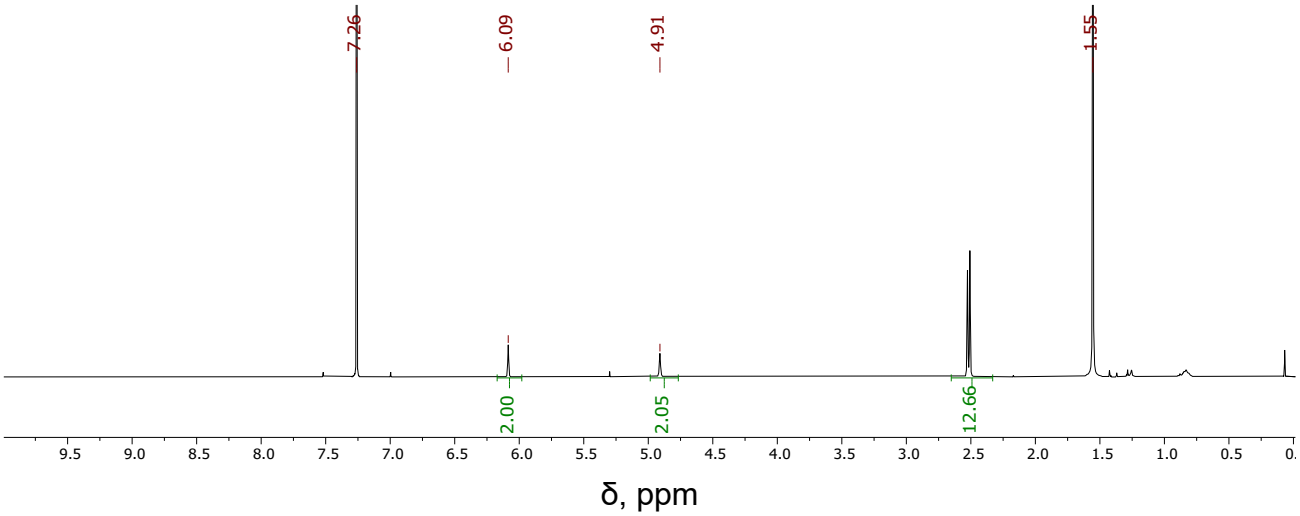

Figure S1. ^{1}H NMR of **2** (BODIPYOH) in $CDCl_3$, RT.

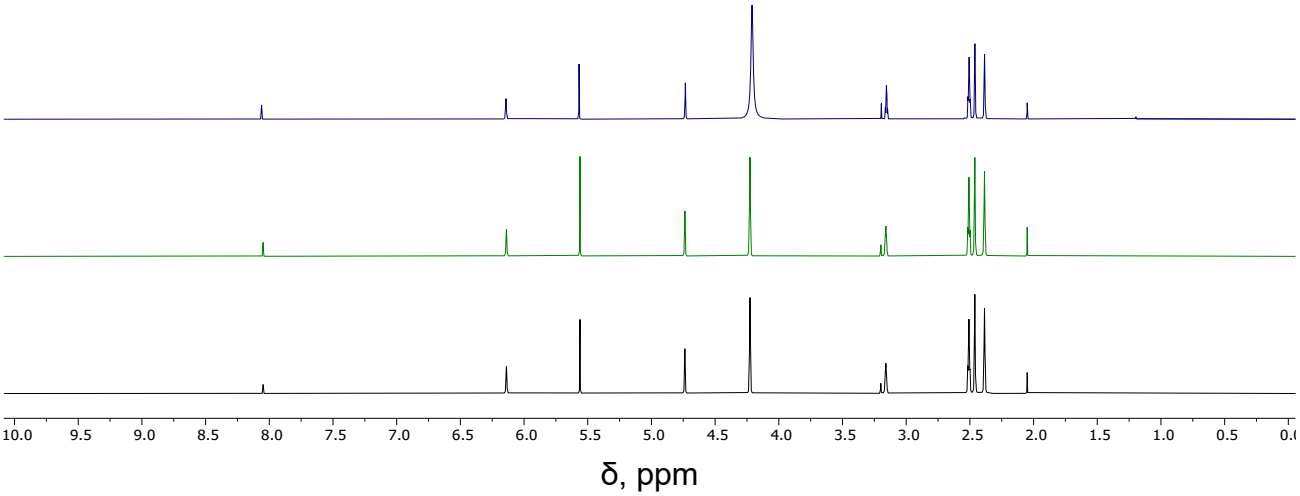

Figure S2. ^{1}H NMR before irradiation (top), after 24 hours (middle), and after irradiation at 510 nm for 10 minutes (bottom) of **2** (BODIPYOH) in DMSO/MeOH (v/v, 1/1), RT.

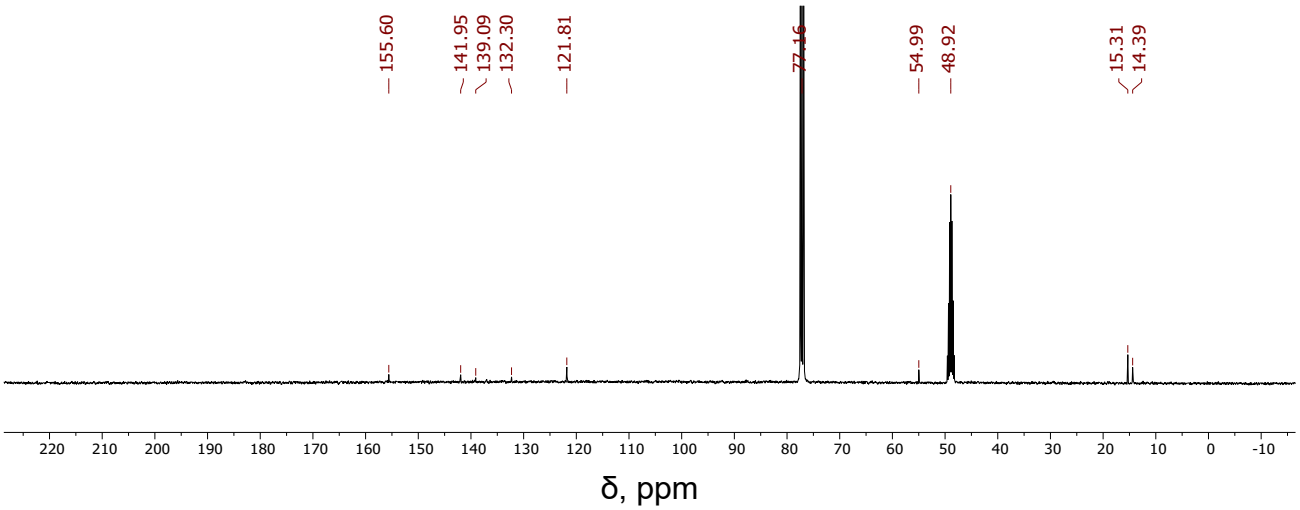

Figure S3. ^{13}C NMR of **2** (BODIPYOH) in $CDCl_3$, RT.

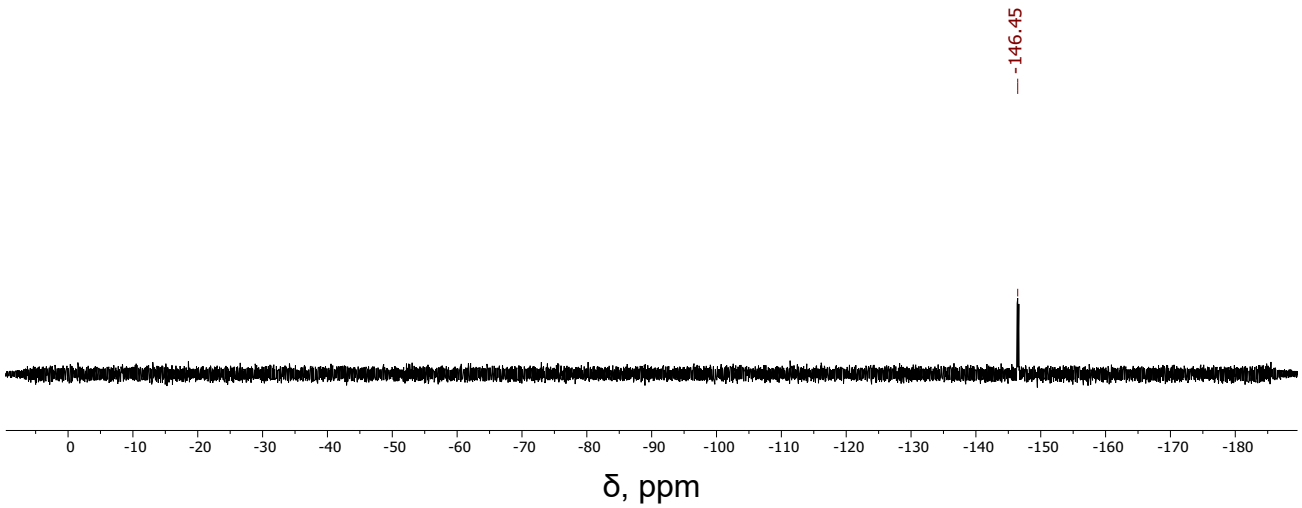

Figure S4. ^{19}F NMR of **2** (BODIPYOH) in $CDCl_3$, RT.

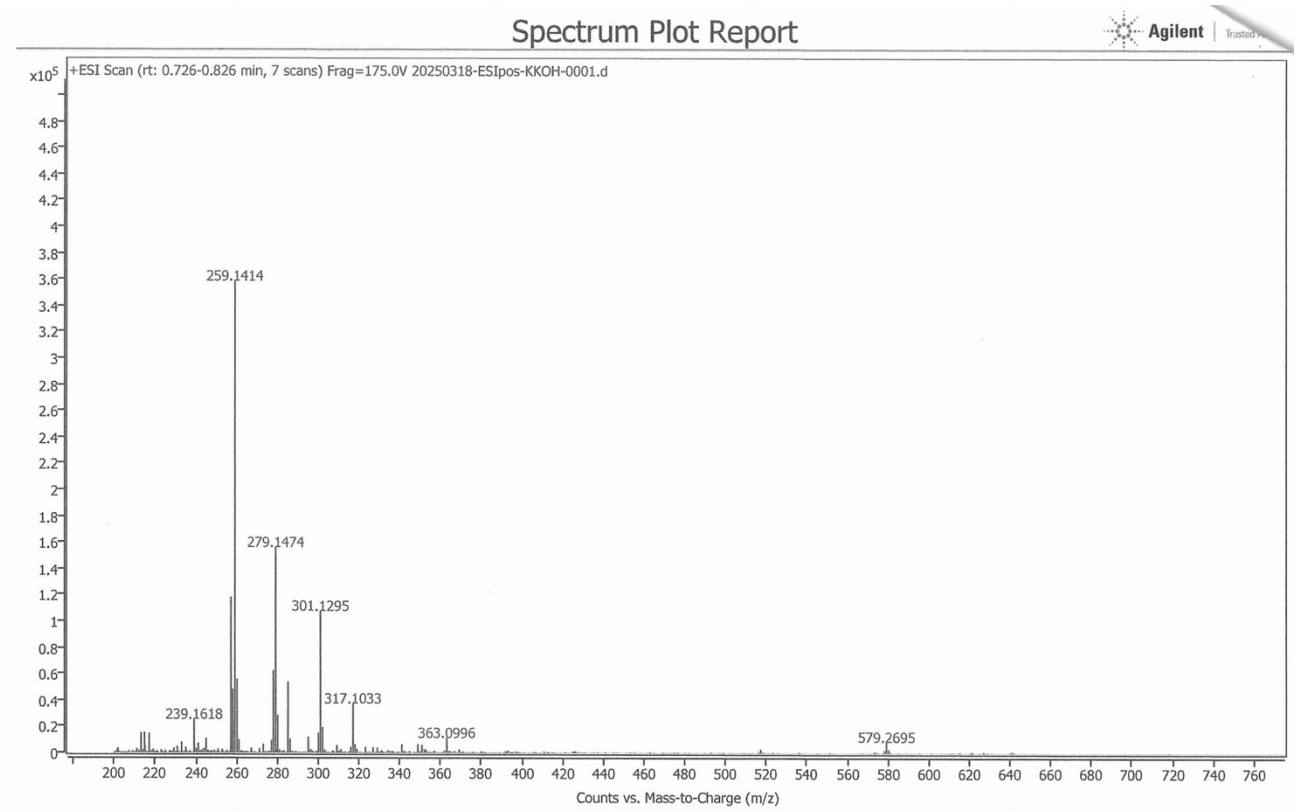

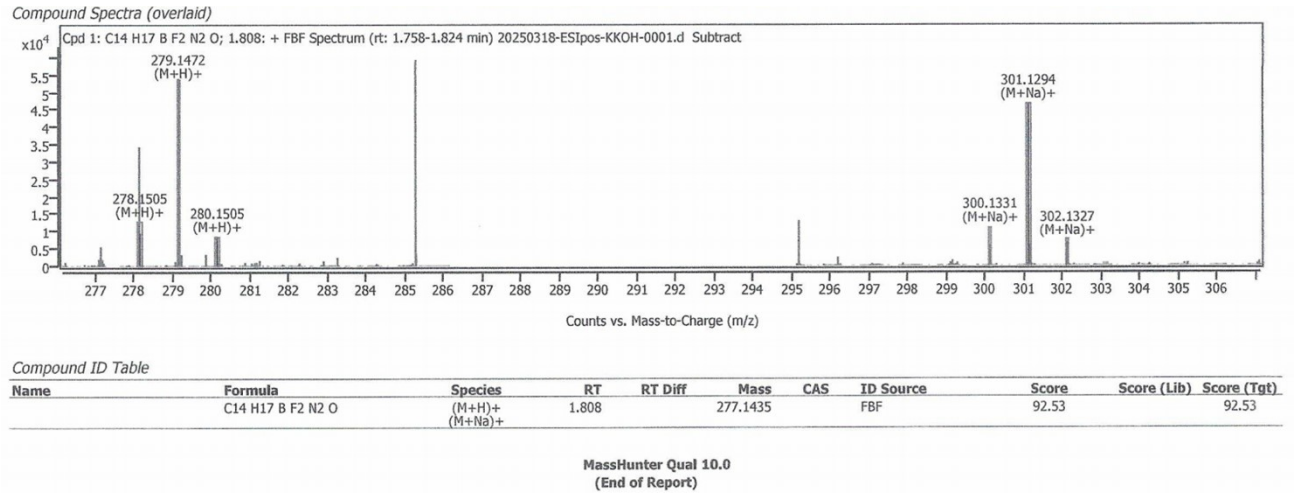

Figure S5. HRMS of **2** (BODIPYOH).

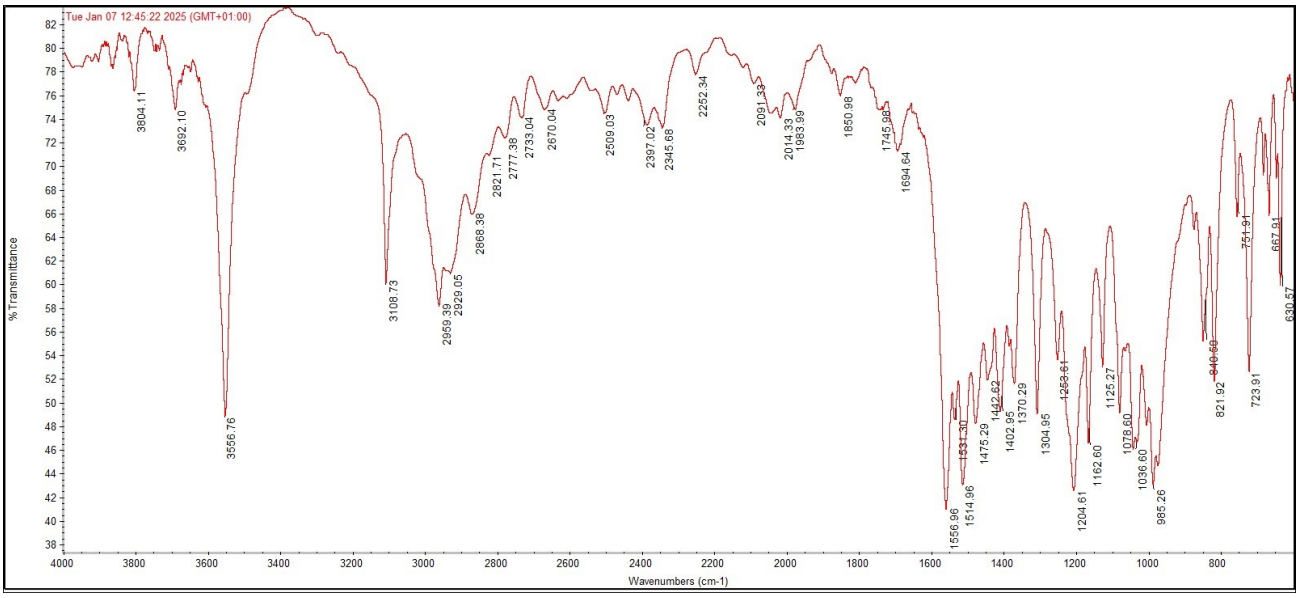

Figure S6. IR of **2** (BODIPYOH).

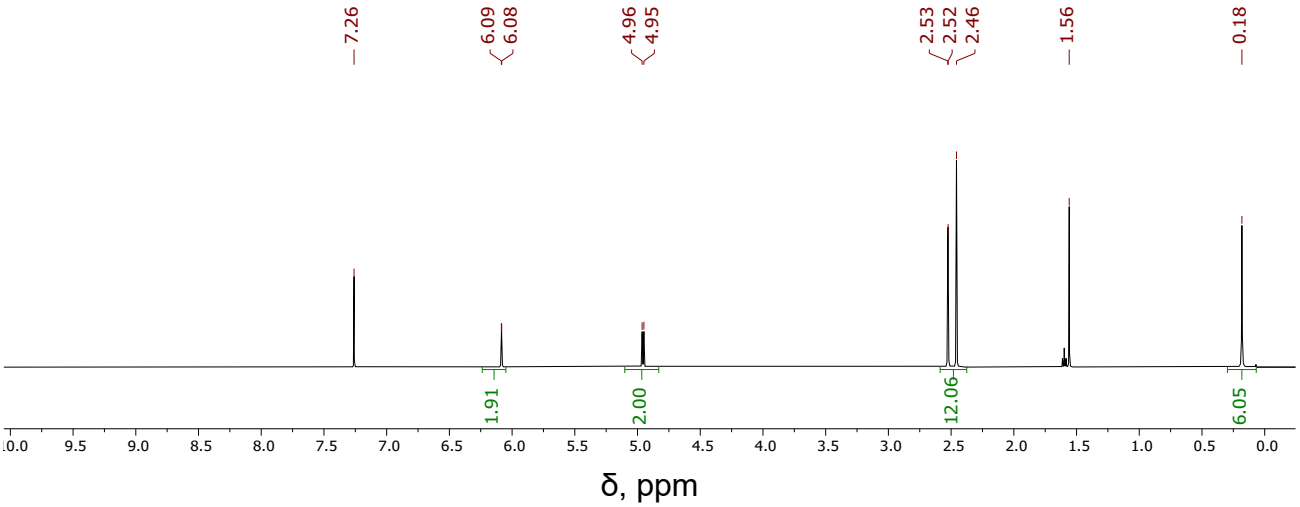

Figure S7. ^{1}H NMR of **3** (BODIPYMeOH) in $CDCl_3$, RT.

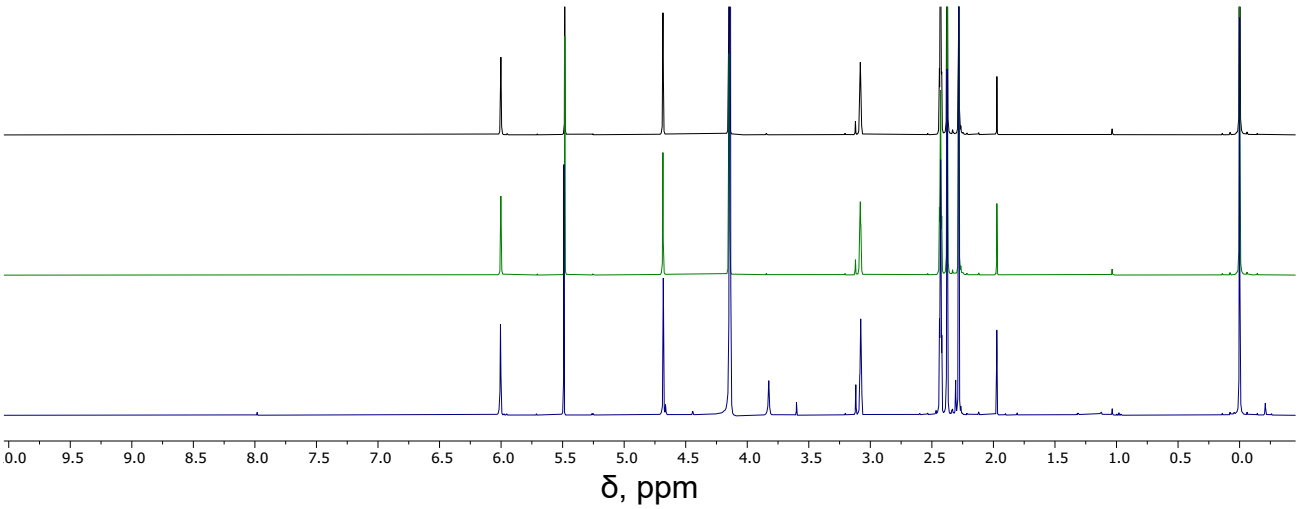

Figure S8. ^{1}H NMR before irradiation (top), after 24 hours (middle), and after irradiation at 510 nm for 10 minutes (bottom) of **3** (BODIPYMeOH) in DMSO/MeOH (v/v, 1/1), RT.

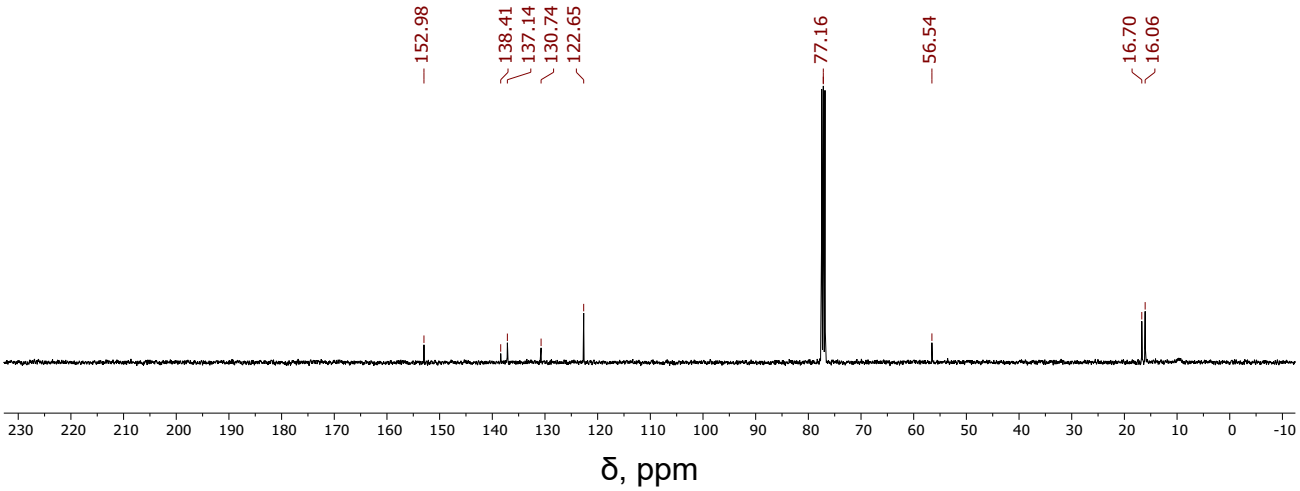

Figure S9. ^{13}C NMR of **3** (BODIPYMeOH) in $CDCl_3$, RT.

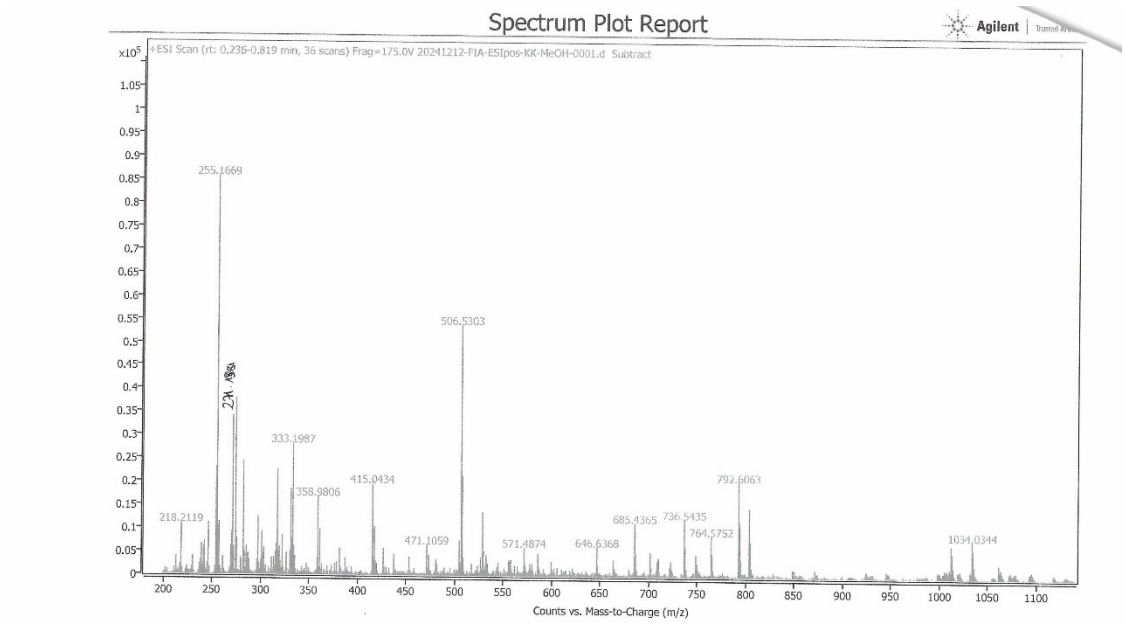

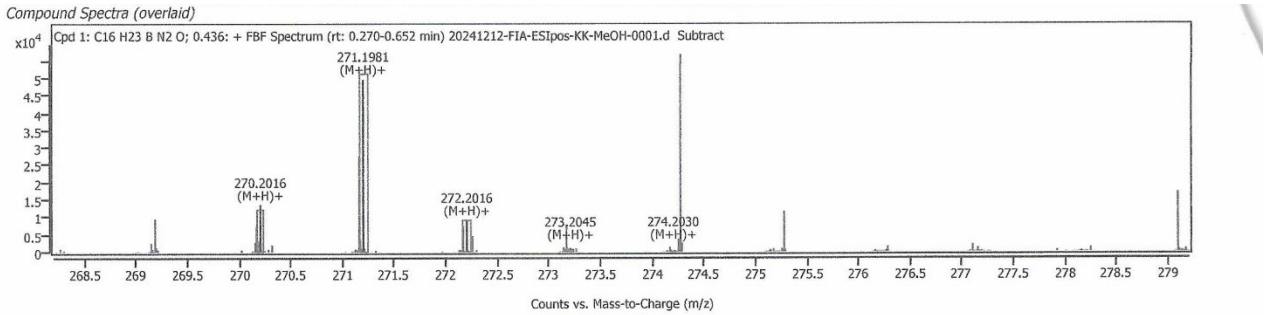

Compound ID Table

Name	Formula	Species	RT	RT Diff	Mass	CAS	ID Source	Score	Score (Lib)	Score (Tgt)
	C16 H23 B N2 O	(M+H)+	0.436		269.1943		FBF	97.41		97.41

Figure S10. HRMS of **3** (BODIPYMeOH).

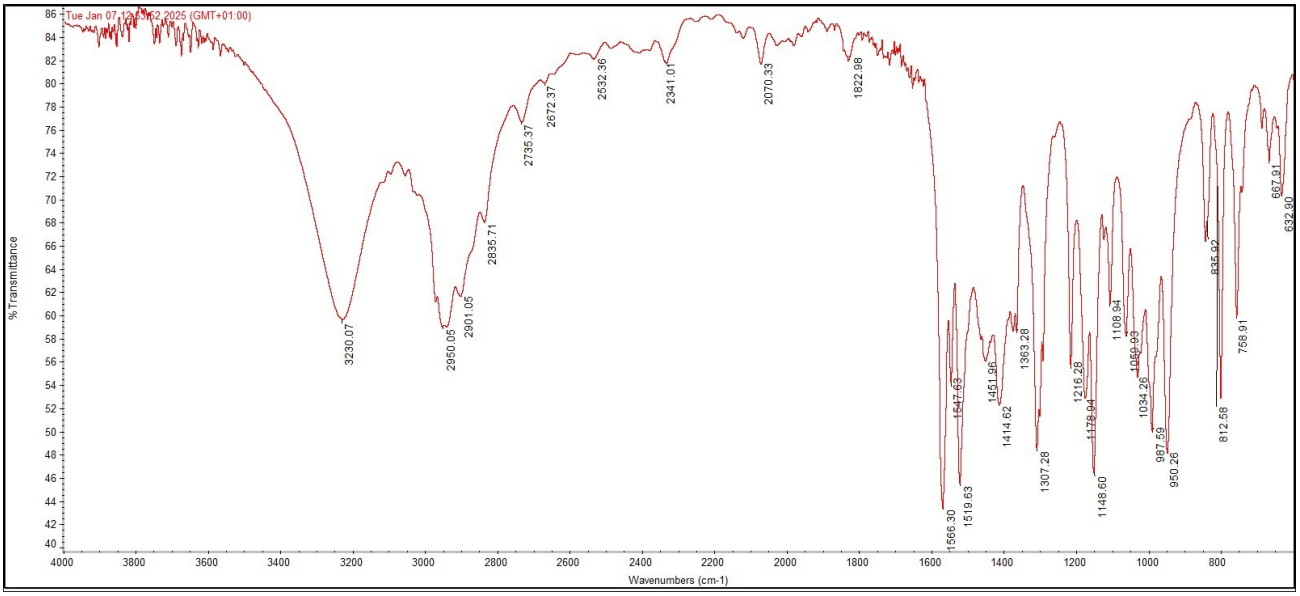

Figure S11. IR of **3** (BODIPYMeOH).

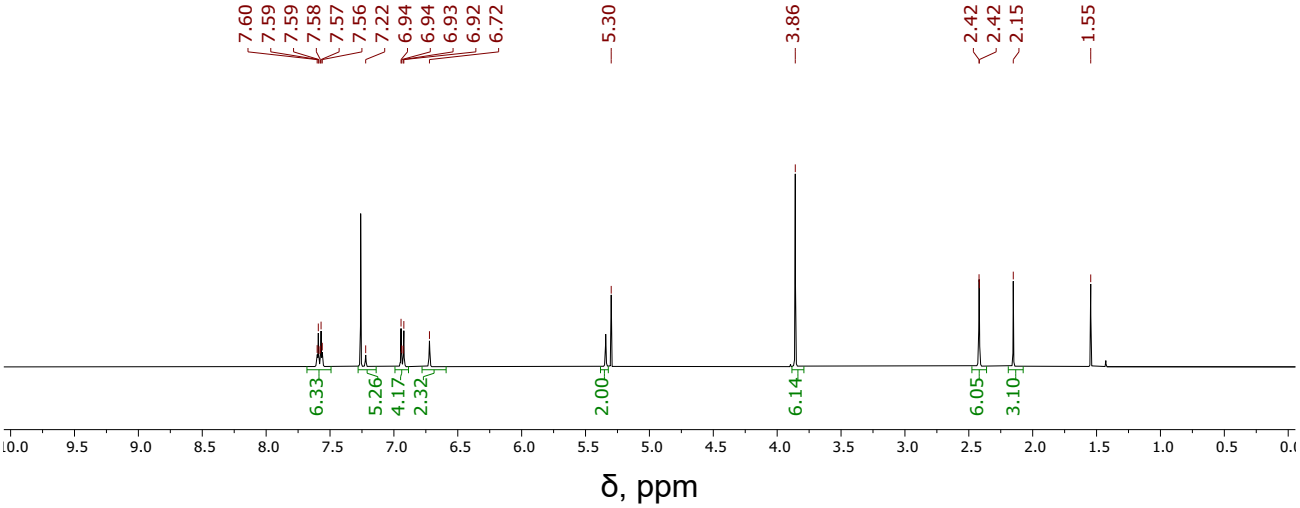

Figure S12. ^{1}H NMR of **4** (BODIPYmodOAc) in $CDCl_3$, RT.

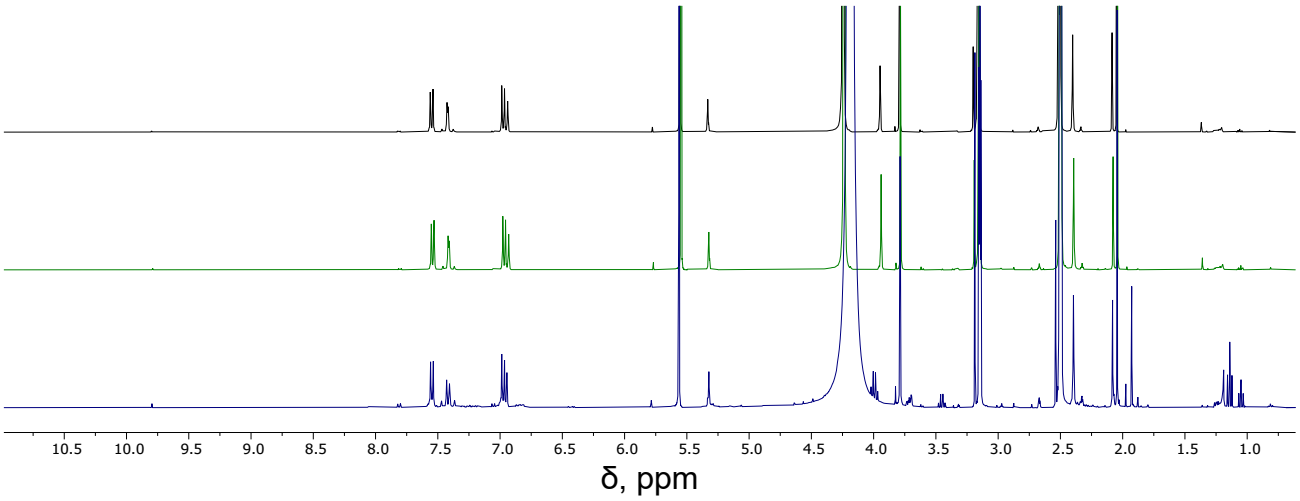

Figure S13. ^{1}H NMR before irradiation (top), after 24 hours (middle), and after irradiation at 645 nm for 1 hour (bottom) of **4** (BODIPYmodOAc) in DMSO/MeOH (v/v, 1/1), RT.

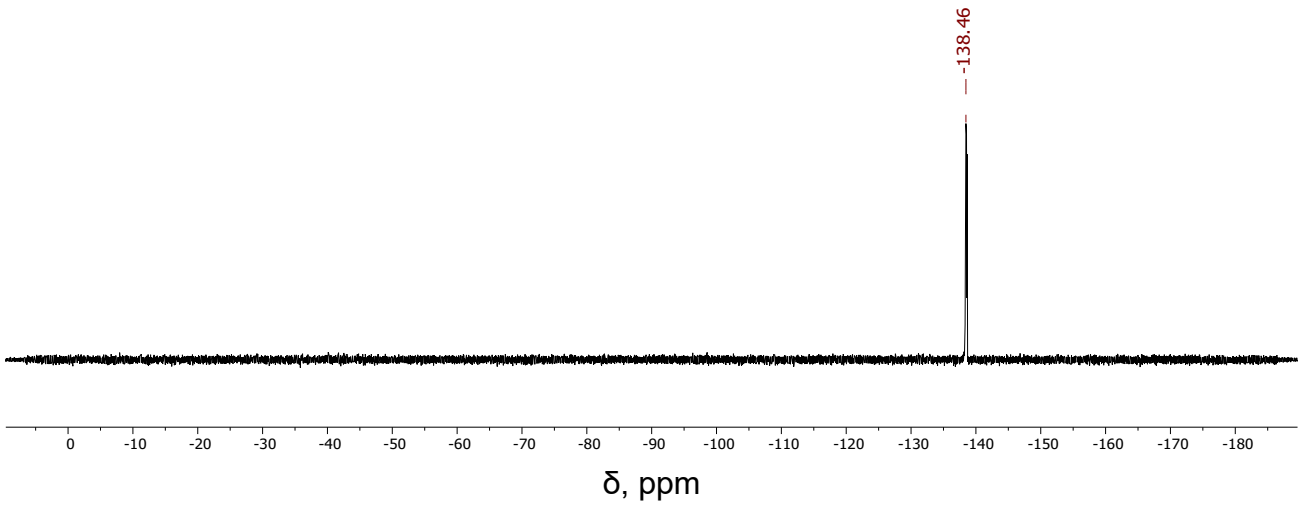

Figure S14. ^{19}F NMR of **4** (BODIPYmodOAc) in $CDCl_3$, RT.

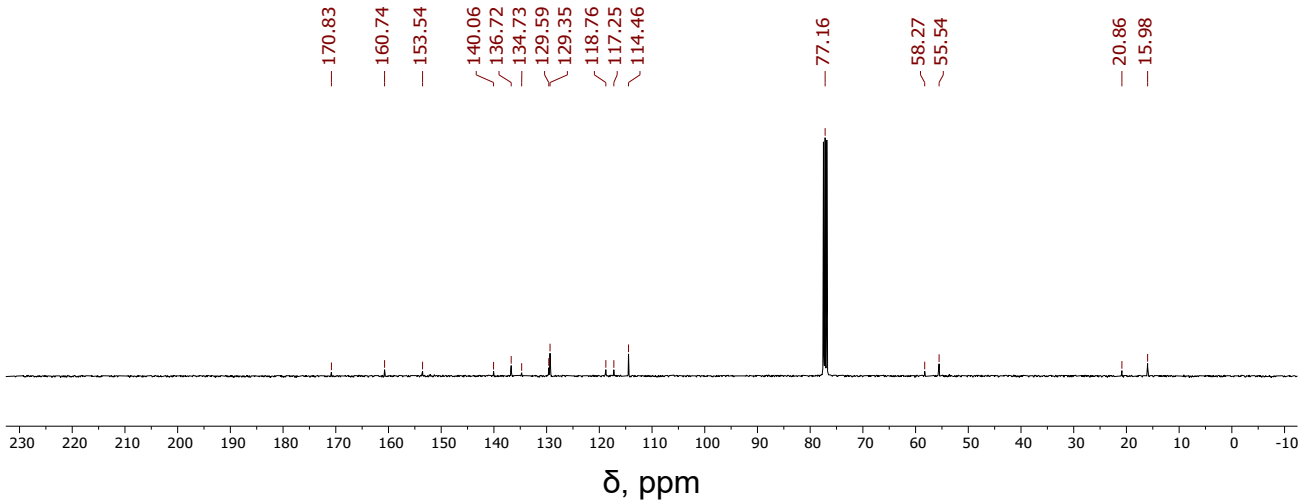

Figure S15. ^{13}C NMR of **4** (BODIPYmodOAc) in $CDCl_3$, RT.

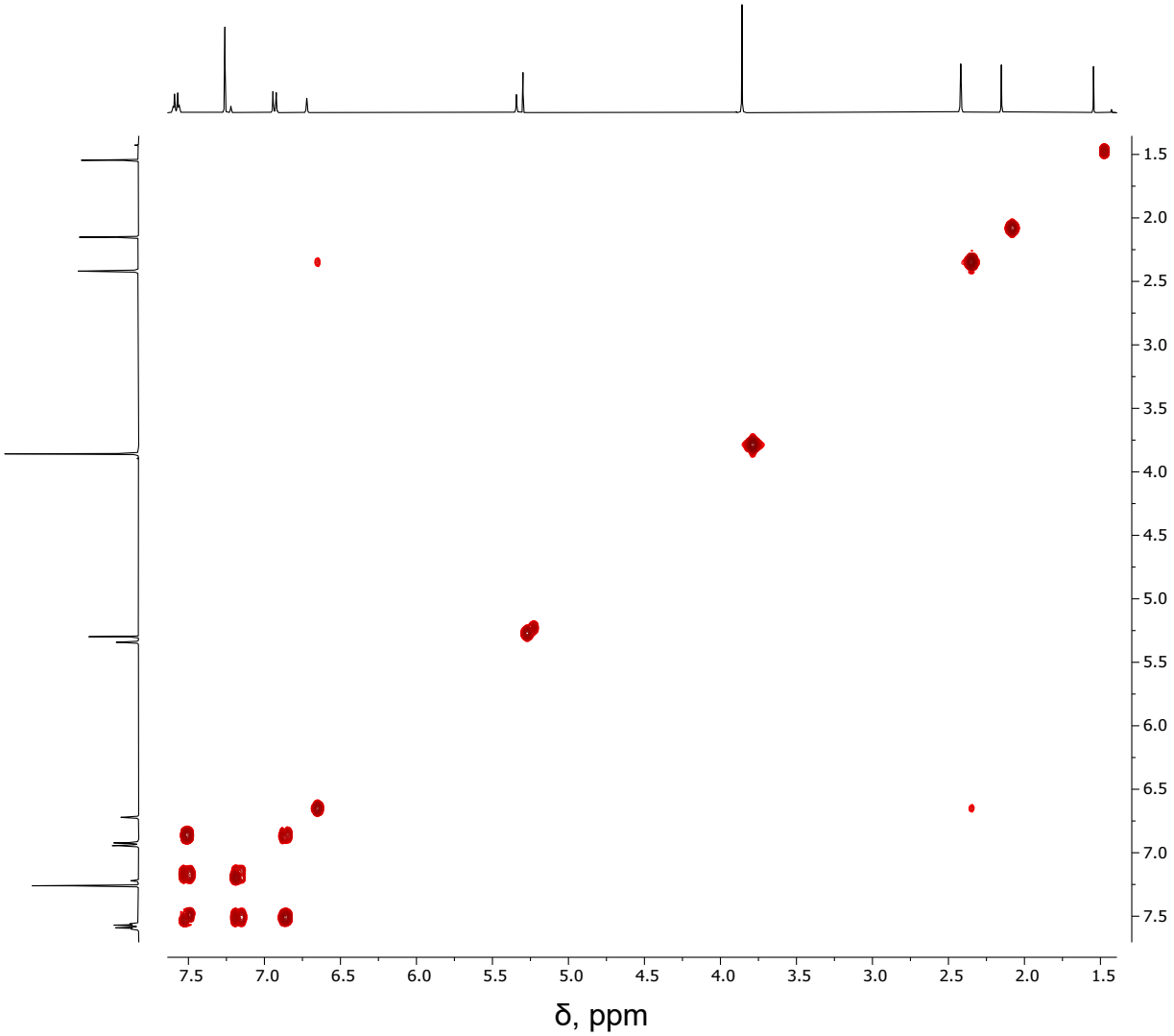

Figure S16. ^{1}H-^{1}H COSY NMR of **4** (BODIPYmodOAc) in $CDCl_3$, RT.

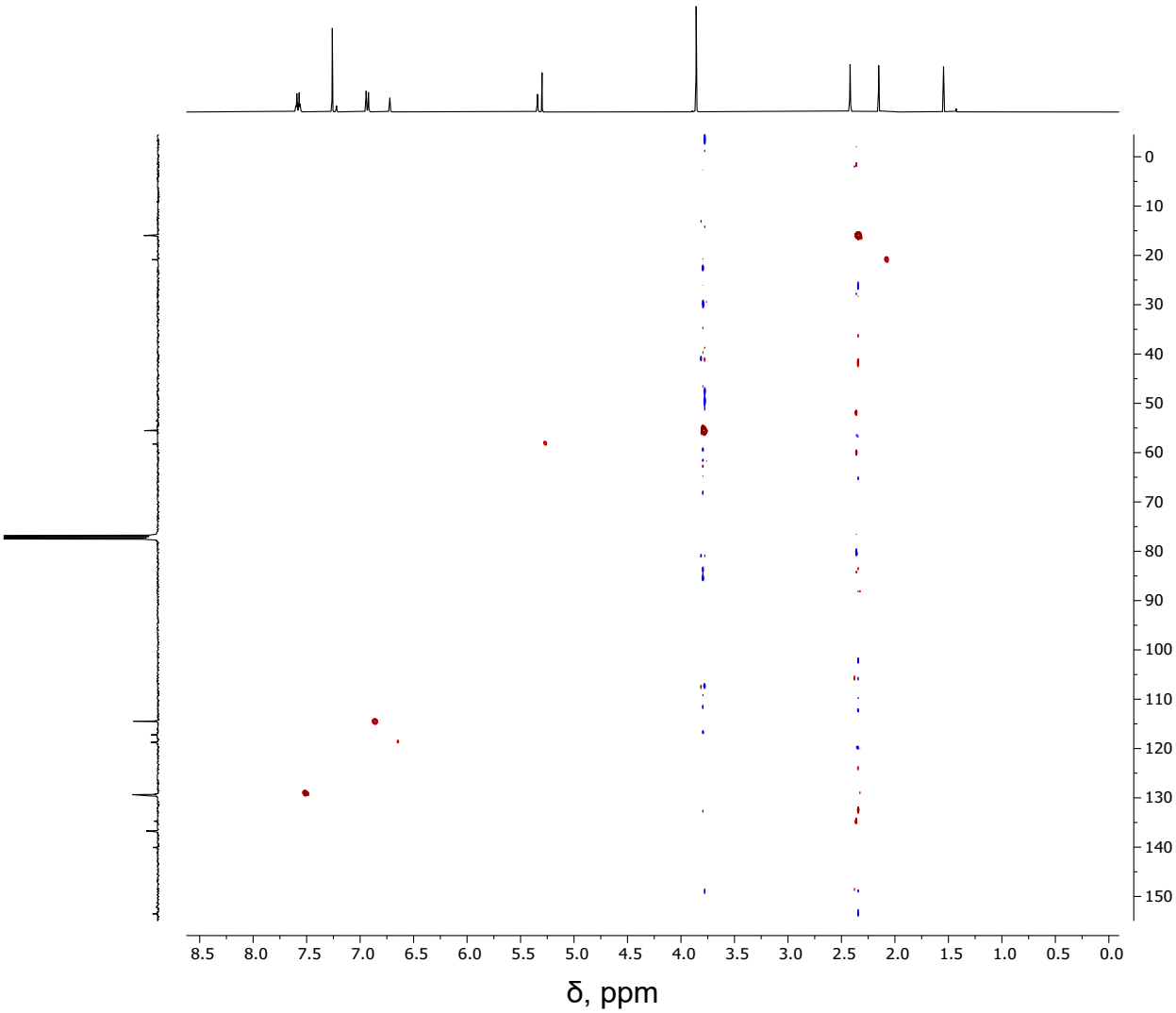

Figure S17. ^{1}H-^{13}C HSQC NMR of **4** (BODIPYmodOAc) in $CDCl_3$, RT.

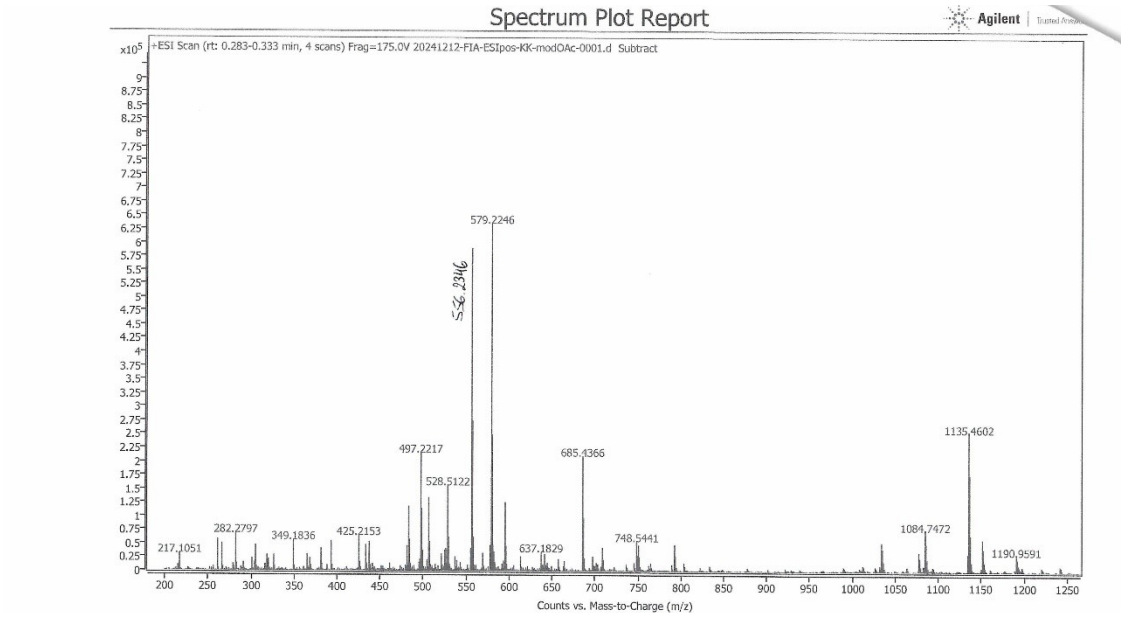

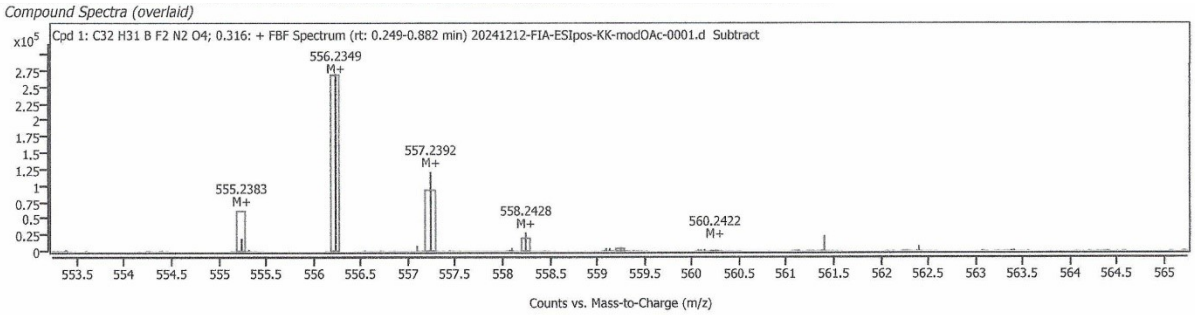

Compound ID Table

Name	Formula	Species	RT	RT Diff	Mass	CAS	ID Source	Score	Score (Lib)	Score (Tgt)
	C32 H31 B F2 N2 O4	M+	0.316		555.2390		FBF	72.06		72.06

Figure S18. HRMS of **4** (BODIPYmodOAc).

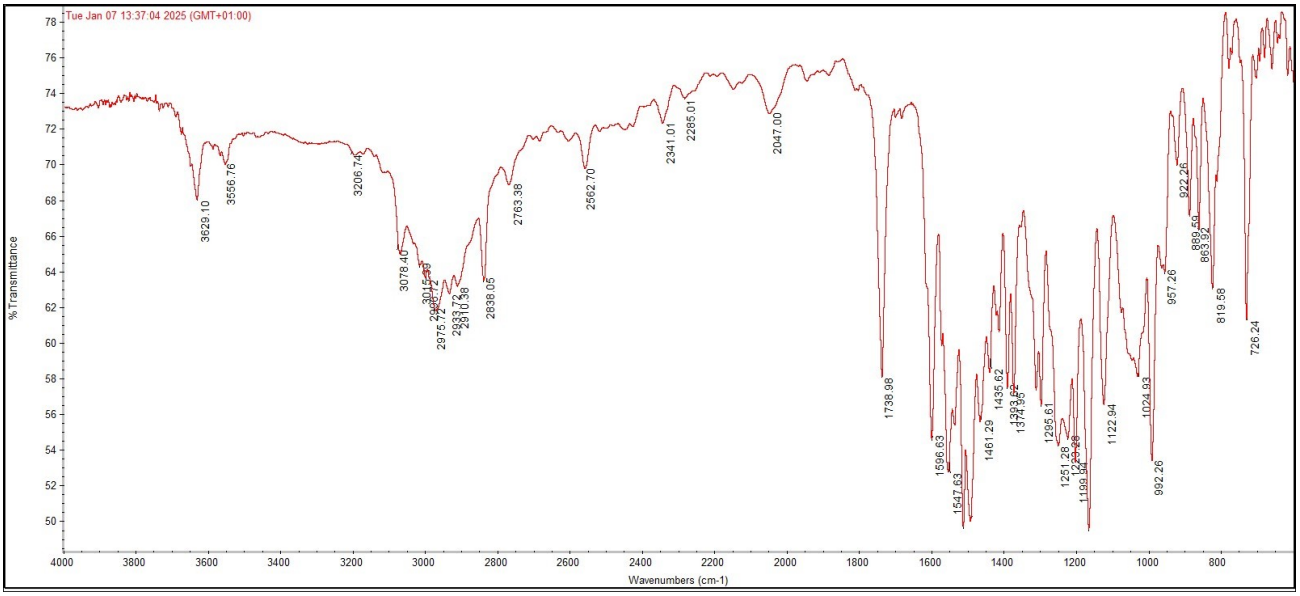

Figure S19. IR of **4** (BODIPYmodOAc).

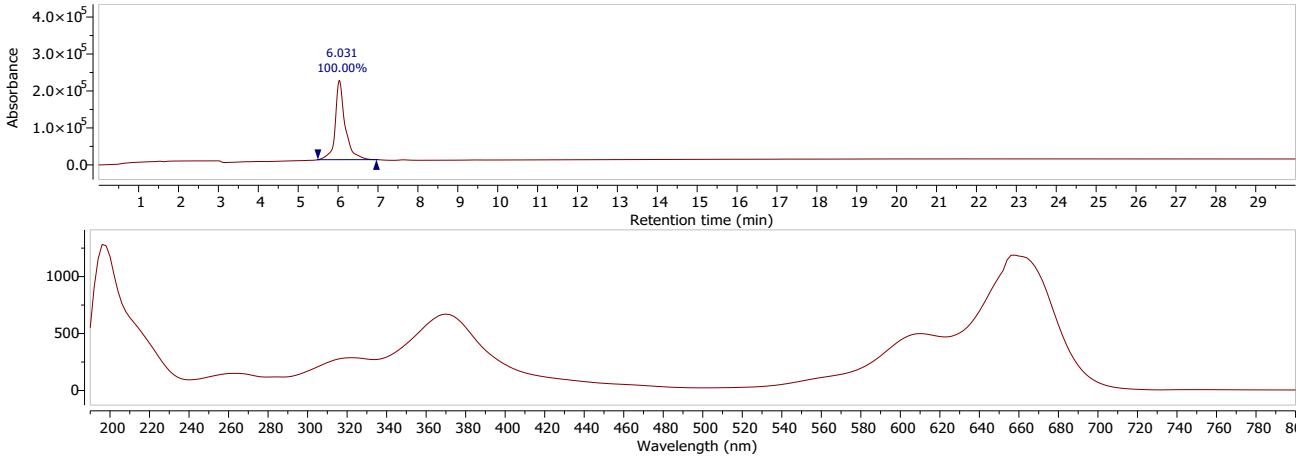

Figure S20. HPLC data of **4** (BODIPYmodOAc) shows absorbance at 250 nm during 30 min (top) and the absorption spectrum corresponding to the peak near 5.5 min (bottom). Isocratic 5% H_2O in MeOH.

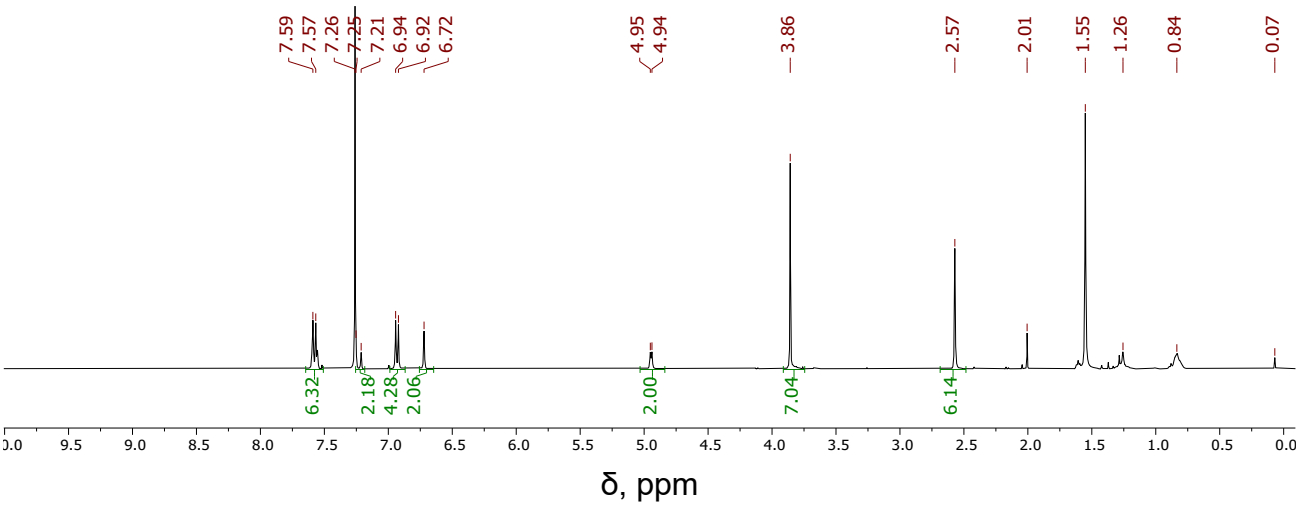

Figure S21. ^{1}H NMR of **5** (BODIPYmodOH) in $CDCl_3$, RT.

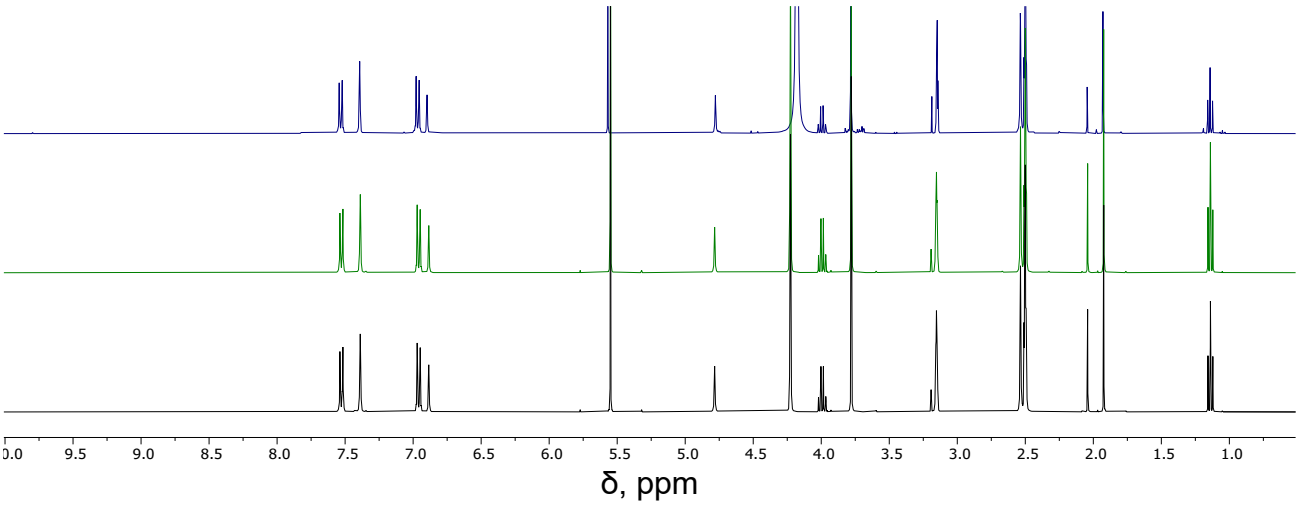

Figure S22. ^{1}H NMR before irradiation (top), after 24 hours (middle), and after irradiation at 645 nm for 1 hour (bottom) of **5** (BODIPYmodOH) in DMSO/MeOH (v/v, 1/1), RT.

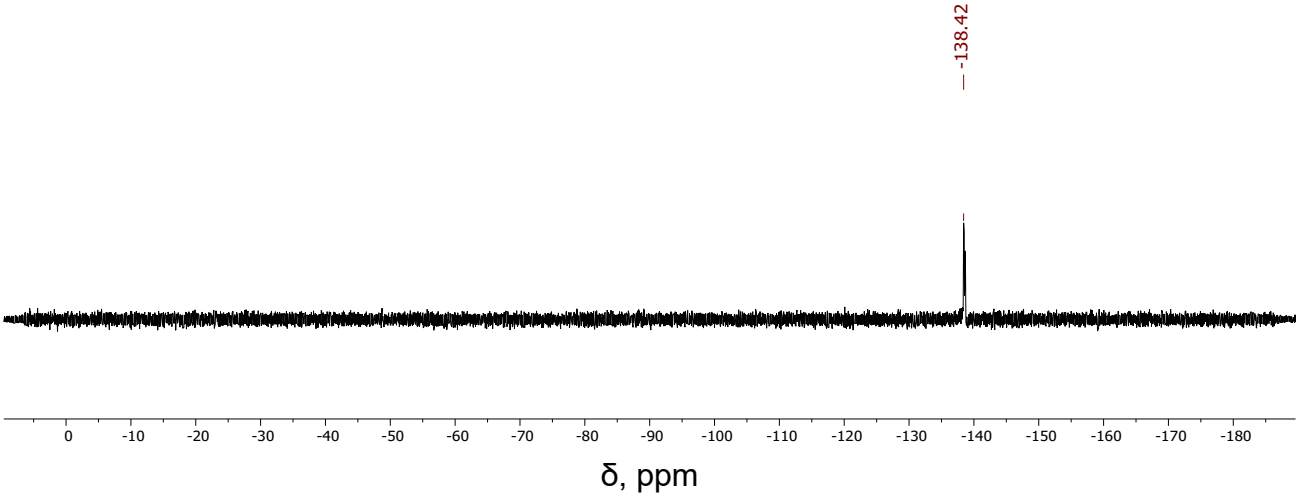

Figure S23. ^{19}F NMR of **5** (BODIPYmodOH) in $CDCl_3$, RT.

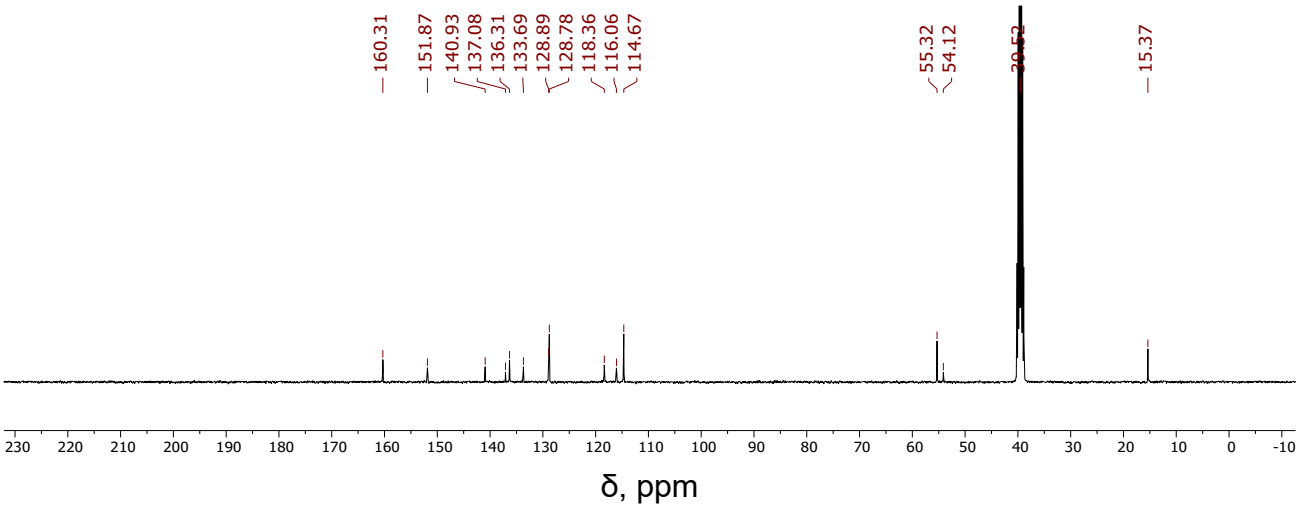

Figure S24. ^{13}C NMR of **5** (BODIPYmodOH) in DMSO-d_6, RT

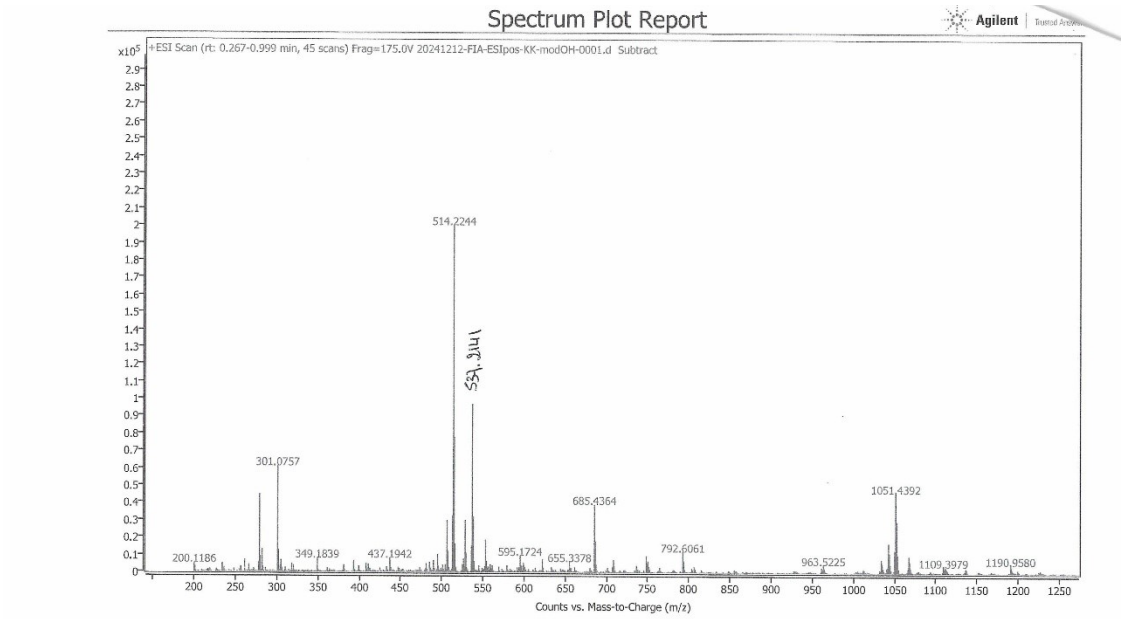

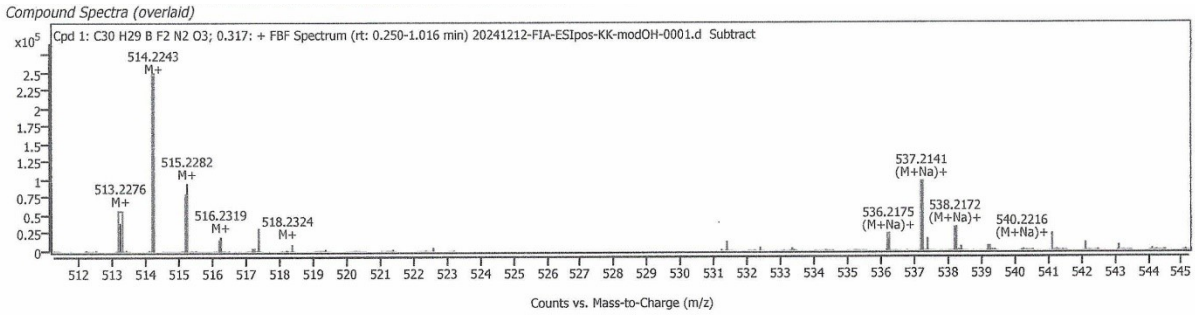

Compound ID Table

Name	Formula	Species	RT	RT Diff	Mass	CAS	ID Source	Score	Score (Lib)	Score (Tgt)
	C30 H29 B F2 N2 O3	M+ (M+Na)+	0.317		513.2282		FBF	92.07		92.07

Figure S25. HRMS of **5** (BODIPYmodOH).

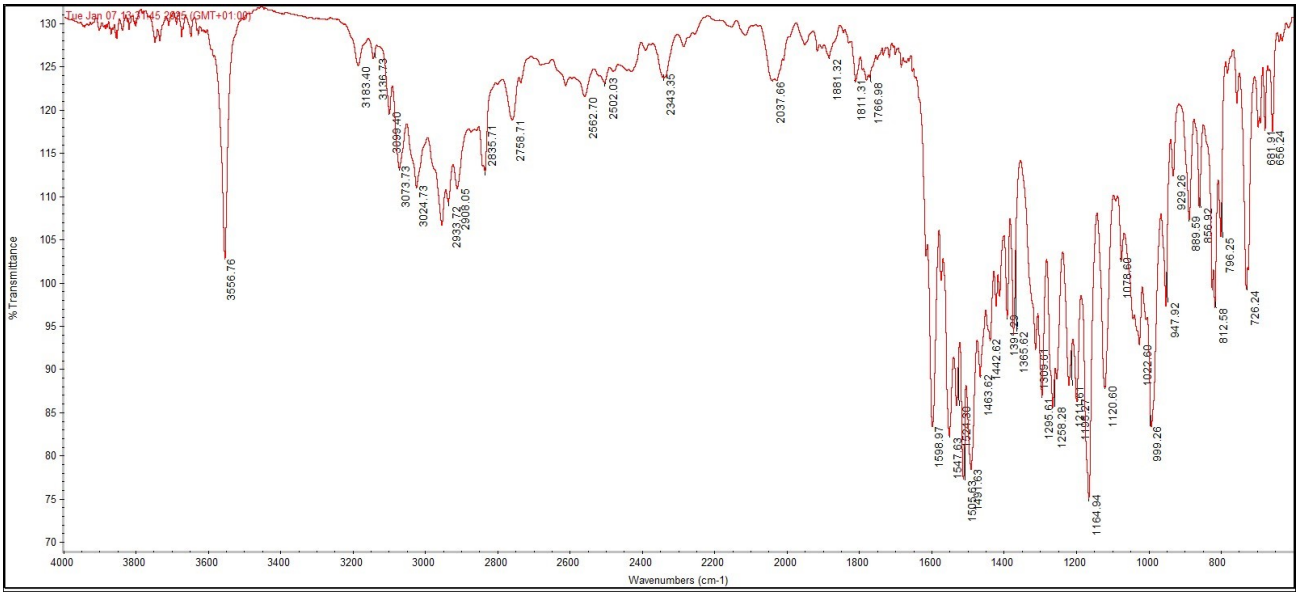

Figure S26. IR of **5** (BODIPYmodOH).

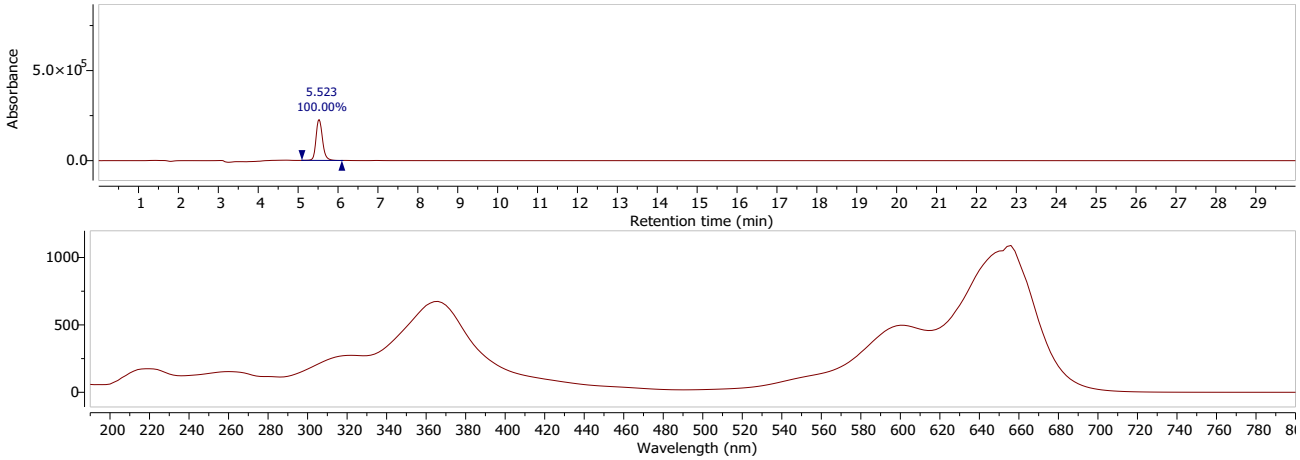

Figure S27. HPLC data of **5** (BODIPYmodOH) shows absorbance at 250 nm during 30 min (top) and the absorption spectrum corresponding to the peak near 5.5 min (bottom). Isocratic 5% H_2O in MeOH.

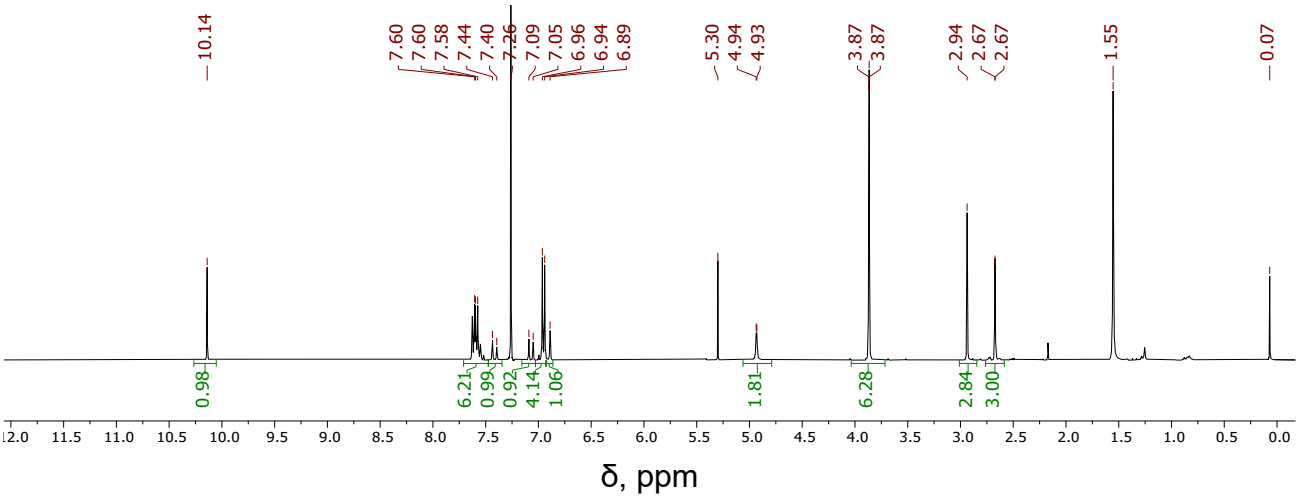

Figure S28. ^{1}H NMR of **6** (BODIPYmodOHCHO) in $CDCl_3$, RT.

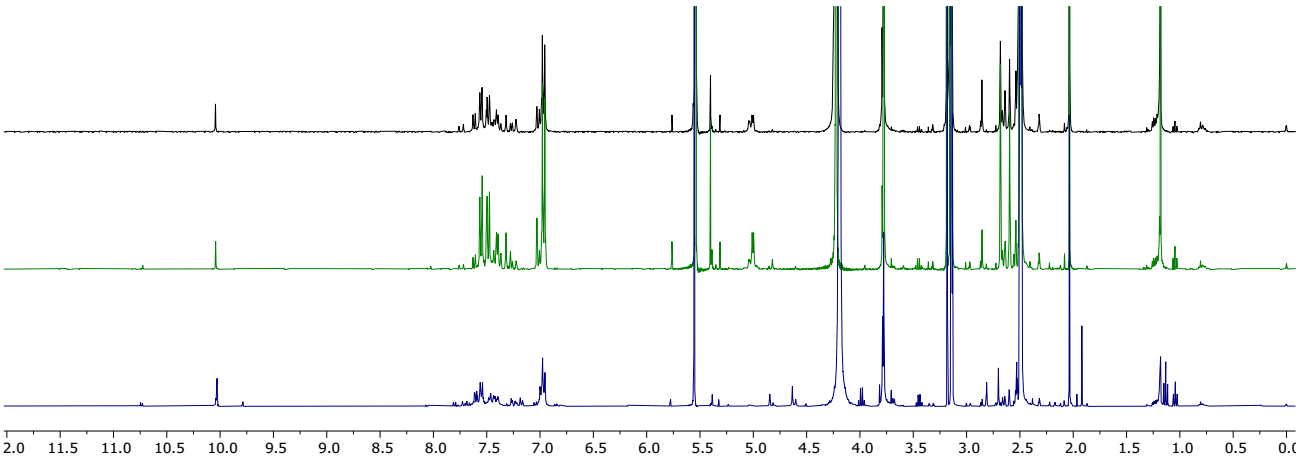

Figure S29. ^{1}H NMR before irradiation (top), after 24 hours (middle), and after irradiation at 645 nm for 1 hour (bottom) of **6** (BODIPYmodOHCHO) in deuterated DMSO/MeOH (v/v, 1/1), RT.

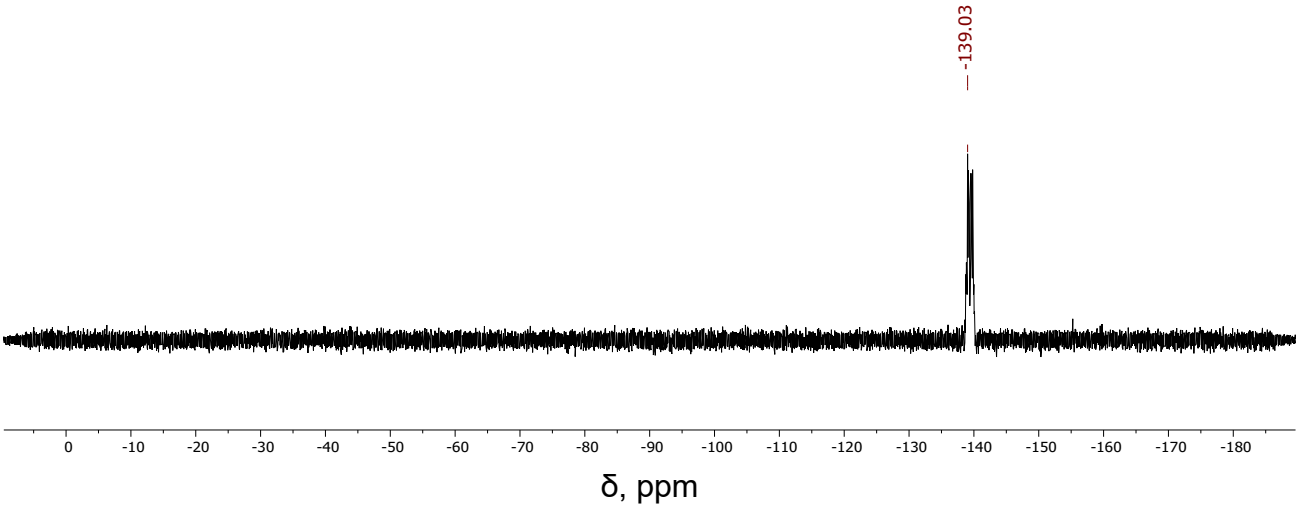

Figure S30. ^{19}F NMR of **6** (BODIPYmodOHCHO) in $CDCl_3$, RT.

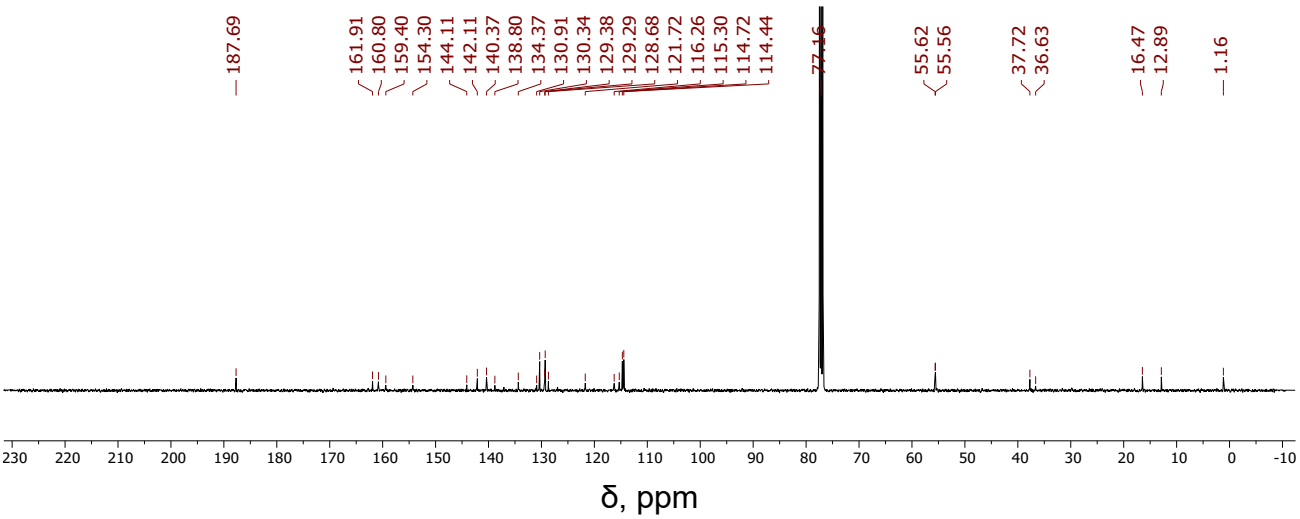

Figure S31. ^{13}C NMR of **6** (BODIPYmodOHCHO) in $CDCl_3$, RT.

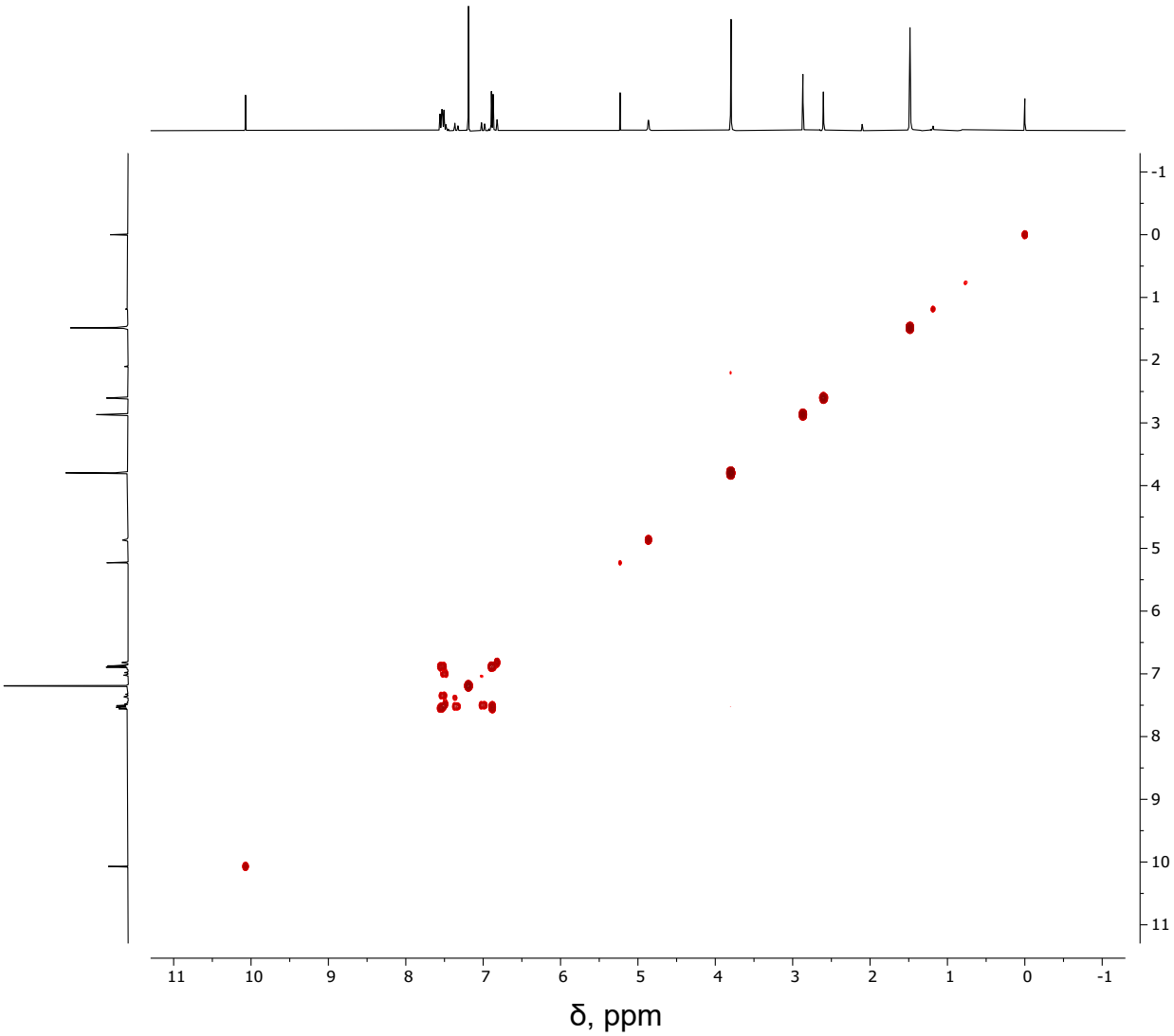

Figure S32. ^{1}H-^{1}H COSY NMR of **6** (BODIPYmodOHCHO) in $CDCl_3$, RT.

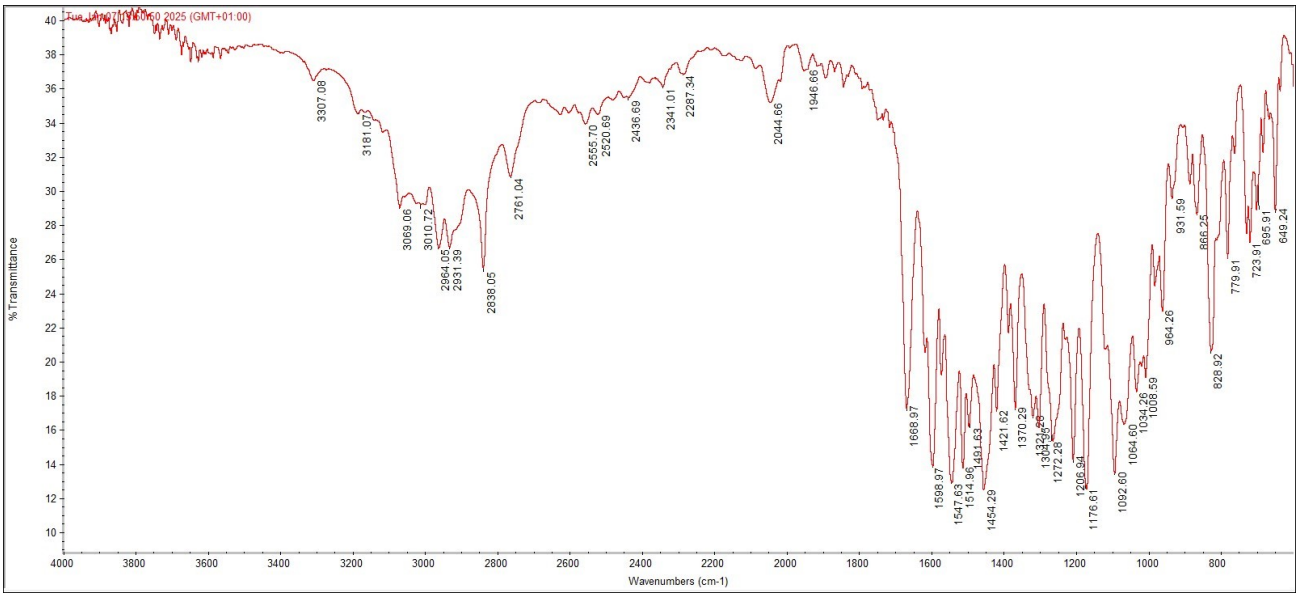

Figure S33. IR of **6** (BODIPYmodOHCHO).

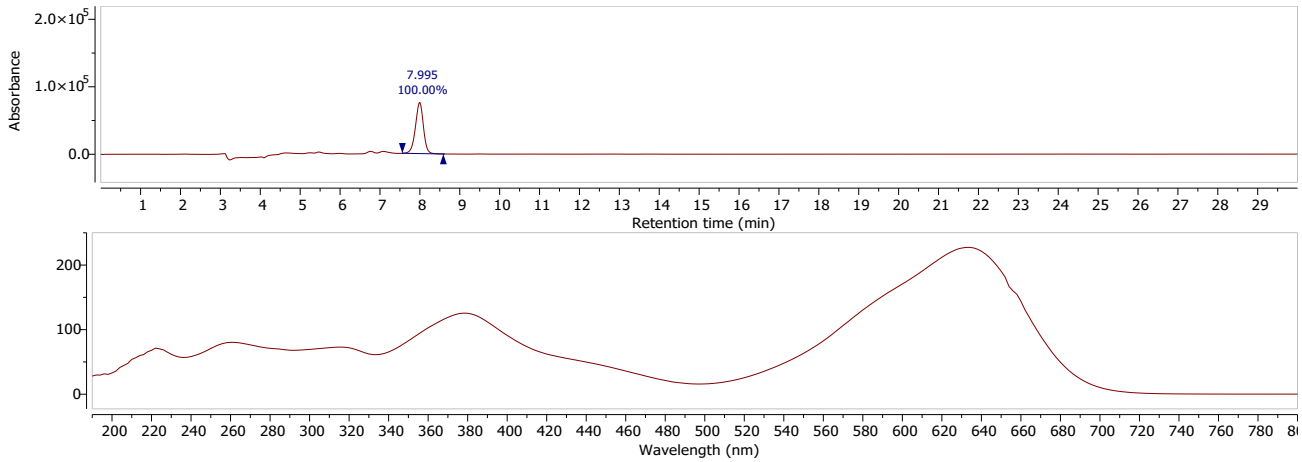

Figure S34. HPLC data of **6** (BODIPYmodOHCHO) shows absorbance at 250 nm during 30 min (top) and the absorption spectrum corresponding to the peak near 8.0 min (bottom). Isocratic 5% H_2O in MeOH.

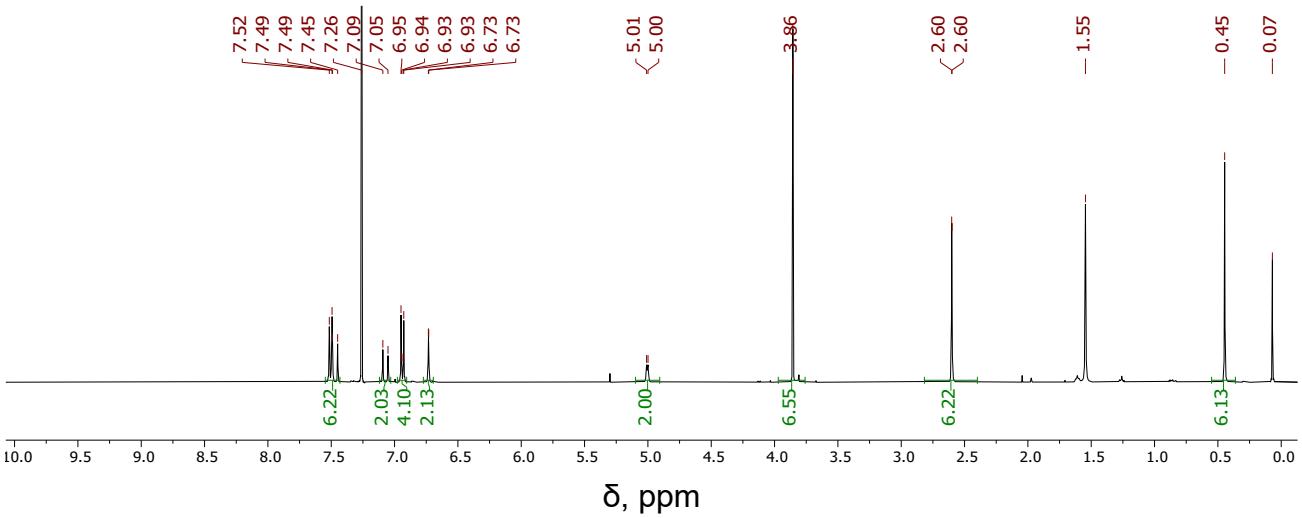

Figure S35. ^{1}H NMR of **7** (BODIPYmodMeOH) in $CDCl_3$, RT.

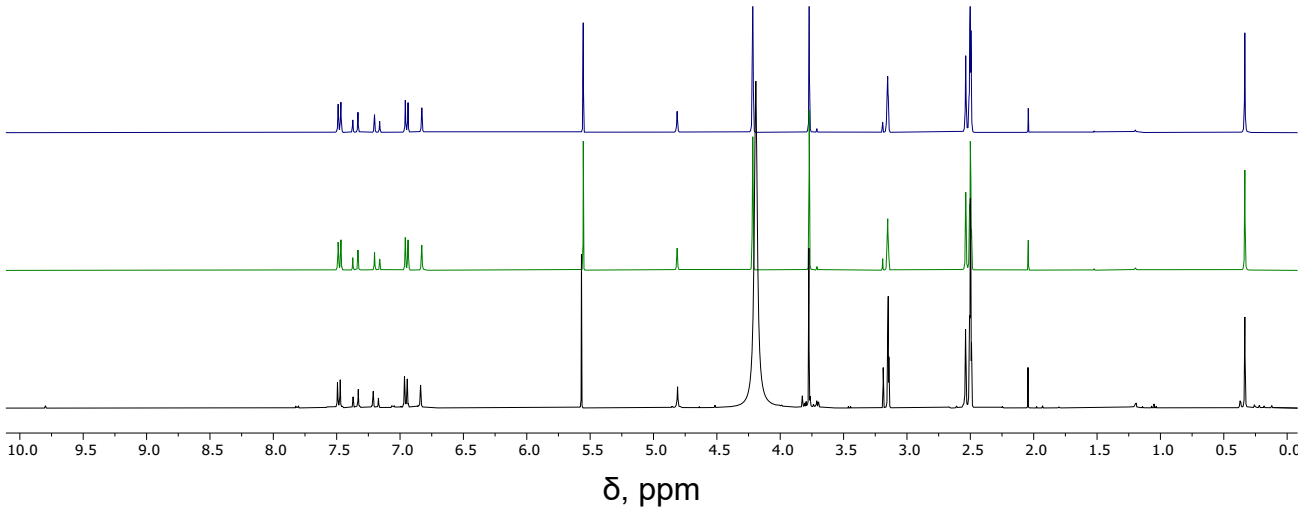

Figure S36. ^{1}H NMR before irradiation (top), after 24 hours (middle), and after irradiation at 645 nm for 1 hour (bottom) of **7** (BODIPYmodMeOH) in deuterated DMSO/MeOH (v/v, 1/1), RT.

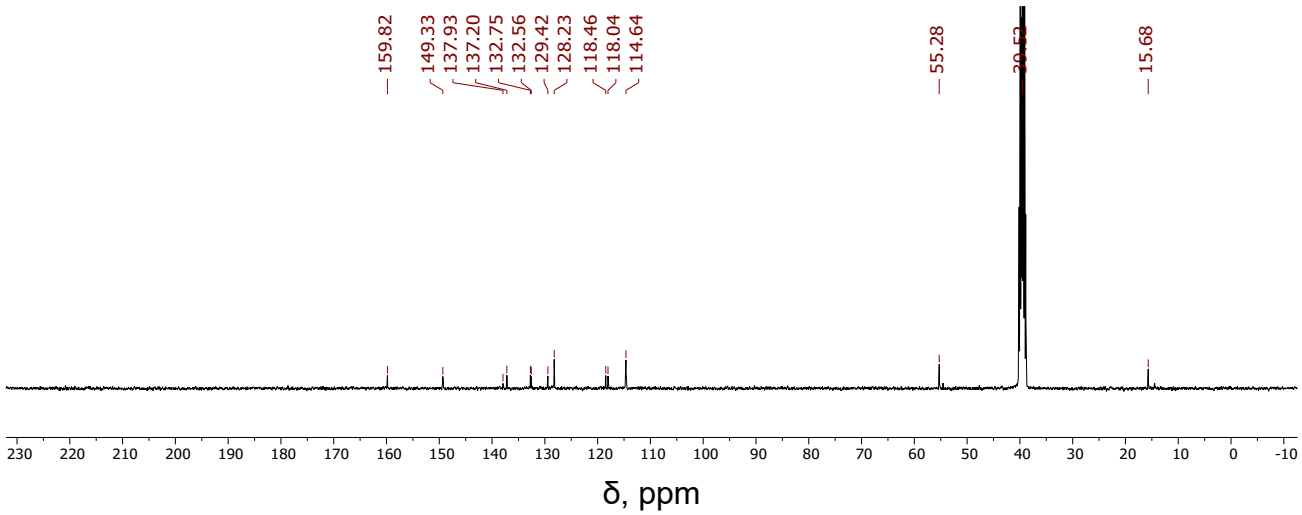

Figure S37. ^{13}C NMR of **7** (BODIPYmodMeOH) in DMSO-d_6, RT

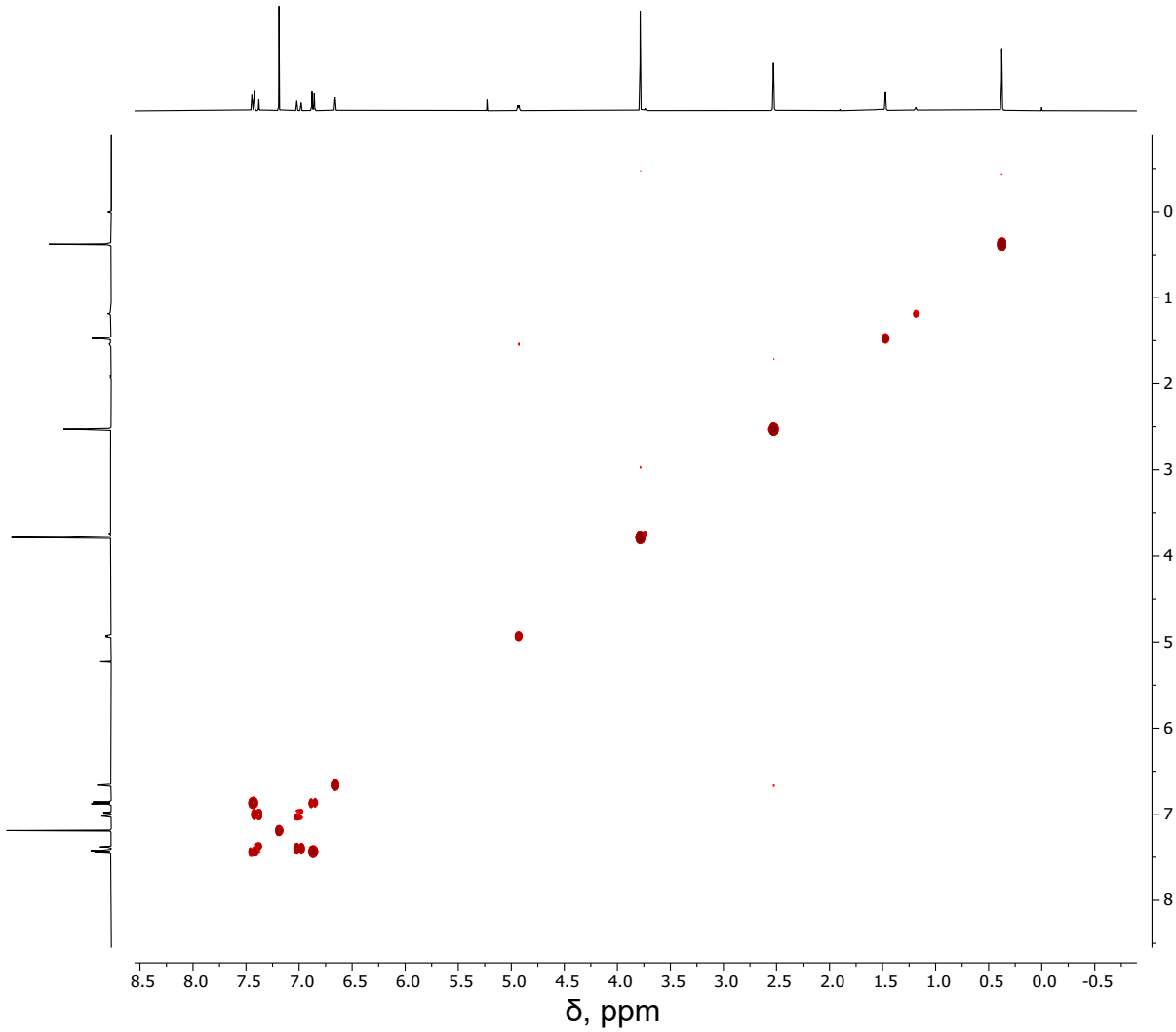

Figure S38. ^{1}H-^{1}H COSY NMR of **7** (BODIPYmodMeOH) in $CDCl_3$, RT.

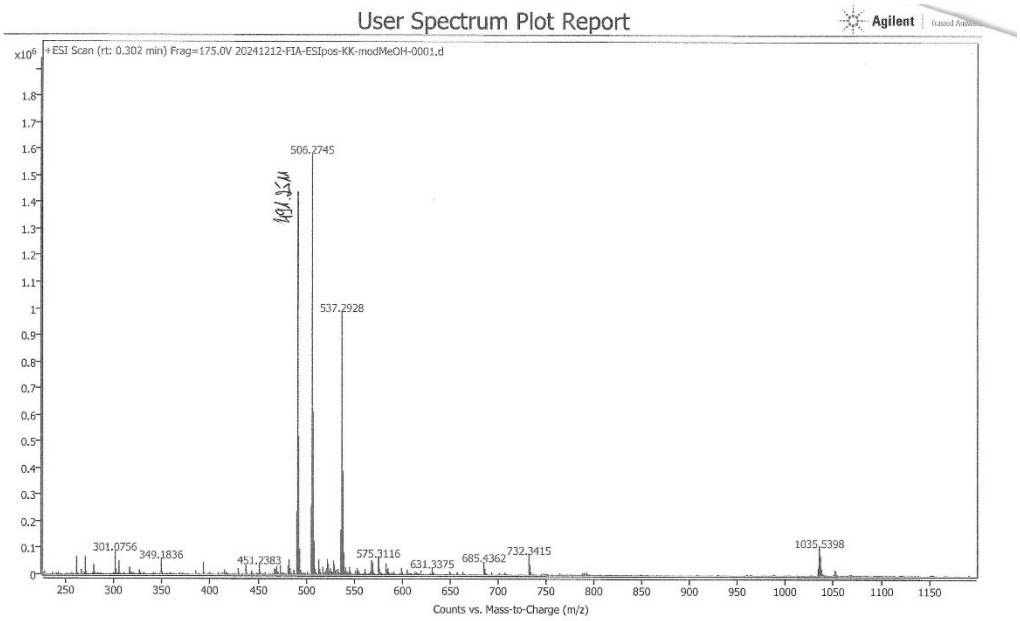

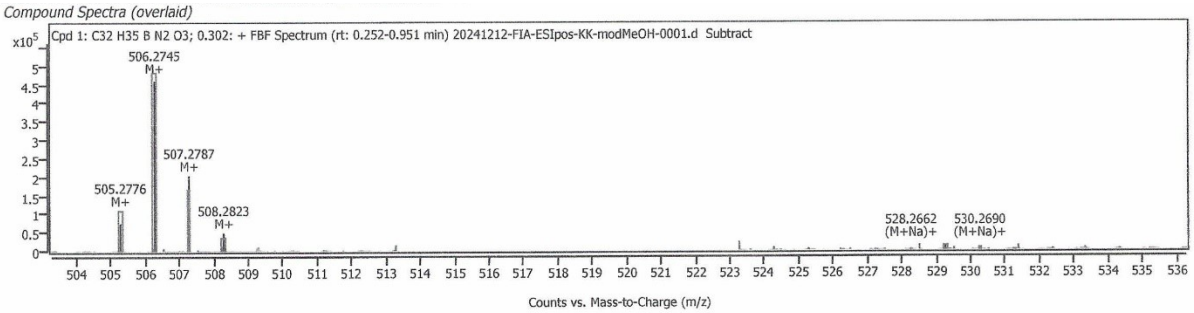

Compound ID Table

Name	Formula	Species	RT	RT Diff	Mass	CAS	ID Source	Score	Score (Lib)	Score (Tgt)
	C32 H35 B N2 O3	M+ (M+Na)+	0.302		505.2785		FBF	82.48		82.48

Figure S39. HRMS of **7** (BODIPYmodMeOH).

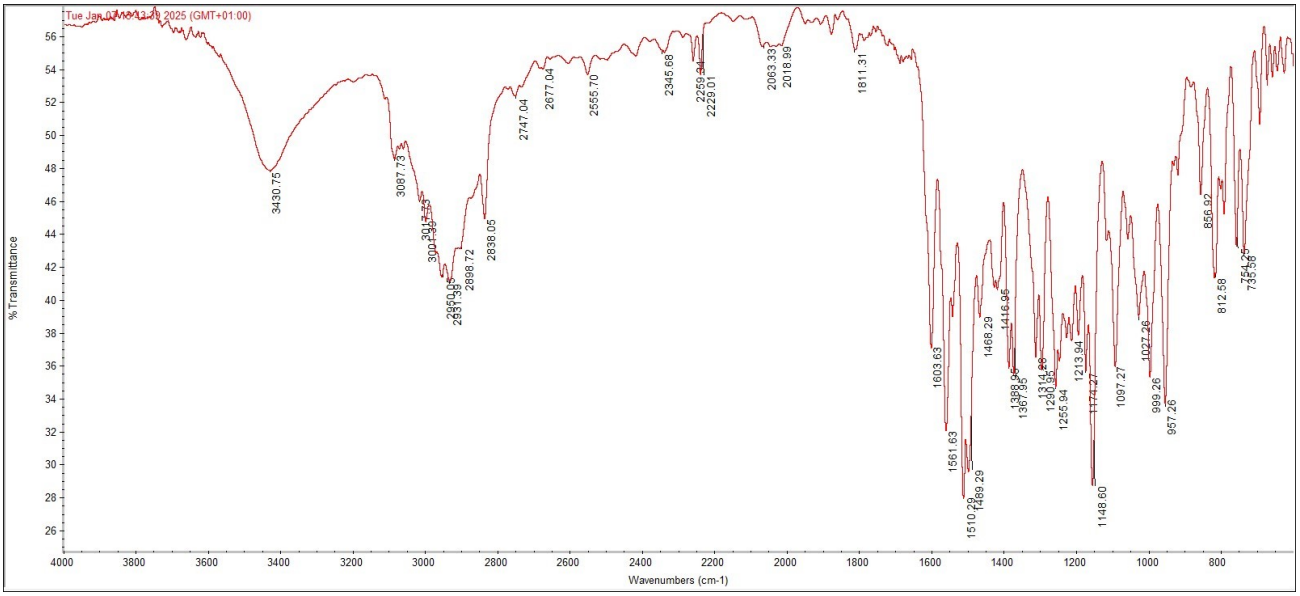

Figure S40. IR of **7** (BODIPYmodMeOH).

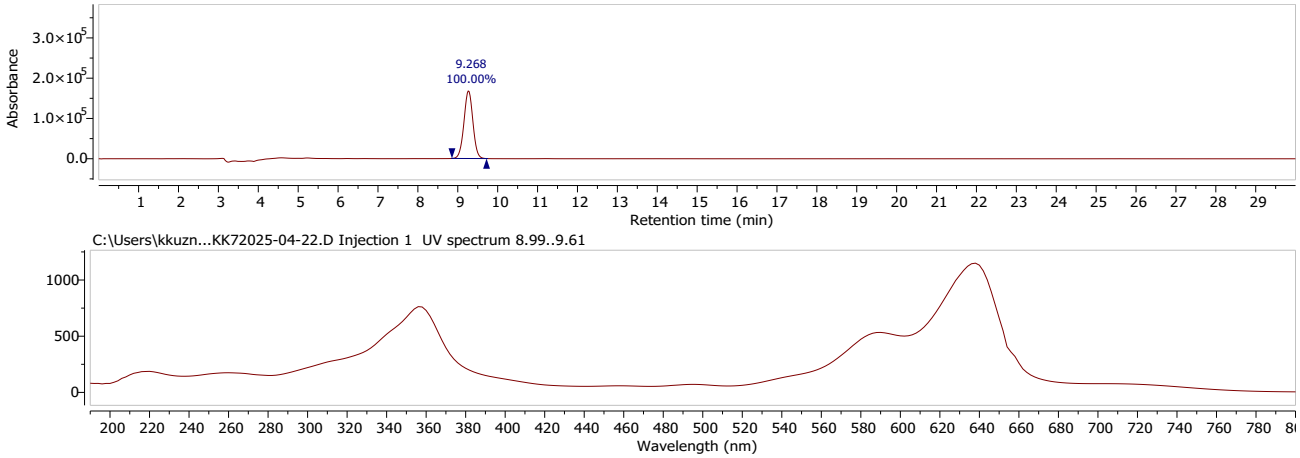

Figure S41. HPLC data of **7** (BODIPYmodMeOH) shows absorbance at 250 nm during 30 min (top) and the absorption spectrum corresponding to the peak near 9.3 min (bottom). Isocratic 5% H_2O in MeOH.

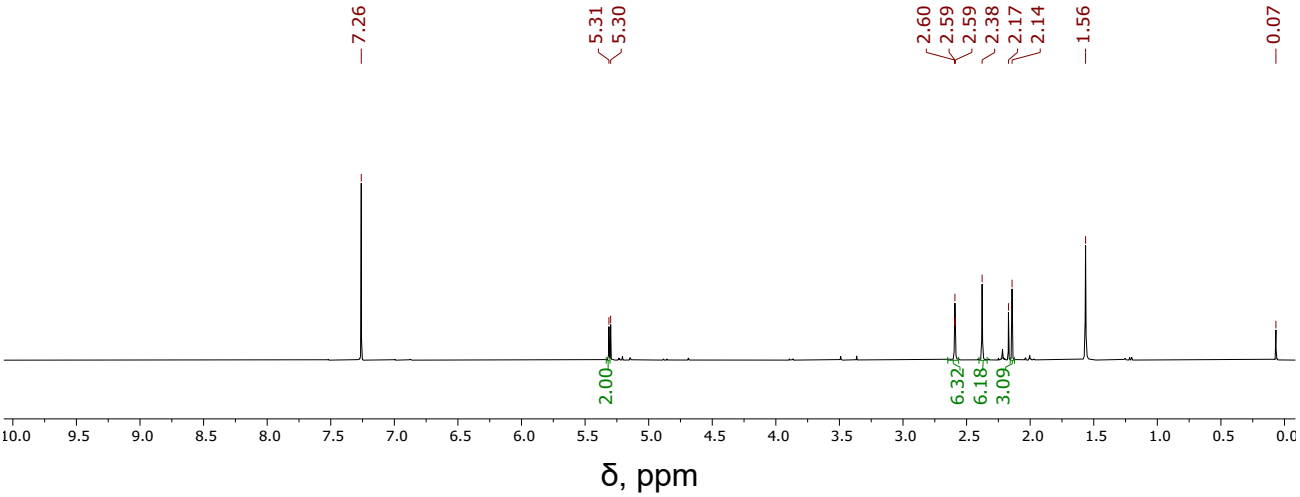

Figure S42. ^{1}H NMR of **8** (BODIPYBrOAc) in $CDCl_3$, RT.

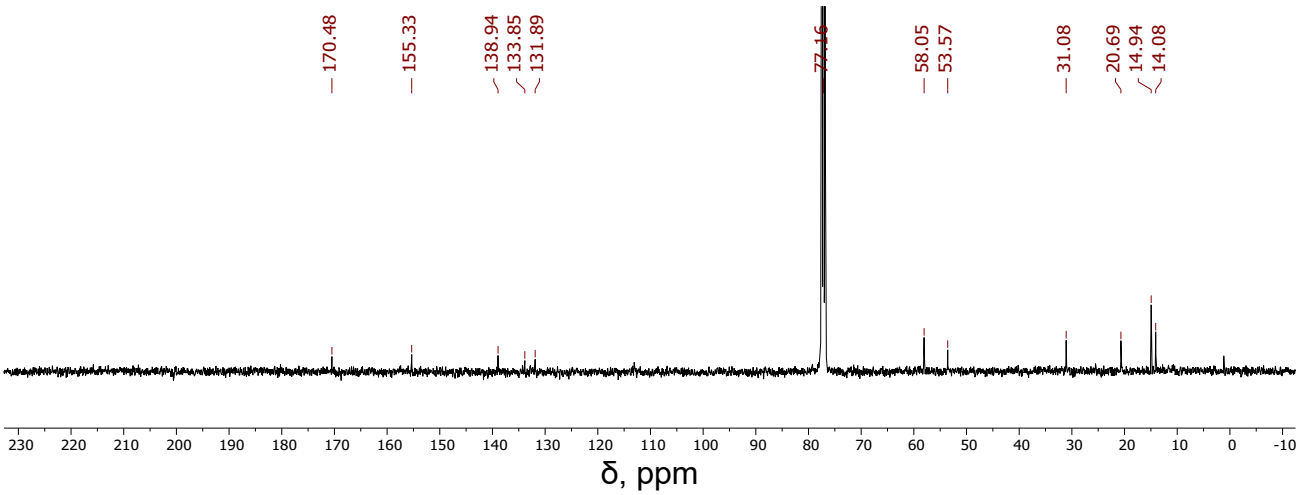

Figure S43. ^{13}C NMR of **8** (BODIPYBrOAc) in $CDCl_3$, RT

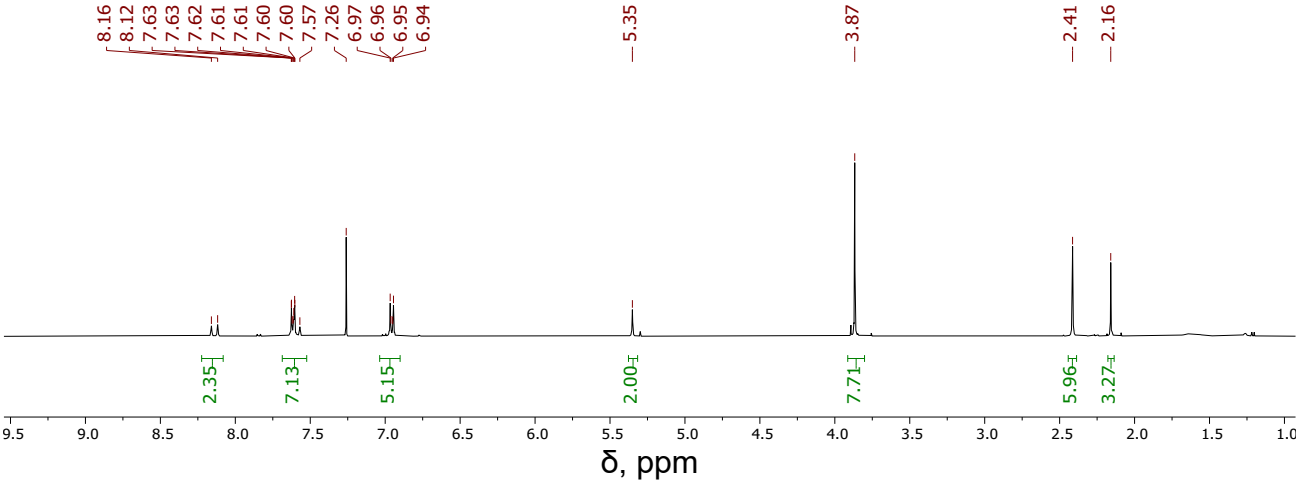

Figure S44. ^{1}H NMR of **9** (BODIPYBrmodOAc) in $CDCl_3$, RT.

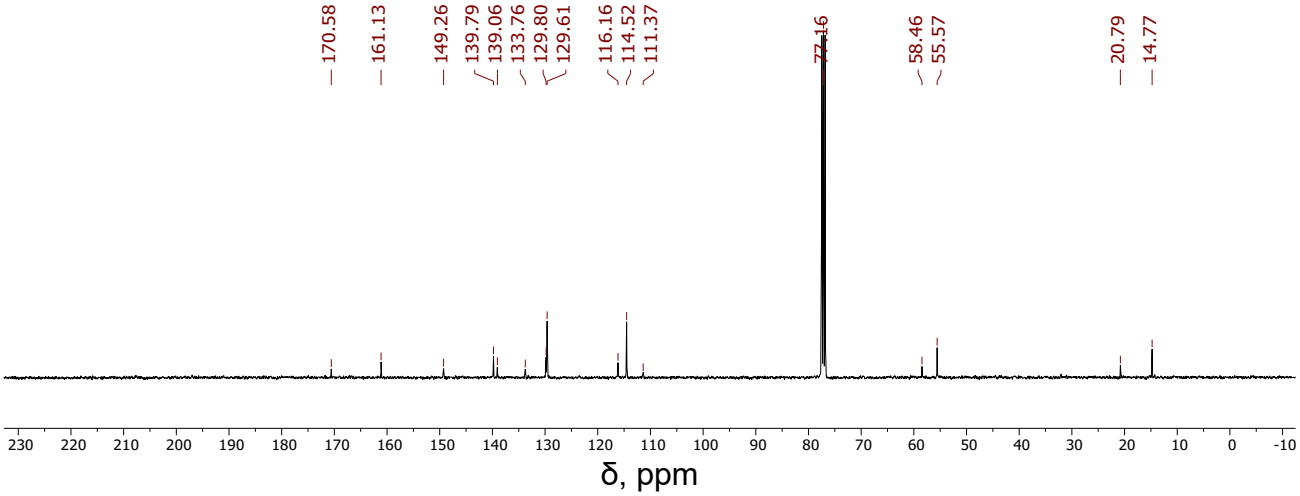

Figure S45. ^{13}C NMR of **9** (BODIPYBrmodOAc) in $CDCl_3$, RT.

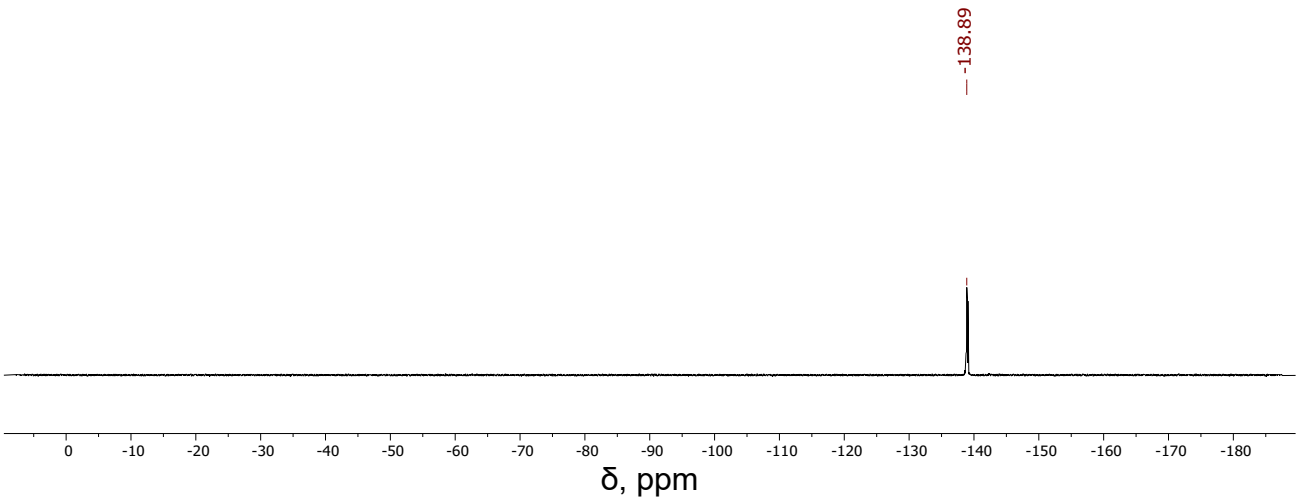

Figure S46. ^{19}F NMR of **9** (BODIPYBrmodOAc) in $CDCl_3$, RT.

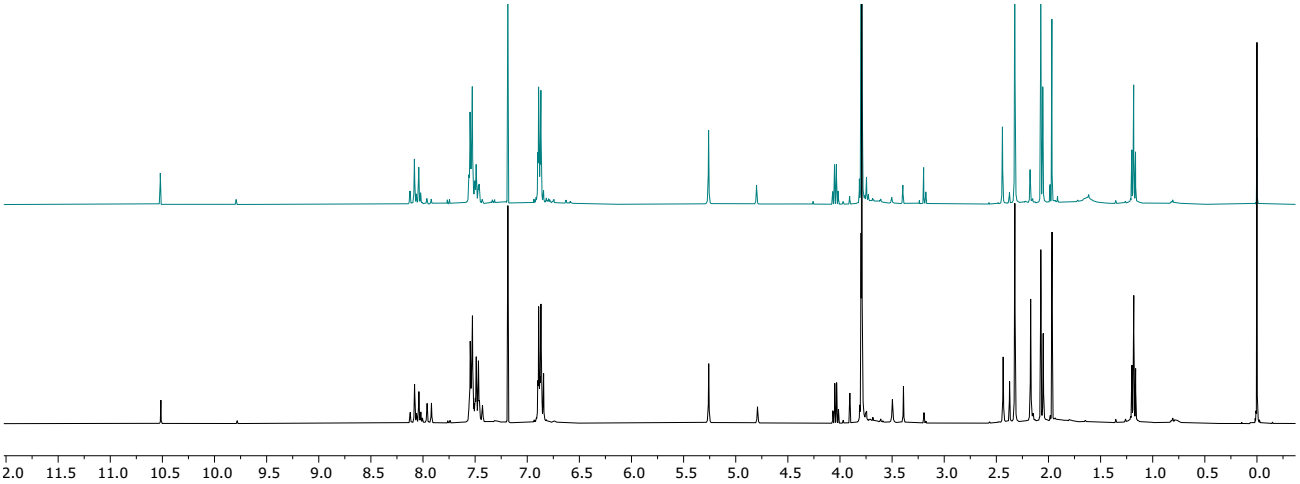

Figure S47. ^{1}H NMR of a crude mixture of hydrolysis with NaOH (0.1 M) of **9** (BODIPYBrmodOAc) under aerated (top) and degassed (bottom, bubbled with nitrogen for 20 minutes) conditions in the dark in $CDCl_3$, RT.

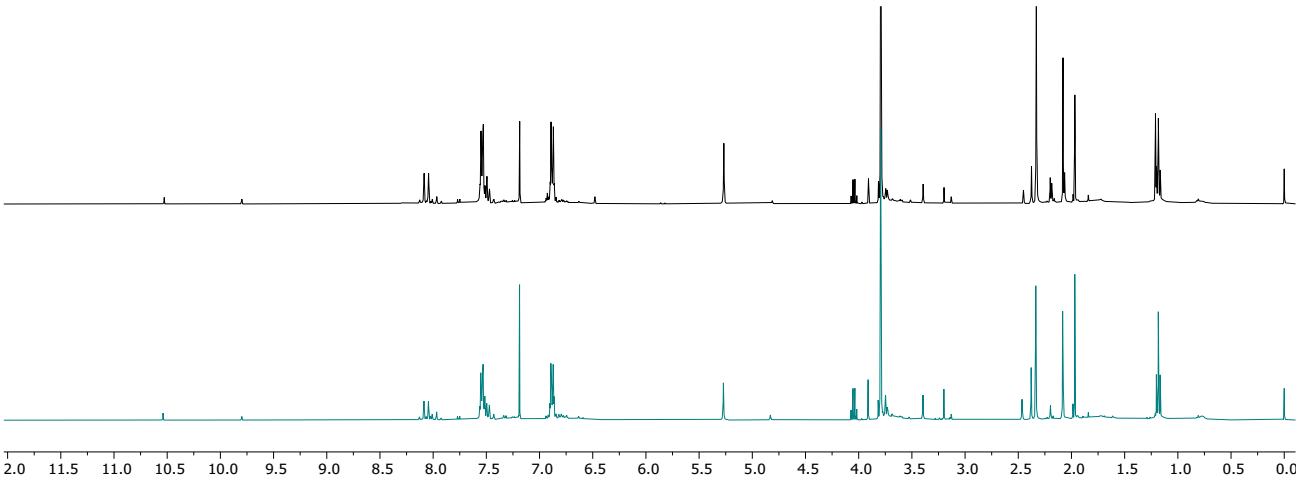

Figure S48. ^{1}H NMR of a crude mixture of hydrolysis with K_2CO_3 of **9** (BODIPYBrmodOAc) under aerated (top) and degassed (bottom, bubbled with nitrogen for 20 minutes) conditions in dark in $CDCl_3$, RT.

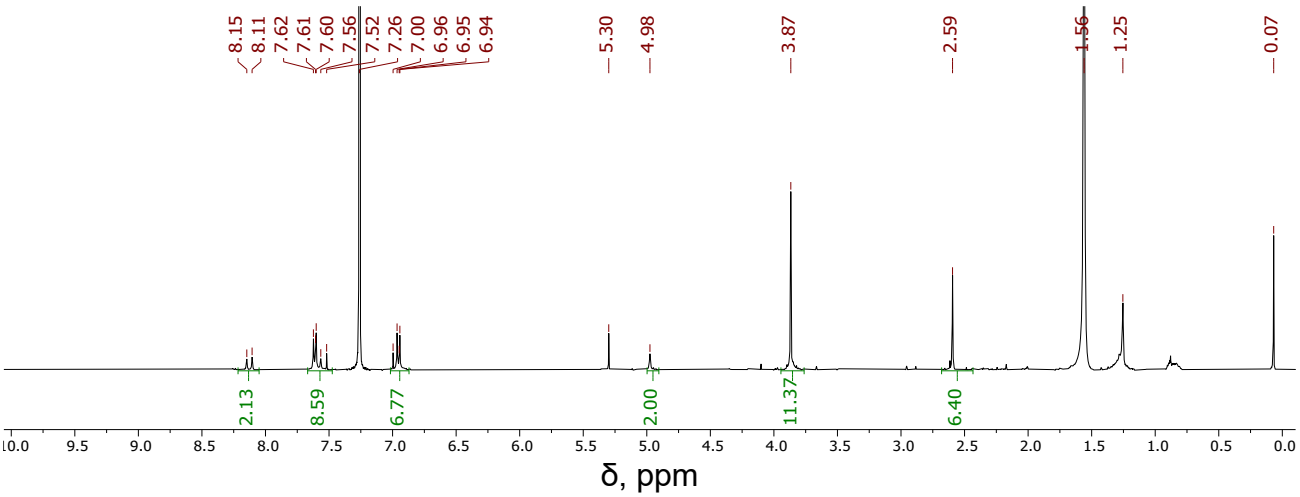

Figure S49. ^{1}H NMR of **10** (BODIPYBrmodOH) in $CDCl_3$, RT.

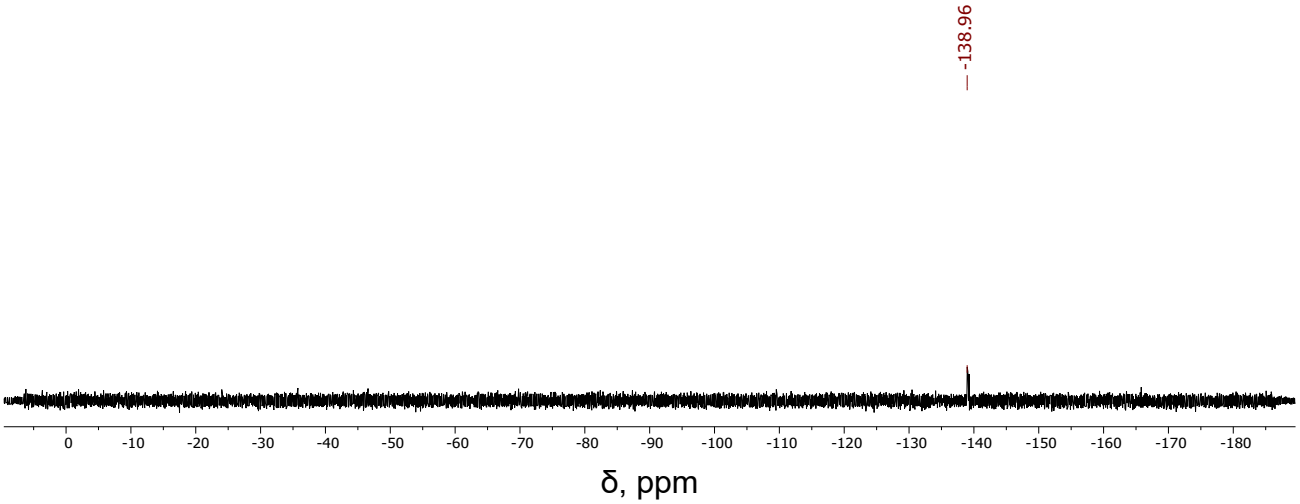

Figure S50. ^{19}F NMR of **10** (BODIPYBrmodOH) in $CDCl_3$, RT.

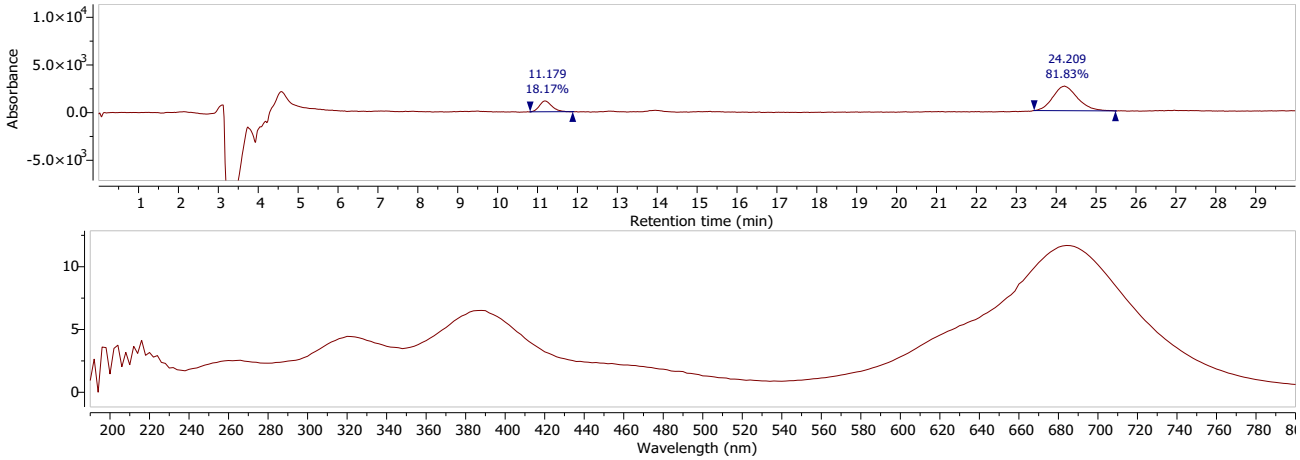

Figure S51. HPLC data of **10** (BODIPYBrmodOH) shows absorbance at 250 nm during 30 min (top) and the absorption spectrum corresponding to the peak near 24.2 min (bottom). Isocratic 5% H_2O in MeOH.

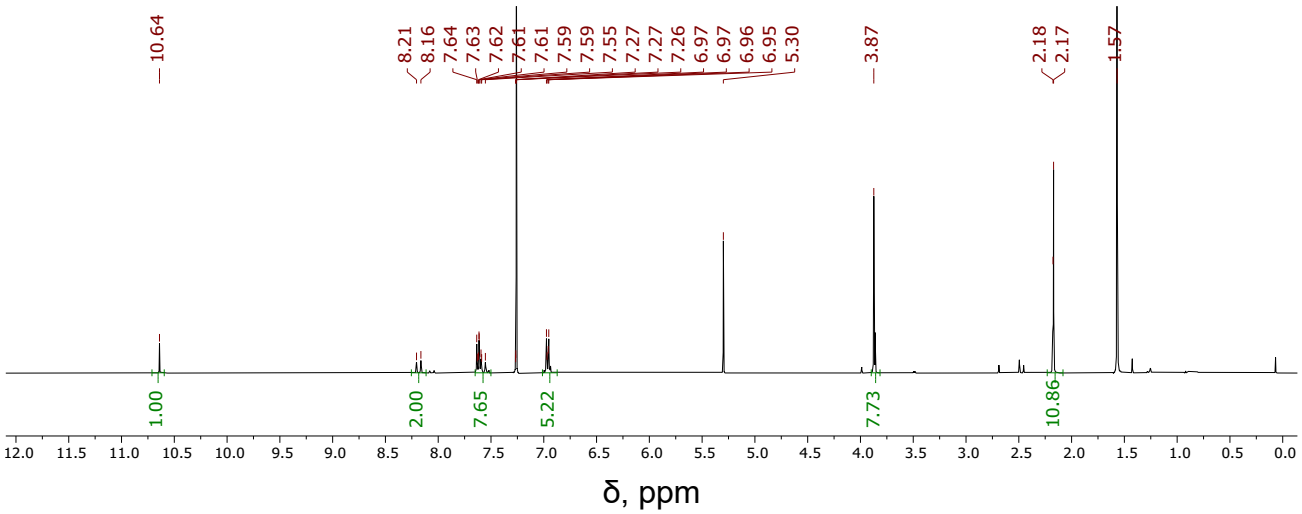

Figure S52. ^{1}H NMR of **11** (BODIPYBrmodCHO) in $CDCl_3$, RT.

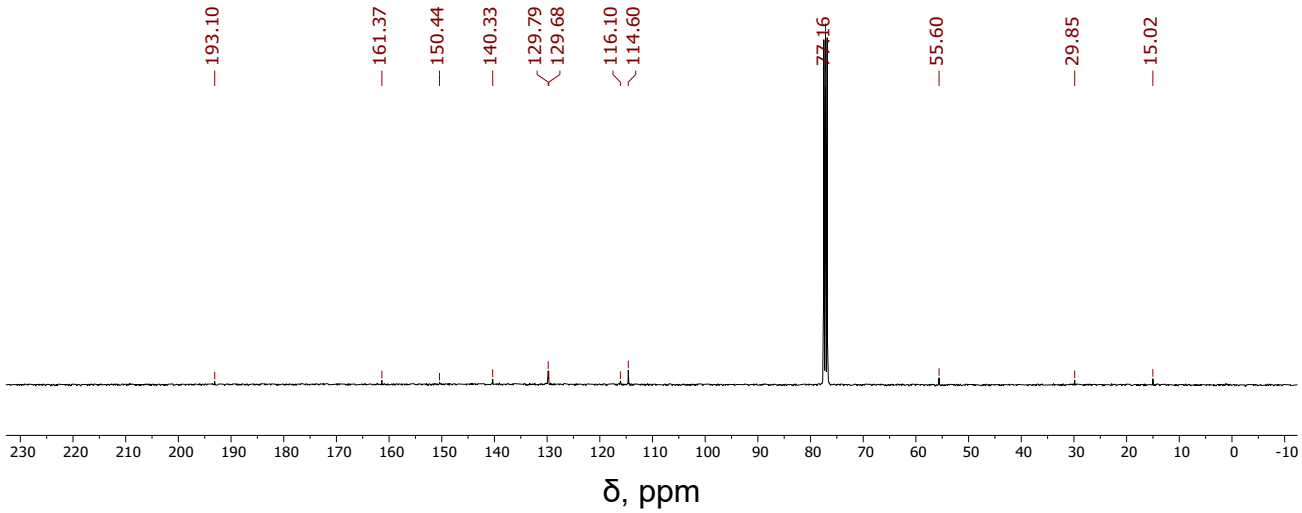

Figure S53. ^{13}C NMR of **11** (BODIPYBrmodCHO) in $CDCl_3$, RT.

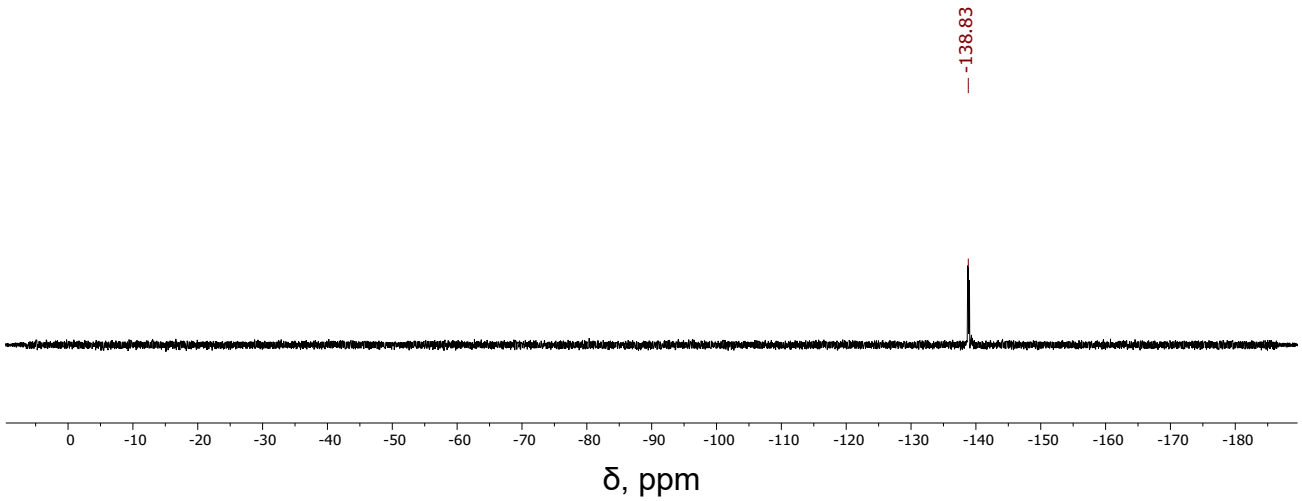

Figure S54. ^{19}F NMR of **11** (BODIPYBrmodCHO) in $CDCl_3$, RT.

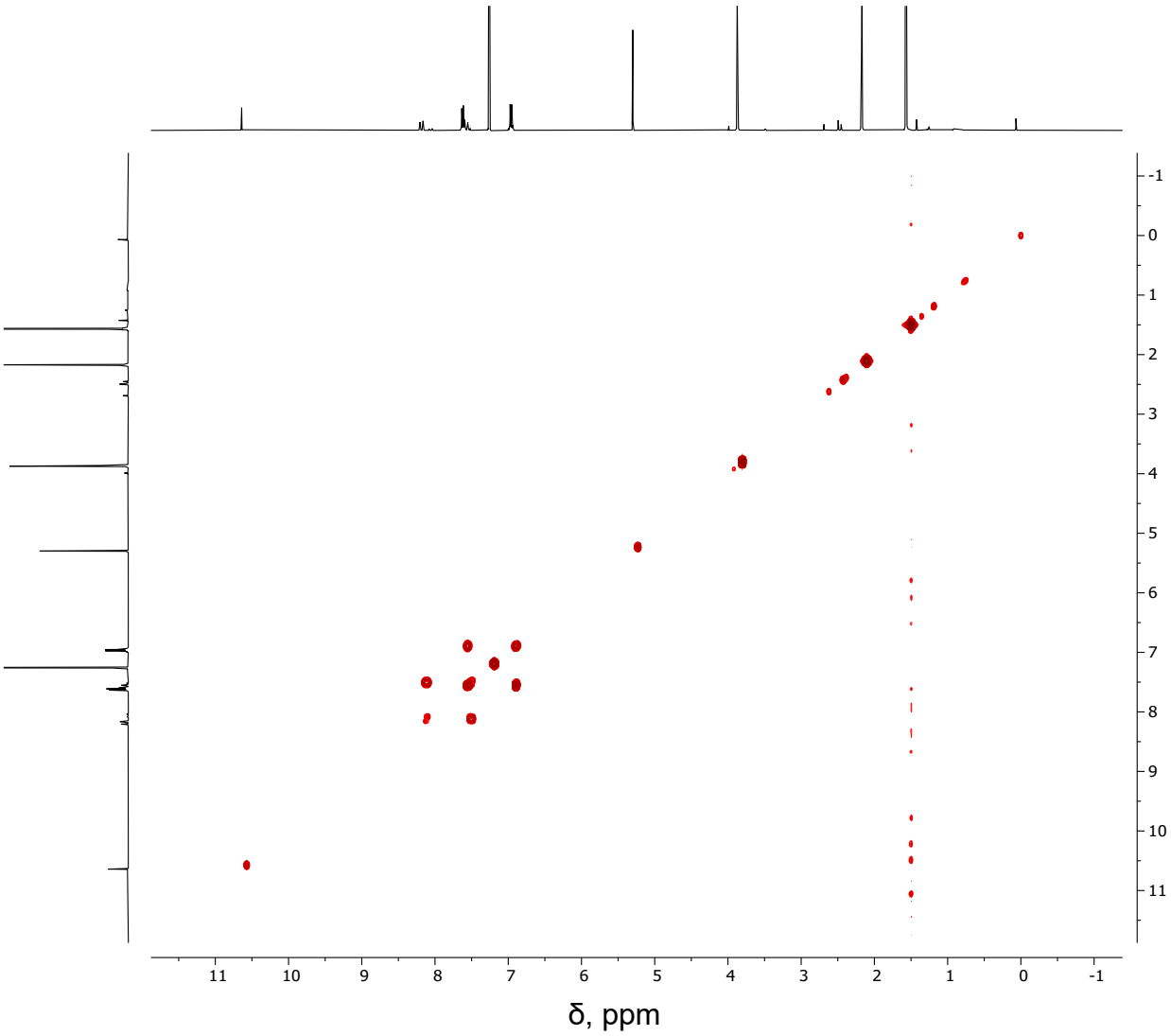

Figure S55. ^{1}H-^{1}H COSY NMR of **11** (BODIPYBrmodCHO) in $CDCl_3$, RT.

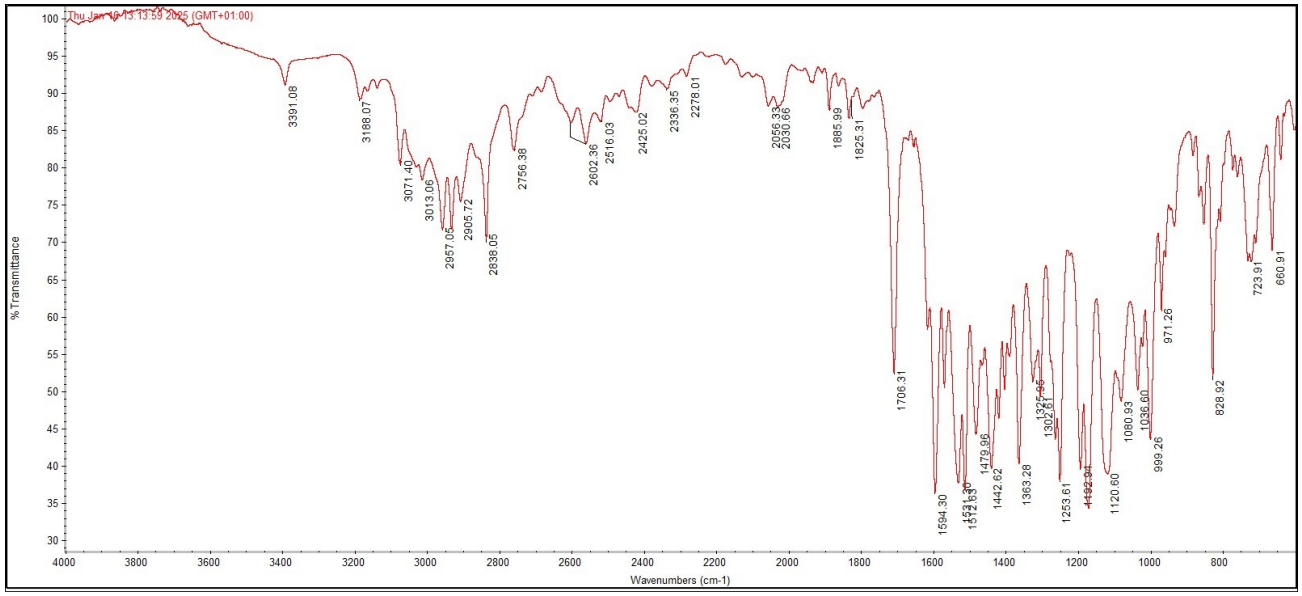

Figure S56. IR of **11** (BODIPYBrmodCHO).

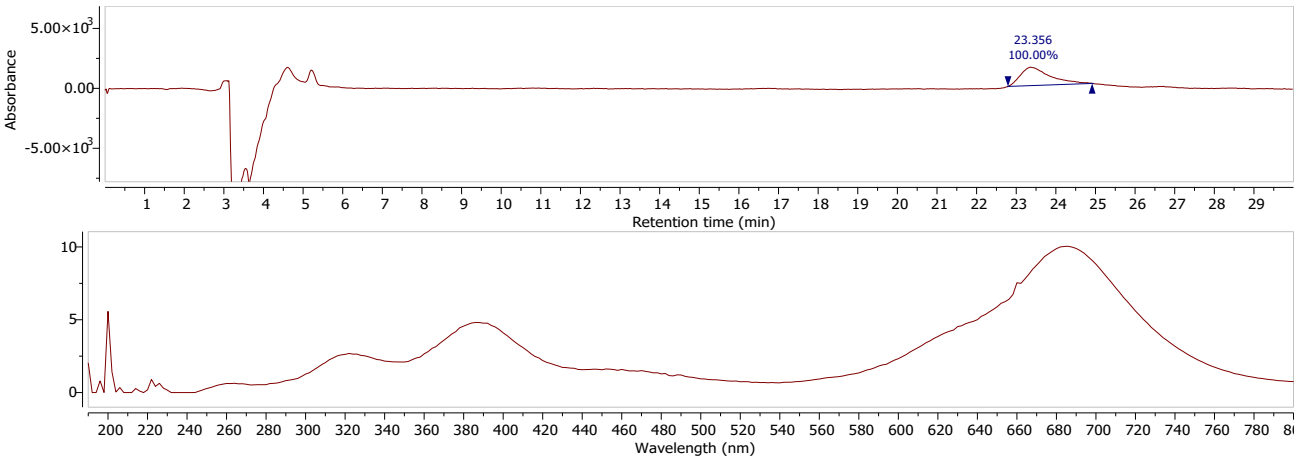

Figure S57. HPLC data of **11** (BODIPYBrmodCHO) shows absorbance at 250 nm during 30 min (top) and the absorption spectrum corresponding to the peak near 23.3 min (bottom). Isocratic 5% H_2O in MeOH.

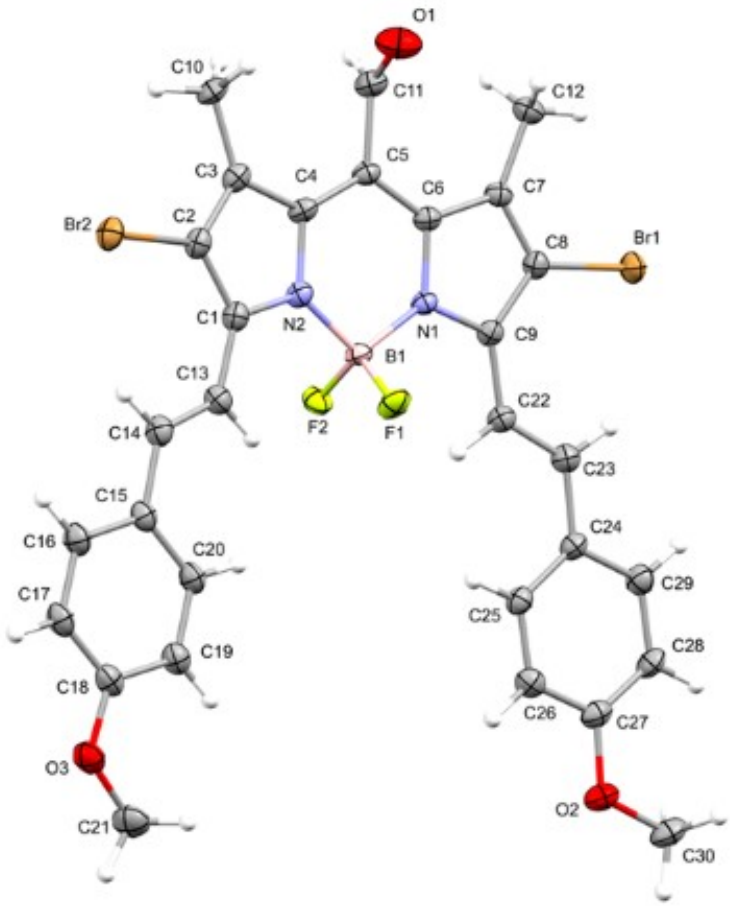

Figure S58. The molecular structure of the title compound. Displacement ellipsoids are drawn at the 30% probability level.

Table S1. Crystal data and structure refinement for **11**.

CCDC number	2454511
Empirical formula	$C_{30}H_{25}BBr_2F_2N_2O_3$
Formula weight	670.15
Temperature/K	160.0(1)
Crystal system	monoclinic
Space group	P21/c
a/Å	7.88303(17)
b/Å	9.5602(3)
c/Å	36.0425(8)
α/°	90
β/°	93.3839(19)
γ/°	90
Volume/Å3	2711.55(11)
Z	4
ρcalcg/cm3	1.642
μ/mm-1	4.220
F(000)	1344.0
Crystal size/mm3	0.31 × 0.1 × 0.02
Radiation	Cu Kα (λ = 1.54184)
2Θ range for data collection/°	4.912 to 154.76
Index ranges	-9 ≤ h ≤ 7, -11 ≤ k ≤ 12, -45 ≤ l ≤ 43
Reflections collected	36993
Independent reflections	5738 [Rint = 0.0548, Rsigma = 0.0312]
Data/restraints/parameters	5738/0/365
Goodness-of-fit on F2	1.194
Final R indexes [I>=2σ (I)]	R1 = 0.0572, wR2 = 0.1396
Final R indexes [all data]	R1 = 0.0669, wR2 = 0.1441
Largest diff. peak/hole / e Å-3	0.76/-1.08

Table S2. Fractional Atomic Coordinates (×104) and Equivalent Isotropic Displacement Parameters (Å2×103) for **11**. Ueq is defined as 1/3 of the trace of the orthogonalised UIJ tensor.

Atom	***x***	***y***	***z***	**U(eq)**
Br1	9625.7(8)	7784.0(7)	4993.2(2)	42.54(17)
Br2	12903.1(8)	274.9(6)	7011.7(2)	41.40(17)

F1	8033(4)	3947(3)	6191.0(9)	44.2(8)
F2	9502(4)	5578(3)	6533.6(8)	41.0(7)
O1	14485(7)	2643(6)	5479.6(16)	70.5(14)
O2	295(5)	9365(4)	6134.9(12)	46.3(10)
O3	3602(5)	1913(5)	8103.1(11)	48.8(10)
N1	10163(5)	5253(4)	5895.8(11)	28.3(8)
N2	10958(5)	3471(4)	6378.7(12)	31.0(9)
C1	10864(7)	2583(5)	6674.8(14)	32.9(11)
C2	12362(7)	1752(5)	6683.2(15)	35.2(11)
C3	13376(6)	2149(5)	6405.5(15)	33.0(11)
C4	12453(6)	3222(5)	6203.2(14)	29.5(10)
C5	12778(6)	3935(5)	5878.1(14)	30.6(10)
C6	11631(6)	4928(5)	5722.0(14)	29.4(10)
C7	11667(6)	5725(5)	5387.9(14)	31.3(10)
C8	10211(6)	6516(5)	5375.2(14)	31.3(10)
C9	9251(6)	6219(5)	5689.6(14)	30.2(10)
C10	15077(7)	1554(6)	6335.5(17)	40.1(12)
C11	14342(7)	3616(6)	5686.1(16)	40.2(12)
C12	12975(7)	5713(6)	5105.3(15)	39.9(12)
C13	9451(7)	2632(6)	6905.1(14)	36.1(11)
C14	9156(7)	1812(6)	7197.2(15)	38.9(12)
C15	7689(7)	1885(6)	7422.1(15)	37.6(12)
C16	7603(8)	995(6)	7731.4(15)	42.4(13)
C17	6233(8)	1023(6)	7951.8(16)	43.2(13)
C18	4897(7)	1944(6)	7873.1(15)	39.8(12)
C19	4954(7)	2836(6)	7566.6(15)	40.1(12)
C20	6334(7)	2794(6)	7347.3(15)	39.0(12)
C21	2327(8)	2973(7)	8062(2)	55.3(17)
C22	7675(6)	6750(5)	5810.9(15)	33.4(11)
C23	6559(7)	7598(6)	5627.4(15)	35.5(11)
C24	4950(6)	8066(5)	5764.7(15)	33.6(11)
C25	4271(7)	7544(5)	6086.6(15)	34.6(11)
C26	2730(7)	7994(6)	6200.9(16)	38.5(12)
C27	1812(6)	8999(6)	5996.1(16)	37.7(12)

C28	2441(7)	9542(6)	5679.9(17)	40.9(13)
C29	3987(7)	9069(6)	5563.0(16)	40.9(12)
C30	-709(7)	10390(7)	5935(2)	49.8(15)
B1	9599(7)	4576(6)	6257.1(16)	30.3(11)

Table S3. Anisotropic Displacement Parameters (Å2×103) for **11**. The Anisotropic displacement factor exponent takes the form: -2π2[h2a*2U11+2hka*b*U12+…].

Atom	**U11**	**U22**	**U33**	**U23**	**U13**	**U12**
Br1	47.0(3)	43.3(3)	37.3(3)	9.8(2)	2.4(2)	3.1(3)
Br2	48.9(3)	30.0(3)	44.4(3)	4.5(2)	-4.8(2)	4.3(3)
F1	26.5(15)	45.5(19)	60(2)	14.7(16)	0.4(13)	-7.2(14)
F2	52.4(18)	35.4(17)	35.9(16)	-1.6(13)	9.3(13)	11.3(14)
O1	67(3)	59(3)	88(4)	-12(3)	27(3)	1(3)
O2	34(2)	45(2)	60(3)	-5(2)	4.9(17)	4.4(18)
O3	51(2)	52(3)	44(2)	8.0(19)	10.4(18)	-9(2)
N1	28(2)	24.7(19)	33(2)	-1.6(16)	2.0(16)	1.7(17)
N2	32(2)	25(2)	36(2)	1.0(17)	1.9(17)	1.0(17)
C1	37(3)	26(2)	35(3)	1(2)	-2(2)	-2(2)
C2	38(3)	29(2)	38(3)	2(2)	-5(2)	-2(2)
C3	31(2)	25(2)	42(3)	-3(2)	-4(2)	-2(2)
C4	24(2)	22(2)	43(3)	-1(2)	1.9(19)	-1.5(19)
C5	28(2)	26(2)	38(3)	-4(2)	2.6(19)	1(2)
C6	27(2)	26(2)	35(3)	-3.4(19)	3.5(19)	-2.7(19)
C7	32(3)	28(2)	34(3)	-4(2)	4.7(19)	-1(2)
C8	33(3)	28(2)	33(2)	3(2)	0.0(19)	-4(2)
C9	29(2)	28(2)	33(2)	2(2)	0.6(19)	-3(2)
C10	31(3)	34(3)	54(3)	2(2)	-1(2)	8(2)
C11	33(3)	38(3)	51(3)	0(3)	6(2)	3(2)
C12	41(3)	41(3)	39(3)	0(2)	10(2)	-1(2)
C13	41(3)	33(3)	35(3)	0(2)	4(2)	-1(2)
C14	46(3)	31(3)	39(3)	2(2)	1(2)	1(2)
C15	46(3)	34(3)	33(3)	-2(2)	2(2)	-4(2)
C16	49(3)	40(3)	38(3)	5(2)	2(2)	-5(3)
C17	56(4)	39(3)	35(3)	6(2)	5(2)	-8(3)
C18	47(3)	40(3)	32(3)	-3(2)	4(2)	-15(3)
C19	45(3)	39(3)	36(3)	1(2)	1(2)	-8(2)

C20	47(3)	38(3)	32(3)	3(2)	3(2)	-6(3)
C21	51(4)	56(4)	61(4)	9(3)	17(3)	-9(3)
C22	33(3)	29(2)	38(3)	0(2)	2(2)	0(2)
C23	37(3)	32(3)	38(3)	-1(2)	2(2)	-2(2)
C24	30(2)	30(3)	40(3)	-1(2)	-1(2)	1(2)
C25	36(3)	30(3)	38(3)	0(2)	-1(2)	2(2)
C26	40(3)	35(3)	41(3)	-1(2)	4(2)	-6(2)
C27	30(3)	34(3)	49(3)	-10(2)	-1(2)	-2(2)
C28	36(3)	35(3)	51(3)	5(2)	-5(2)	8(2)
C29	42(3)	38(3)	43(3)	5(2)	2(2)	0(3)
C30	35(3)	42(3)	72(4)	-6(3)	1(3)	8(3)
B1	24(3)	29(3)	38(3)	4(2)	5(2)	5(2)

Table S4. Bond Lengths for **11**.

Atom	**Atom**	**Length/Å**	**Atom**	**Atom**	**Length/Å**
Br1	C8	1.872(5)	C5	C11	1.481(7)
Br2	C2	1.876(5)	C6	C7	1.427(7)
F1	B1	1.381(6)	C7	C8	1.373(7)
F2	B1	1.387(7)	C7	C12	1.491(7)
O1	C11	1.201(7)	C8	C9	1.428(7)
O2	C27	1.369(6)	C9	C22	1.434(7)
O2	C30	1.427(7)	C13	C14	1.344(7)
O3	C18	1.353(7)	C14	C15	1.453(8)
O3	C21	1.429(8)	C15	C16	1.407(8)
N1	C6	1.383(6)	C15	C20	1.390(8)
N1	C9	1.364(6)	C16	C17	1.378(8)
N1	B1	1.543(7)	C17	C18	1.389(8)
N2	C1	1.369(6)	C18	C19	1.399(8)
N2	C4	1.390(6)	C19	C20	1.383(8)
N2	B1	1.549(7)	C22	C23	1.342(7)
C1	C2	1.422(7)	C23	C24	1.458(7)
C1	C13	1.429(7)	C24	C25	1.398(7)
C2	C3	1.371(7)	C24	C29	1.400(7)
C3	C4	1.432(7)	C25	C26	1.374(7)
C3	C10	1.491(7)	C26	C27	1.389(8)

C4	C5	1.393(7)	C27	C28	1.371(8)
C5	C6	1.406(7)	C28	C29	1.389(8)

Table S5. Bond Angles for **11**.

Atom	Atom	Atom	Angle/°	Atom	Atom	Atom	Angle/°
C27	O2	C30	117.5(5)	N1	C9	C22	120.8(4)
C18	O3	C21	118.2(5)	C8	C9	C22	132.9(5)
C6	N1	B1	125.4(4)	O1	C11	C5	124.1(6)
C9	N1	C6	109.5(4)	C14	C13	C1	127.8(5)
C9	N1	B1	125.1(4)	C13	C14	C15	126.1(5)
C1	N2	C4	109.6(4)	C16	C15	C14	119.3(5)
C1	N2	B1	125.1(4)	C20	C15	C14	123.3(5)
C4	N2	B1	125.4(4)	C20	C15	C16	117.3(5)
N2	C1	C2	106.3(4)	C17	C16	C15	121.4(6)
N2	C1	C13	120.8(5)	C16	C17	C18	120.3(5)
C2	C1	C13	132.9(5)	O3	C18	C17	116.9(5)
C1	C2	Br2	126.3(4)	O3	C18	C19	123.9(6)
C3	C2	Br2	123.3(4)	C17	C18	C19	119.2(5)
C3	C2	C1	110.4(5)	C20	C19	C18	119.8(6)
C2	C3	C4	105.6(4)	C19	C20	C15	121.9(5)
C2	C3	C10	125.9(5)	C23	C22	C9	128.2(5)
C4	C3	C10	128.5(5)	C22	C23	C24	125.2(5)
N2	C4	C3	108.1(4)	C25	C24	C23	123.8(5)
N2	C4	C5	120.1(4)	C25	C24	C29	116.9(5)
C5	C4	C3	131.7(5)	C29	C24	C23	119.3(5)
C4	C5	C6	121.4(4)	C26	C25	C24	121.7(5)
C4	C5	C11	119.5(5)	C25	C26	C27	119.9(5)
C6	C5	C11	119.1(5)	O2	C27	C26	115.0(5)
N1	C6	C5	120.4(4)	O2	C27	C28	125.0(5)
N1	C6	C7	108.8(4)	C28	C27	C26	120.1(5)
C5	C6	C7	130.8(5)	C27	C28	C29	119.7(5)
C6	C7	C12	128.4(5)	C28	C29	C24	121.6(5)
C8	C7	C6	105.3(4)	F1	B1	F2	109.8(4)
C8	C7	C12	126.3(5)	F1	B1	N1	109.6(4)
C7	C8	Br1	123.4(4)	F1	B1	N2	110.4(4)

C7	C8	C9	110.2(4)	F2	B1	N1	110.3(4)
C9	C8	Br1	126.4(4)	F2	B1	N2	109.5(4)
N1	C9	C8	106.2(4)	N1	B1	N2	107.2(4)

Table S6. Hydrogen Bonds for **11**.

D	H	A	d(D-H)/Å	d(H-A)/Å	d(D-A)/Å	D-H-A/°
C21	H21C	F21	0.98	2.49	3.114(7)	121.6
C22	H22	F2	0.95	2.49	3.110(6)	123.2

11-X,-1/2+Y,3/2-Z

Table S7. Torsion Angles for **11**.

A	B	C	D	Angle/°	A	B	C	D	Angle/°
Br1	C8	C9	N1	-179.2(4)	C9	N1	C6	C5	-179.1(4)
Br1	C8	C9	C22	-0.8(8)	C9	N1	C6	C7	0.1(5)
Br2	C2	C3	C4	175.5(4)	C9	N1	B1	F1	56.1(6)
Br2	C2	C3	C10	-4.1(8)	C9	N1	B1	F2	-64.9(6)
O2	C27	C28	C29	-178.9(5)	C9	N1	B1	N2	176.0(4)
O3	C18	C19	C20	179.9(5)	C9	C22	C23	C24	178.2(5)
N1	C6	C7	C8	0.5(5)	C10	C3	C4	N2	-177.6(5)
N1	C6	C7	C12	-178.8(5)	C10	C3	C4	C5	5.3(9)
N1	C9	C22	C23	-173.5(5)	C11	C5	C6	N1	-179.7(5)
N2	C1	C2	Br2	-176.5(4)	C11	C5	C6	C7	1.4(8)
N2	C1	C2	C3	1.8(6)	C12	C7	C8	Br1	-1.4(8)
N2	C1	C13	C14	178.1(5)	C12	C7	C8	C9	178.4(5)
N2	C4	C5	C6	0.8(7)	C13	C1	C2	Br2	4.2(9)
N2	C4	C5	C11	-177.5(5)	C13	C1	C2	C3	-177.5(5)
C1	N2	C4	C3	-1.8(5)	C13	C14	C15	C16	-176.9(6)
C1	N2	C4	C5	175.6(5)	C13	C14	C15	C20	3.5(9)
C1	N2	B1	F1	-56.4(7)	C14	C15	C16	C17	-179.7(5)
C1	N2	B1	F2	64.6(6)	C14	C15	C20	C19	179.9(5)
C1	N2	B1	N1	-175.7(4)	C15	C16	C17	C18	-0.2(9)
C1	C2	C3	C4	-2.8(6)	C16	C15	C20	C19	0.3(8)
C1	C2	C3	C10	177.6(5)	C16	C17	C18	O3	-179.7(5)
C1	C13	C14	C15	-179.2(5)	C16	C17	C18	C19	0.3(9)
C2	C1	C13	C14	-2.7(10)	C17	C18	C19	C20	-0.1(8)
C2	C3	C4	N2	2.8(5)	C18	C19	C20	C15	-0.2(9)
C2	C3	C4	C5	-174.2(5)	C20	C15	C16	C17	-0.1(8)

C3	C4	C5	C6	177.5(5)	C21	O3	C18	C17	171.4(5)
C3	C4	C5	C11	-0.8(8)	C21	O3	C18	C19	-8.6(8)
C4	N2	C1	C2	0.1(6)	C22	C23	C24	C25	-8.3(9)
C4	N2	C1	C13	179.5(5)	C22	C23	C24	C29	173.2(5)
C4	N2	B1	F1	123.1(5)	C23	C24	C25	C26	-178.5(5)
C4	N2	B1	F2	-115.9(5)	C23	C24	C29	C28	179.5(5)
C4	N2	B1	N1	3.8(7)	C24	C25	C26	C27	-0.5(8)
C4	C5	C6	N1	2.0(7)	C25	C24	C29	C28	0.9(8)
C4	C5	C6	C7	-176.9(5)	C25	C26	C27	O2	179.8(5)
C4	C5	C11	O1	81.6(8)	C25	C26	C27	C28	0.0(8)
C5	C6	C7	C8	179.5(5)	C26	C27	C28	C29	0.9(8)
C5	C6	C7	C12	0.2(9)	C27	C28	C29	C24	-1.4(9)
C6	N1	C9	C8	-0.6(5)	C29	C24	C25	C26	0.0(8)
C6	N1	C9	C22	-179.3(4)	C30	O2	C27	C26	-179.7(5)
C6	N1	B1	F1	-120.8(5)	C30	O2	C27	C28	0.0(8)
C6	N1	B1	F2	118.2(5)	B1	N1	C6	C5	-1.8(7)
C6	N1	B1	N2	-0.9(7)	B1	N1	C6	C7	177.4(4)
C6	C5	C11	O1	-96.7(7)	B1	N1	C9	C8	-177.9(4)
C6	C7	C8	Br1	179.2(4)	B1	N1	C9	C22	3.4(7)
C6	C7	C8	C9	-0.9(6)	B1	N2	C1	C2	179.7(5)
C7	C8	C9	N1	0.9(6)	B1	N2	C1	C13	-0.9(8)
C7	C8	C9	C22	179.4(5)	B1	N2	C4	C3	178.6(4)
C8	C9	C22	C23	8.2(10)	B1	N2	C4	C5	-4.0(7)

Table S8. Hydrogen Atom Coordinates (Å×104) and Isotropic Displacement Parameters (Å2×103) for **11**.

Atom	***x***	***y***	***z***	**U(eq)**
H10A	14959.89	876.5	6131.53	60
H10B	15546.14	1085.84	6560.62	60
H10C	15841.91	2308.9	6268.24	60
H11	15290.85	4219.21	5728.86	48
H12A	13051.66	4771.68	4999.8	60
H12B	14079.22	5979.26	5223.34	60
H12C	12652.31	6379.34	4906.88	60
H13	8619.6	3327.15	6844.33	43
H14	9985.08	1120.26	7262.87	47

H16	8507.77	361.01	7789.37	51
H17	6203.06	409.42	8158.61	52
H19	4047.06	3469.47	7509.33	48
H20	6357.88	3403.11	7139.42	47
H21A	1690.49	2859.84	7821.77	83
H21B	2867.33	3896.74	8072.51	83
H21C	1547.75	2890.96	8262.76	83
H22	7383.71	6463.94	6051.43	40
H23	6839.09	7920.09	5389.25	43
H25	4891.03	6861.62	6230.11	42
H26	2294.01	7617.95	6419.86	46
H28	1821.08	10239.03	5541.49	49
H29	4401.88	9435.86	5340.69	49
H30A	-1042.51	10032.98	5686.57	75
H30B	-44.21	11248.92	5913.03	75
H30C	-1728.46	10590.82	6068.64	75

Crystal data

C30H25BBr2F2N2O3 (*M* = 670.15 g/mol): monoclinic, space group P21/c (no. 14), *a* = 7.88303(17) Å, *b* = 9.5602(3) Å, *c* = 36.0425(8) Å, *β* = 93.3839(19)°, *V* = 2711.55(11) Å3, *Z* = 4, *T* = 160.0(1) K, μ(Cu Kα) = 4.220 mm-1, *Dcalc* = 1.642 g/cm3, 36993 reflections measured (4.912° ≤ 2Θ ≤ 154.76°), 5738 unique (*R*int = 0.0548, Rsigma = 0.0312) which were used in all calculations. The final *R*1 was 0.0572 (I > 2σ(I)) and *wR*2 was 0.1441 (all data).

Photophysical properties and aggregates analysis

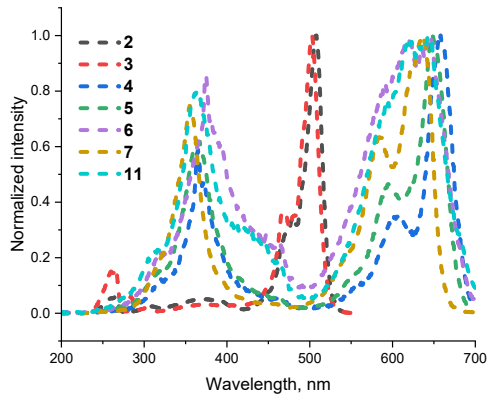

Figure S59. Normalized excitation spectra, λ_{ex} = 350 nm, acetonitrile, RT.

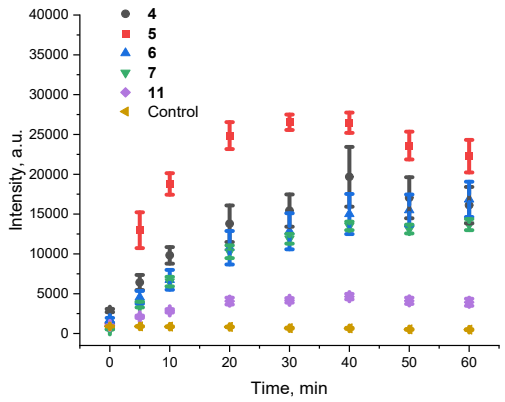

Figure S60. The study of the generation of superoxide anion in a DMSO/MeOH (v/v, 1/1) solution using 645 nm with Dihydrorhodamine 123 over time, 25°C.

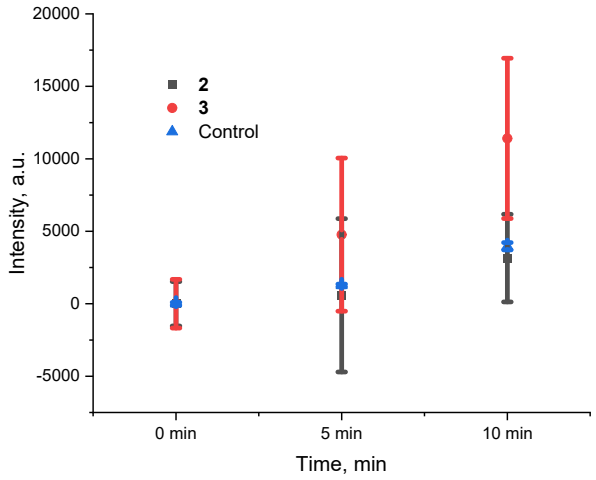

Figure S61. The study of the generation of superoxide anion in a DMSO/MeOH (v/v, 1/1) solution using 510 nm with Dihydrorhodamine 123 (control) over time, 25°C.

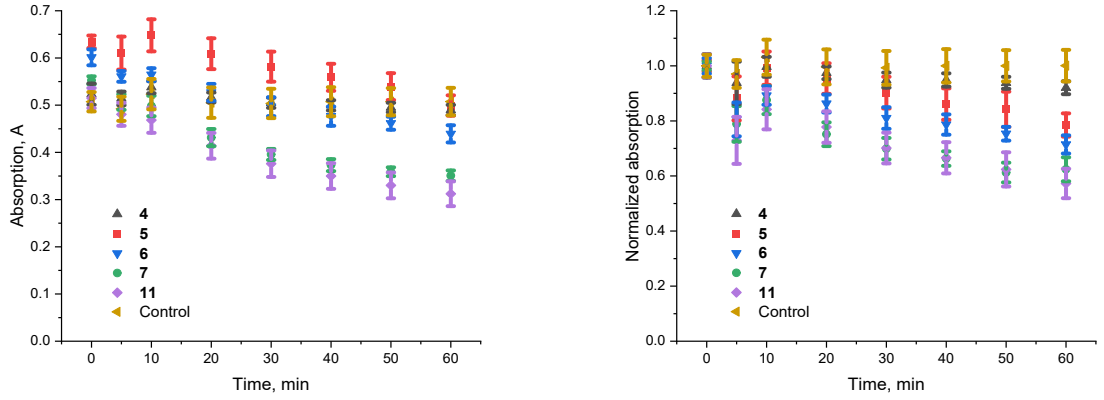

Figure S62. The study of the generation of singlet oxygen in a DMSO/MeOH (v/v, 1/1) solution using 645 nm with 9,10-Anthracenediyl-bis(methylene)dimalonic acid (ABDA, control) over time without correction (left) and with correction (right), 25°C.

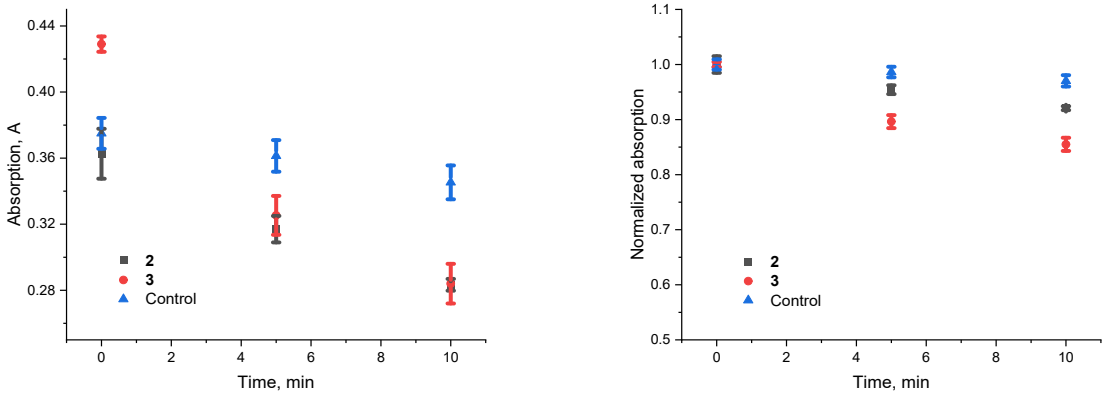

Figure S63. The study of the generation of singlet oxygen in a DMSO/MeOH (v/v, 1/1) solution using 510 nm with 9,10-Anthracenediyl-bis(methylene)dimalonic acid (ABDA, control) over time without correction (left) and normalized with correction (right), 25°C.

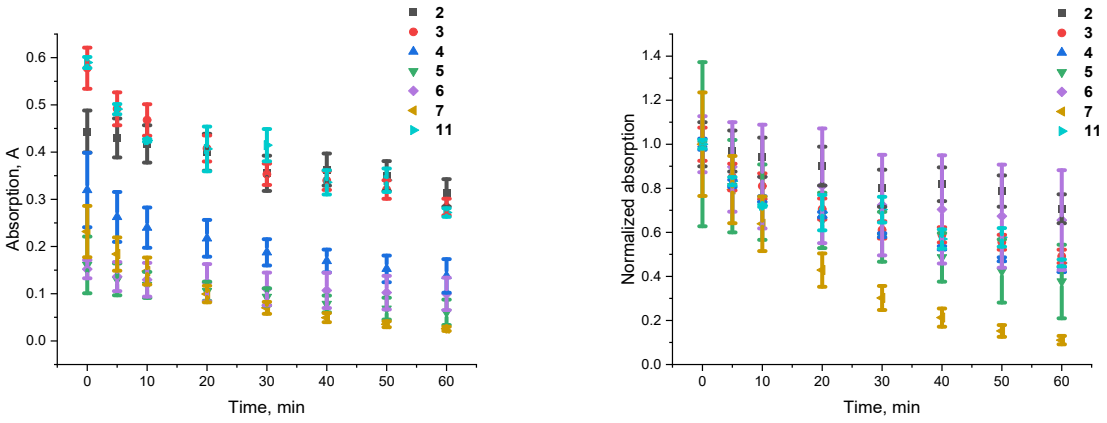

Figure S64. The changes of absorption maximum in DMSO/MeOH (v/v, 1/1) upon irradiation (510 nm for **2**, **3**, 645 nm for other BODIPYs, left) with normalized absorption (right), 25°C.

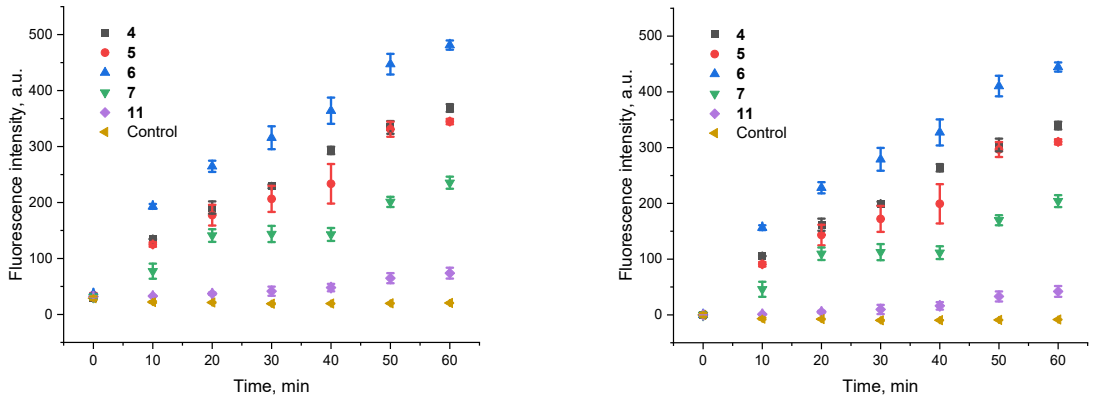

Figure S65. The study of the generation of superoxide anion in PBS solution using 645 nm with Dihydrorhodamine 123 over time without (left) and with (right) normalization to 0 at t = 0 min, 25°C.

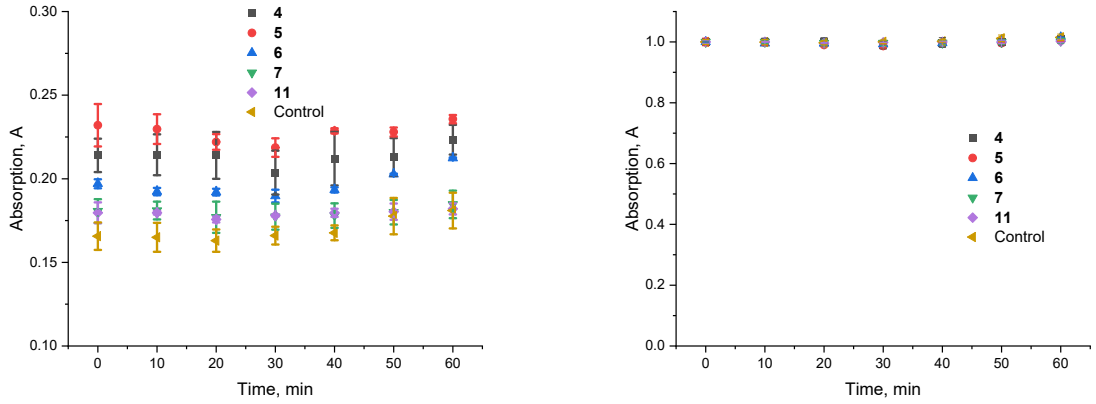

Figure S66. The changes of absorption maximum in PBS upon irradiation (645 nm) without (left) and with normalized absorption (right), 25°C.

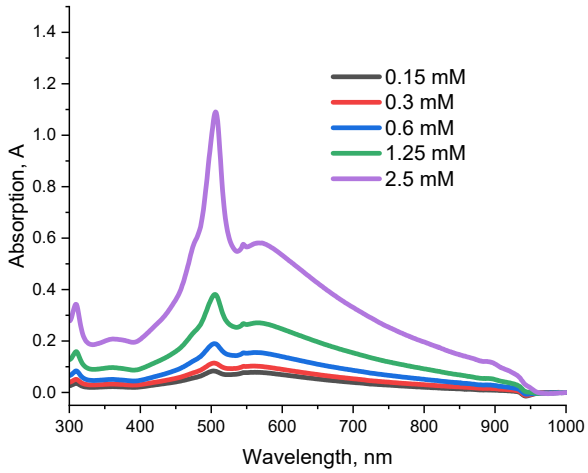

Figure S67. The changes of absorption spectra in PBS varying concentrations of **3**, RT.

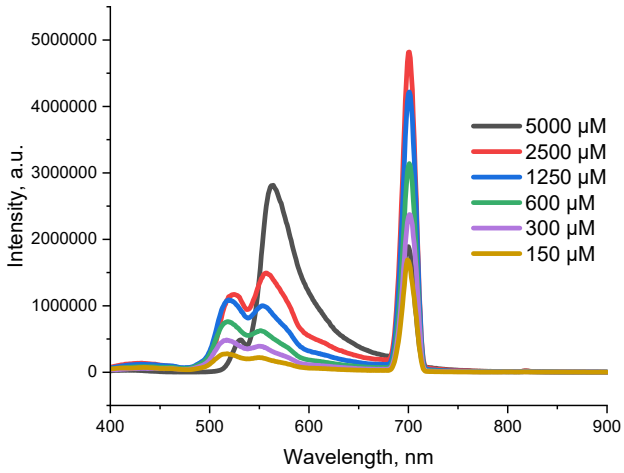

Figure S68. The emission spectra change in PBS of **3** in varying concentrations (λ_{ex} = 350 nm). At 700 nm, we observe the Raman peak.

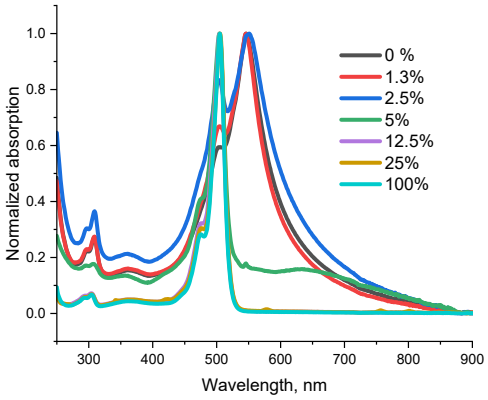

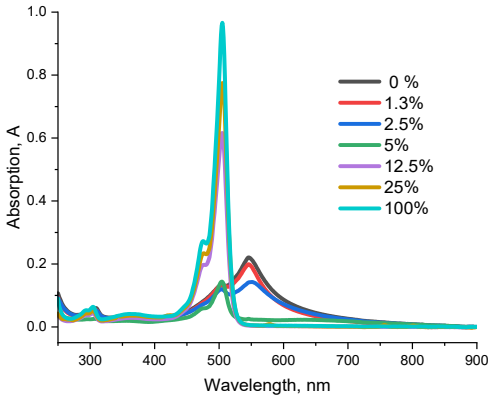

Figure S69. The changes of absorption spectra in MeCN/H_2O mixture of **3** with an indication of the volume fraction of MeCN in H_2O. The concentration of **3** is 25 μM with (left) and without normalization (right).

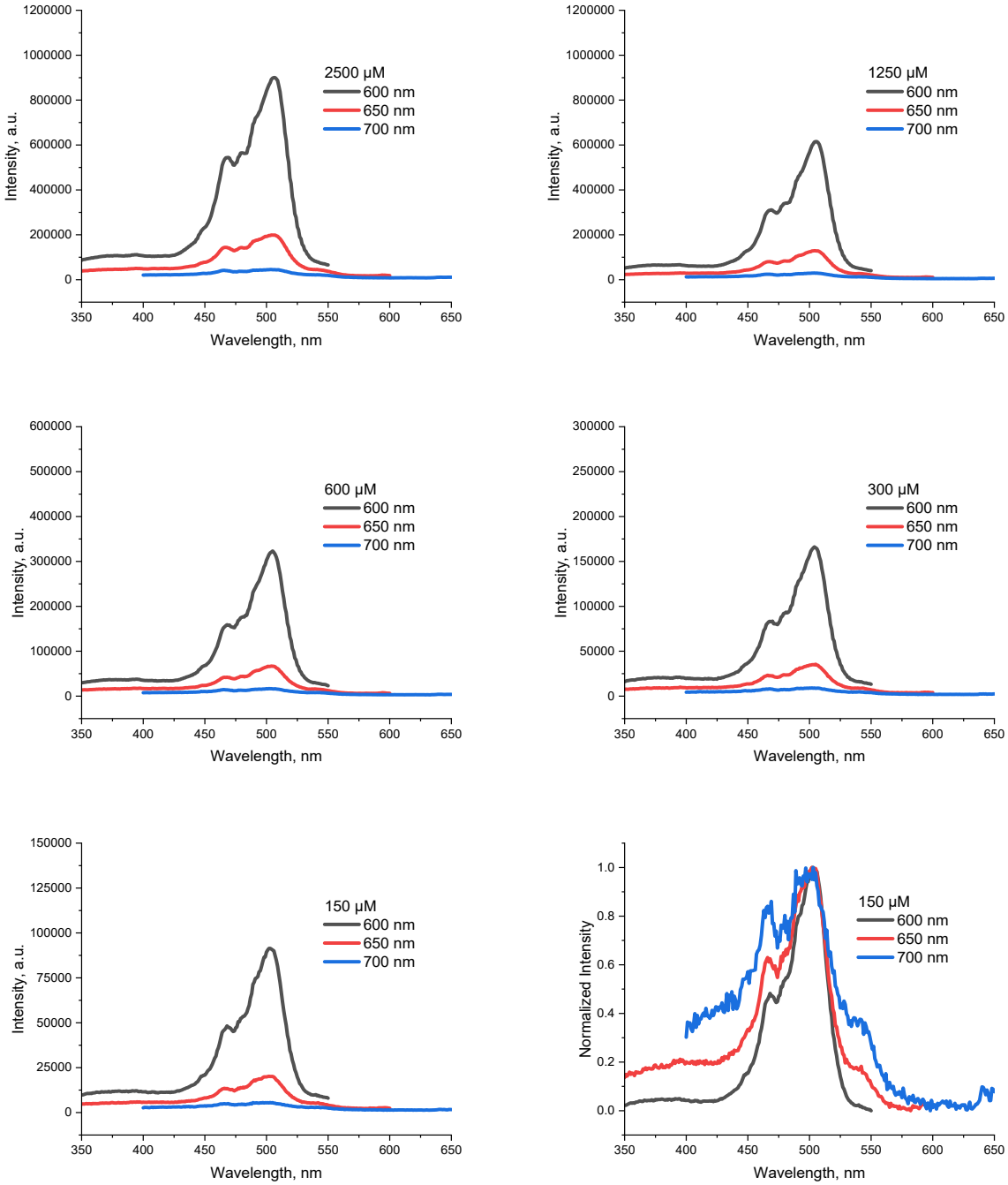

Figure S70. The excitation spectra in PBS of **3,** depending on the emission wavelength at varying concentrations, RT.

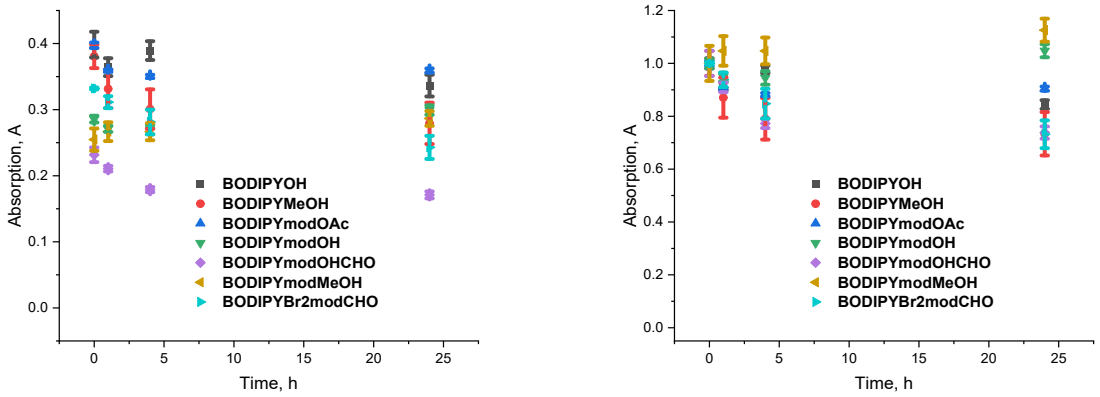

Figure S71. The changes of absorption spectra maxima in DMSO/MeOH (v/v, 1/1) without irradiation (left) and normalized maxima changes (right), 37°C.

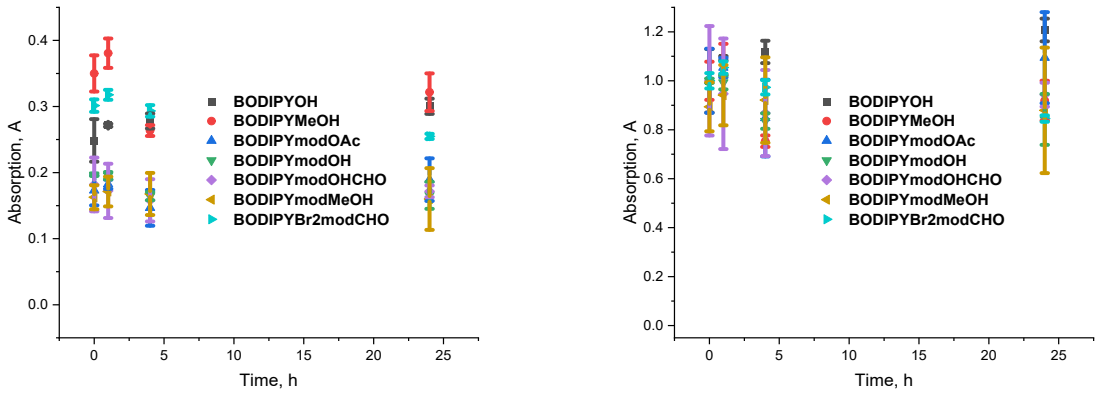

Figure S72. The changes of absorption spectra maxima in PBS without irradiation, 37°C.

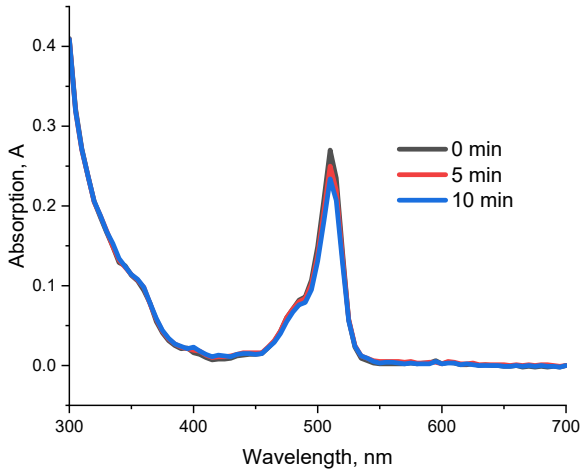

Figure S73. The absorption spectra changes of **2** upon irradiation (510 nm) with indicated time in DMSO/MeOH (v/v, 1/1), 25°C.

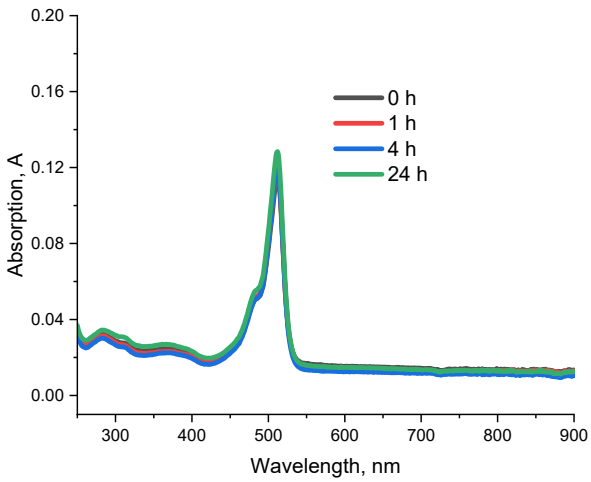

Figure S74. The absorption spectra changes of **2** in PBS without irradiation, the sample was mixed before measurements, 37°C.

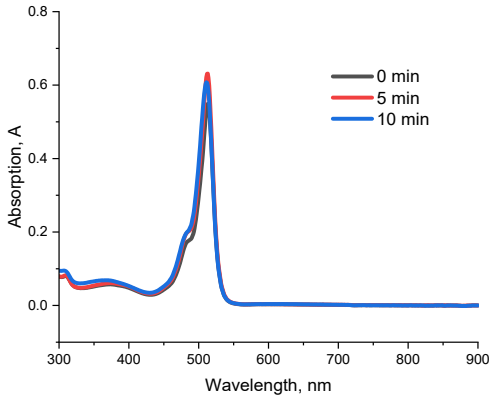

Figure S75. The absorption spectra changes of **3** upon irradiation (510 nm) with indicated time in DMSO/MeOH (v/v, 1/1), 25°C.

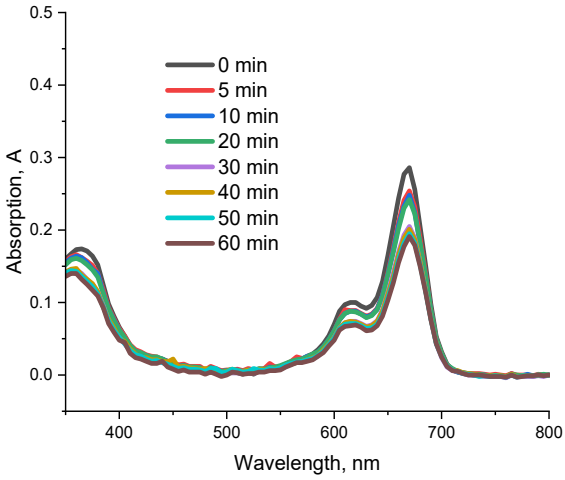

Figure S76. The absorption spectra changes of **4** upon irradiation (645 nm) with indicated time in DMSO/MeOH (v/v, 1/1), 25°C.

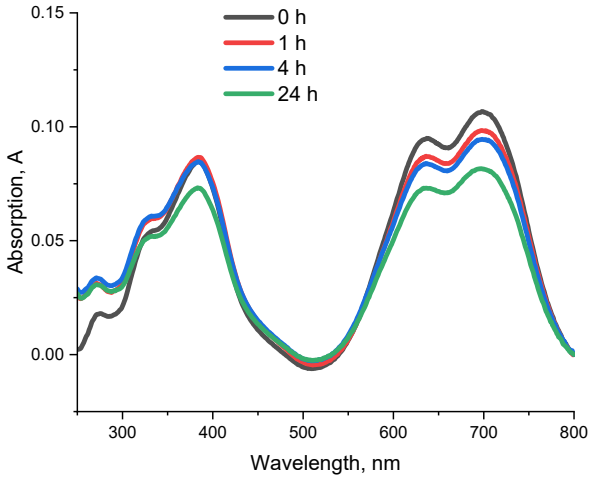

Figure S77. The absorption spectra changes of **4** in PBS without irradiation, 37°C.

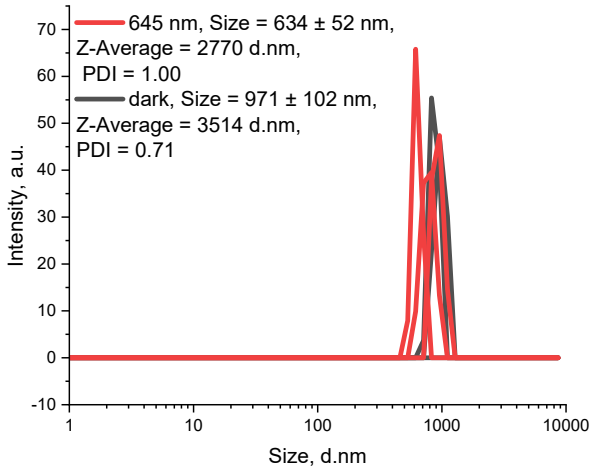

Figure S78. The nanoparticle size changes of **4** in PBS after irradiation at 37°C at 510 nm (light) and without irradiation (dark).

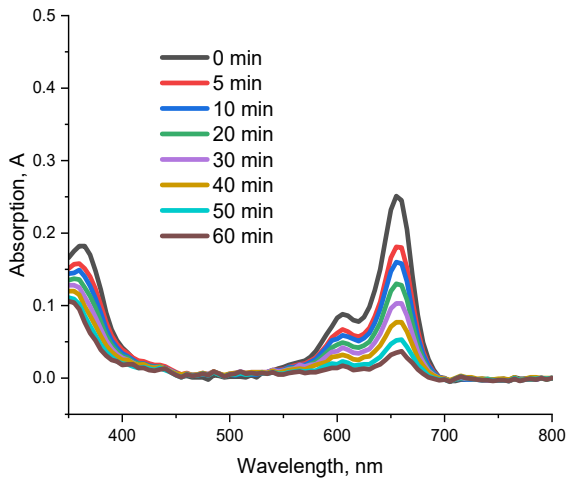

Figure S79. The absorption spectra changes of **5** upon irradiation (645 nm) with indicated time in DMSO/MeOH (v/v, 1/1), 25°C.

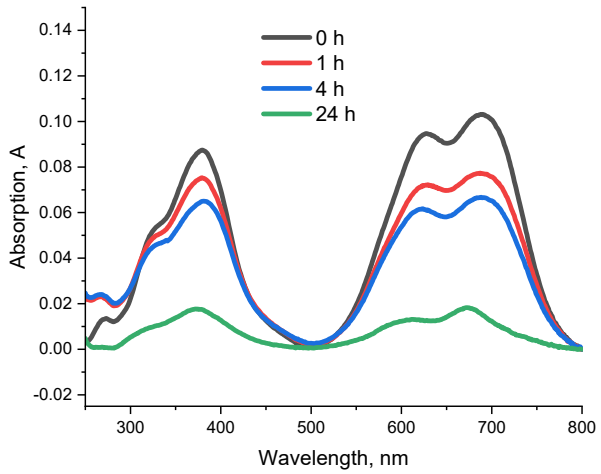

Figure S80. The absorption spectra changes of **5** in PBS without irradiation, 37°C.

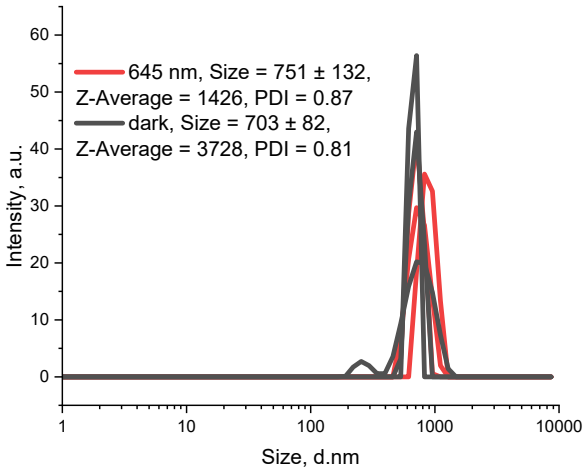

Figure S81. The nanoparticle size changes of **5** in PBS after irradiation at 37°C at 645 nm (light) and without irradiation (dark).

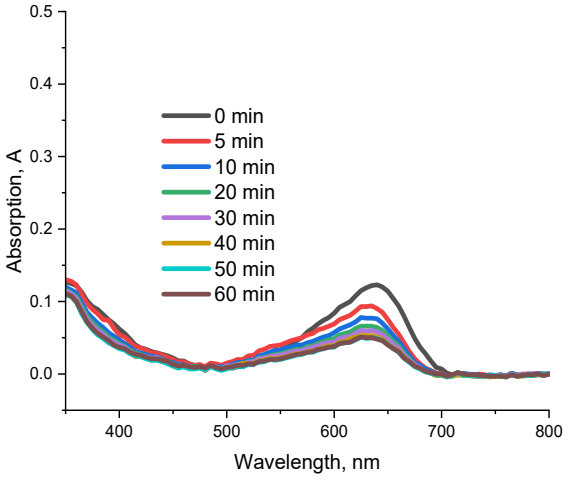

Figure S82. The absorption spectra changes of **6** upon irradiation (645 nm) with indicated time in DMSO/MeOH (v/v, 1/1), 25°C.

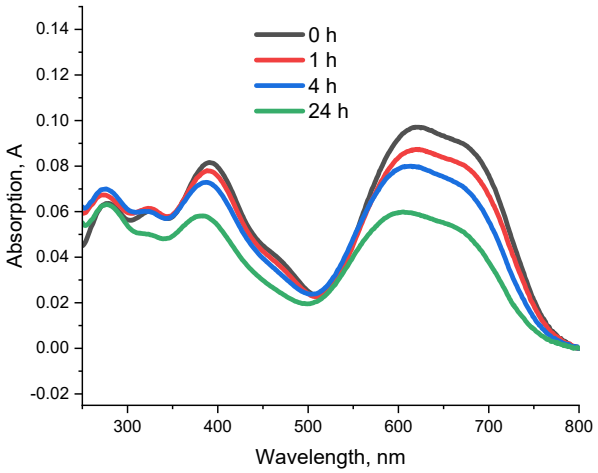

Figure S83. The absorption spectra changes of **6** in PBS without irradiation, 37°C.

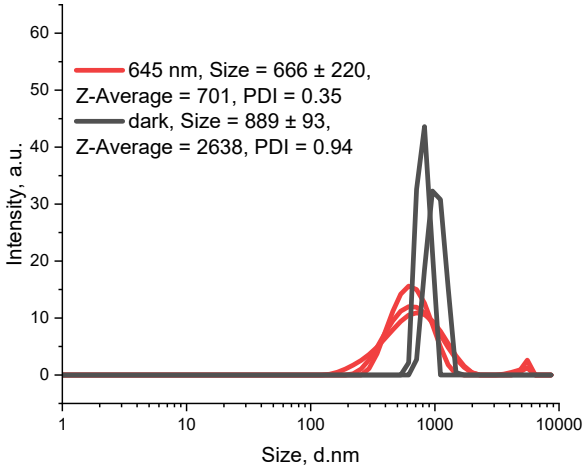

Figure S84. The nanoparticle size changes of **6** in PBS after irradiation at 37°C at 645 nm (light) and without irradiation (dark).

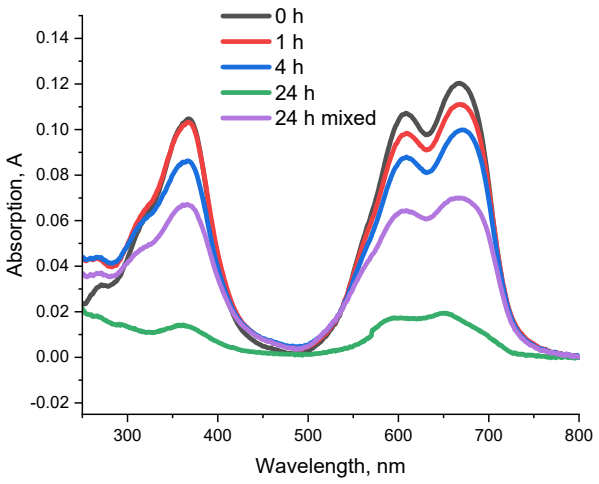

Figure S85. The absorption spectra changes of **7** in PBS without irradiation, 37°C.

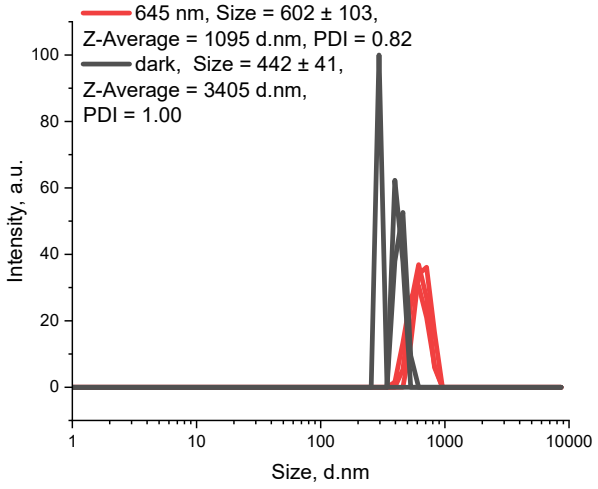

Figure S86. The nanoparticle size changes of **7** in PBS after irradiation at 37°C at 645 nm (light) and without irradiation (dark).

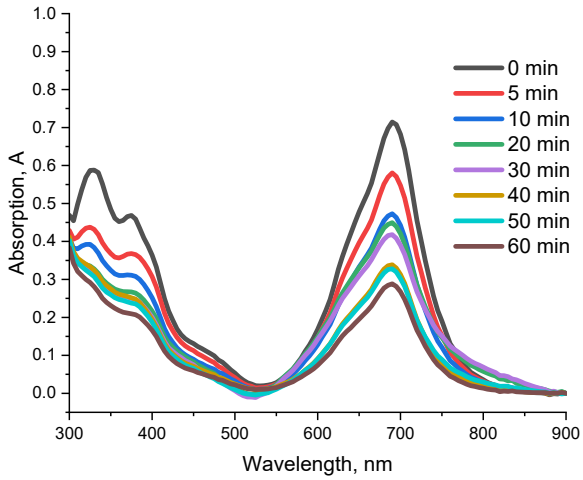

Figure S87. The absorption spectra changes of **11** upon irradiation (645 nm) with indicated time in DMSO/MeOH (v/v, 1/1), 25°C.

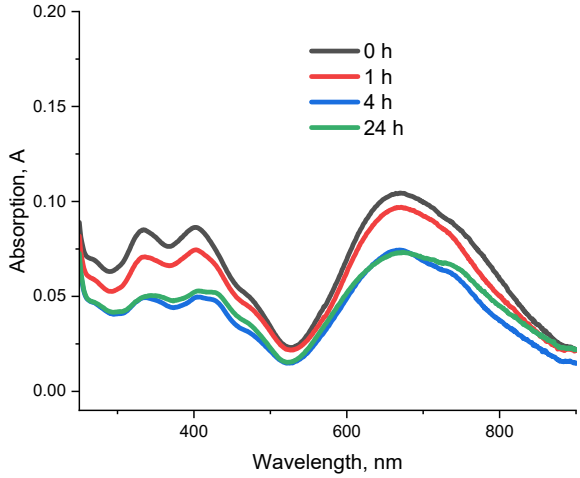

Figure S88. The absorption spectra changes of **11** in PBS without irradiation, 37°C.

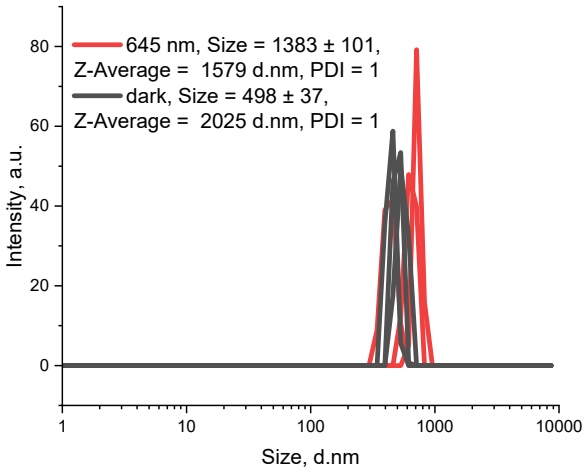

Figure S89. The nanoparticle size changes of **11** in PBS after irradiation at 37°C at 645 nm and without irradiation (dark).

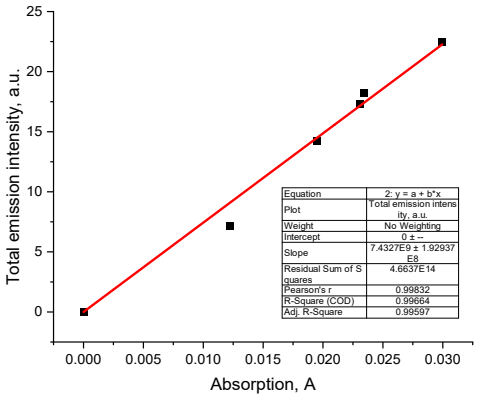

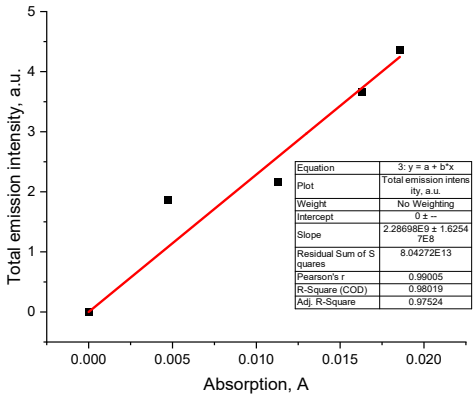

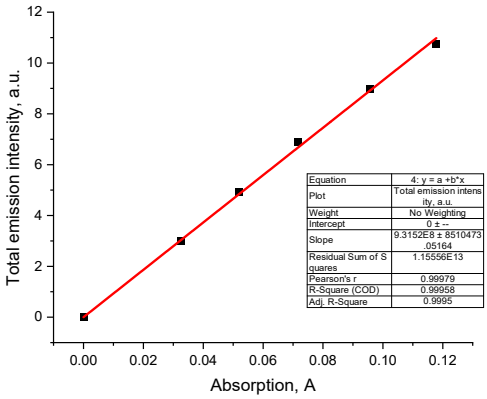

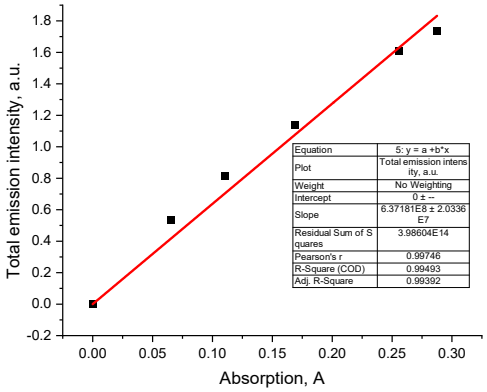

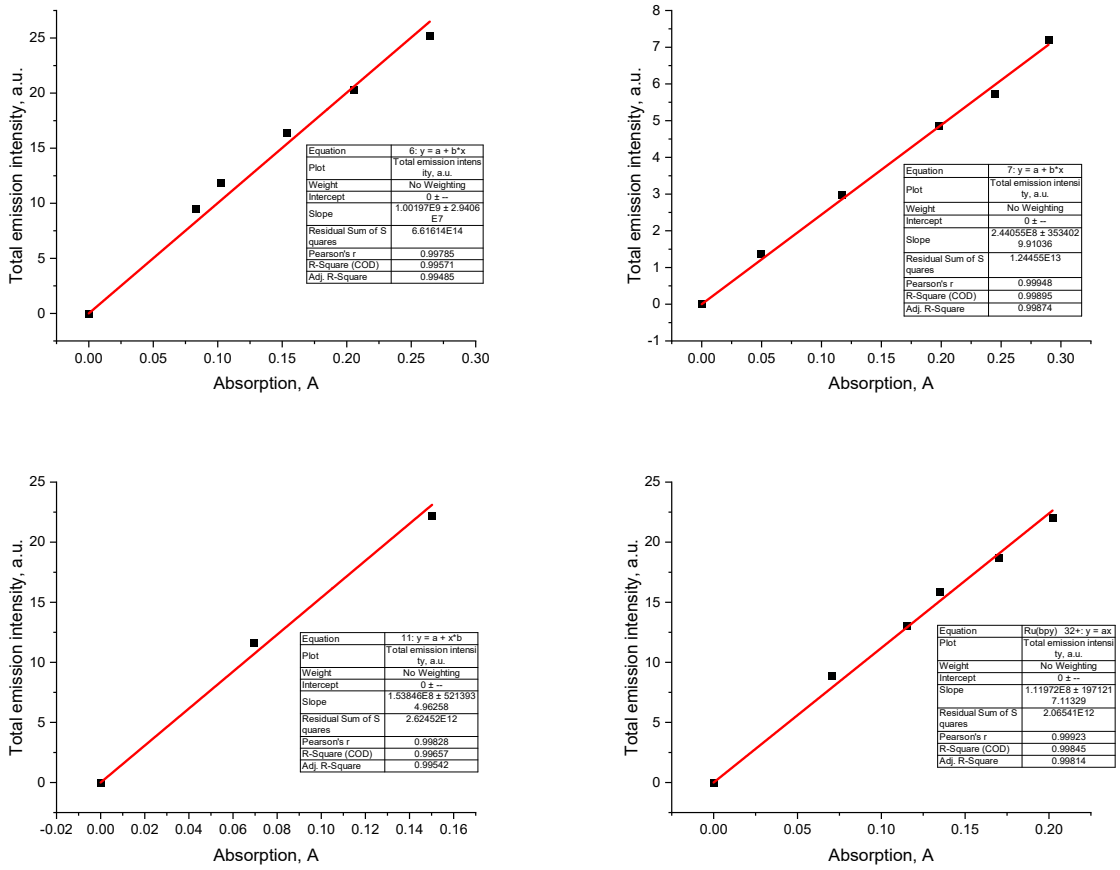

Figure S90. Absorbance and emission dependency curves for target compounds and the control ($[Ru(bpy)_3]Cl_2 \cdot 6H_2O$) for calculation of quantum yields.

(Photo-)toxicity evaluation

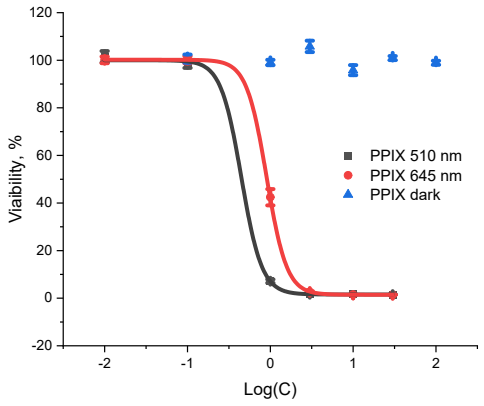

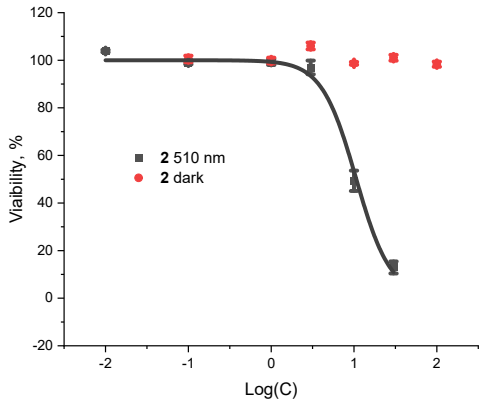

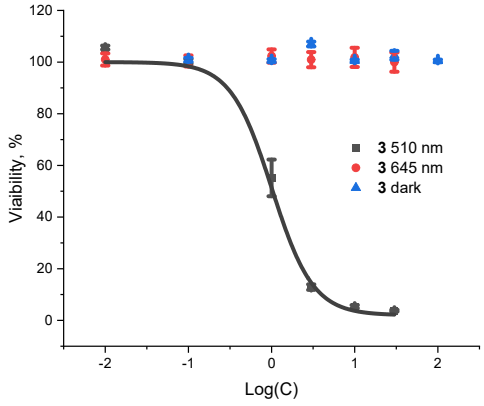

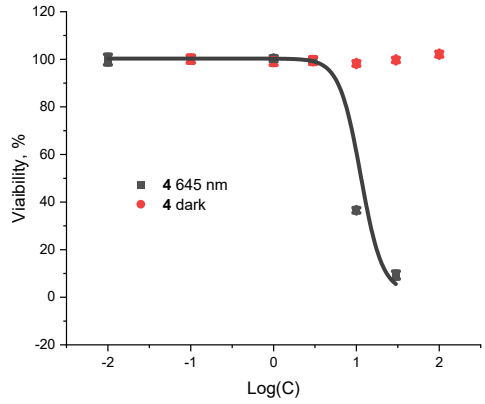

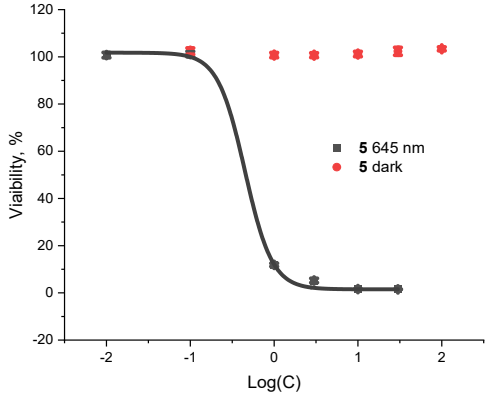

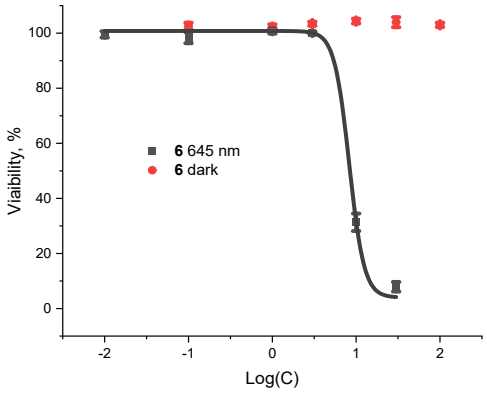

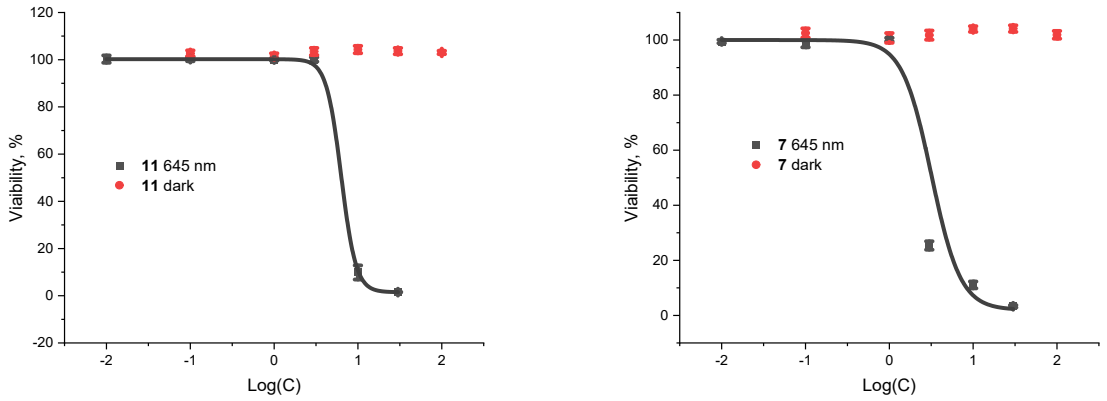

Figure S91. The dependencies between A549 cell viability in percentages and the indicated compounds' concentrations in the dark (without irradiation) and irradiated with 510 nm/645 nm were obtained following resazurin assay, 48 h.

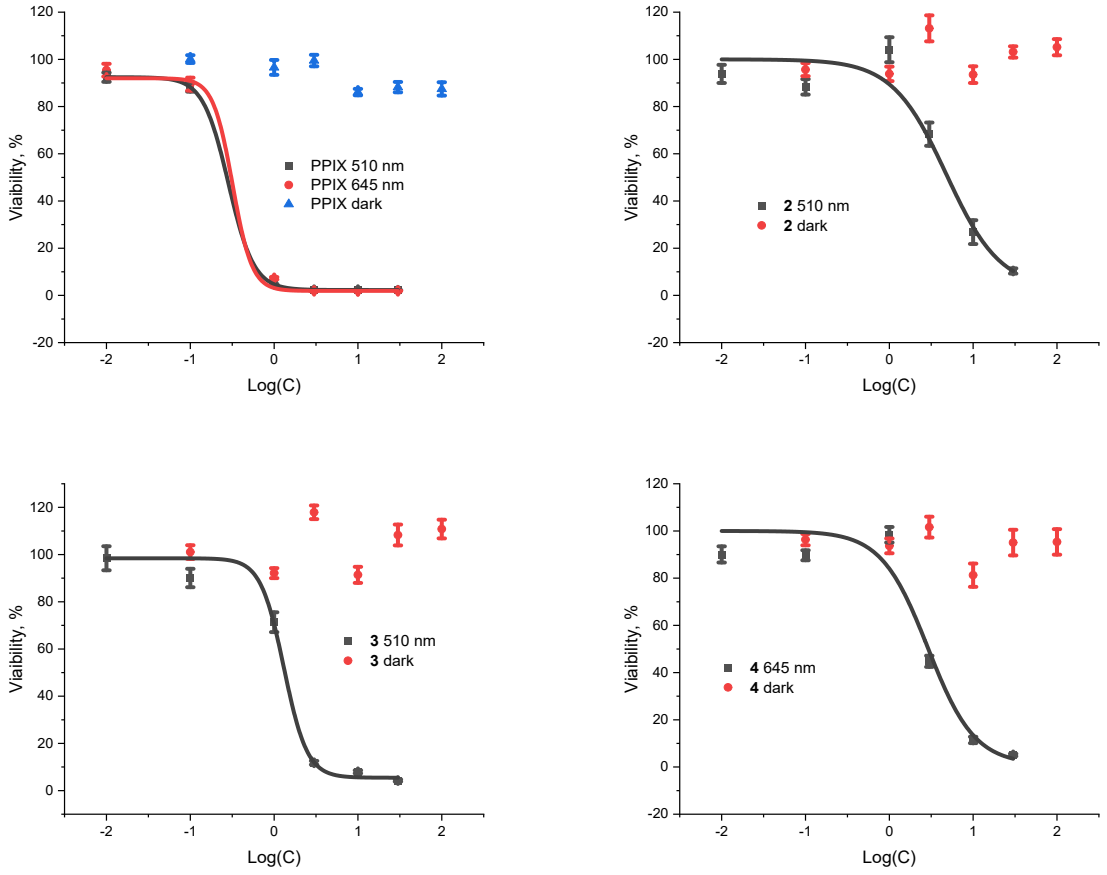

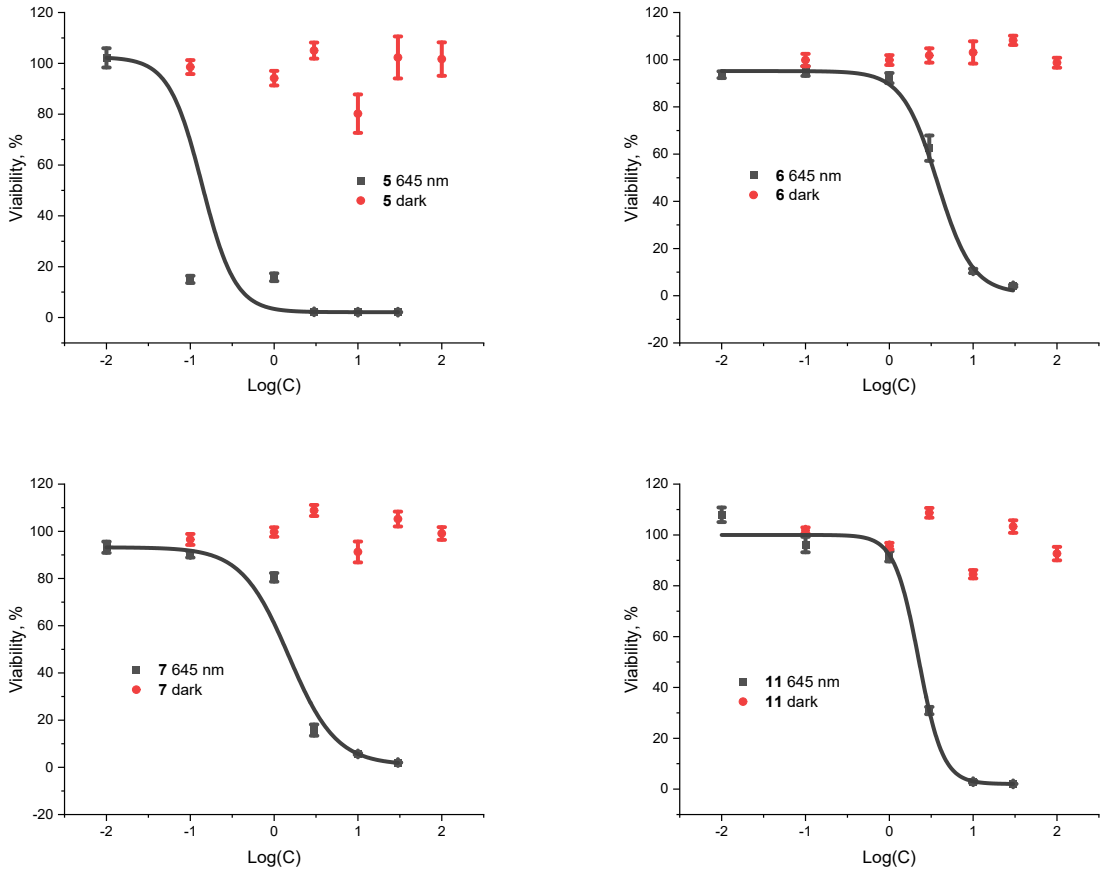

Figure S92. The dependencies between RPE-1 cell viability in percentages and the indicated compounds' concentrations in the dark (without irradiation) and irradiated with 510 nm/645 nm were obtained following resazurin assay, 48 h.

Confocal microscopy

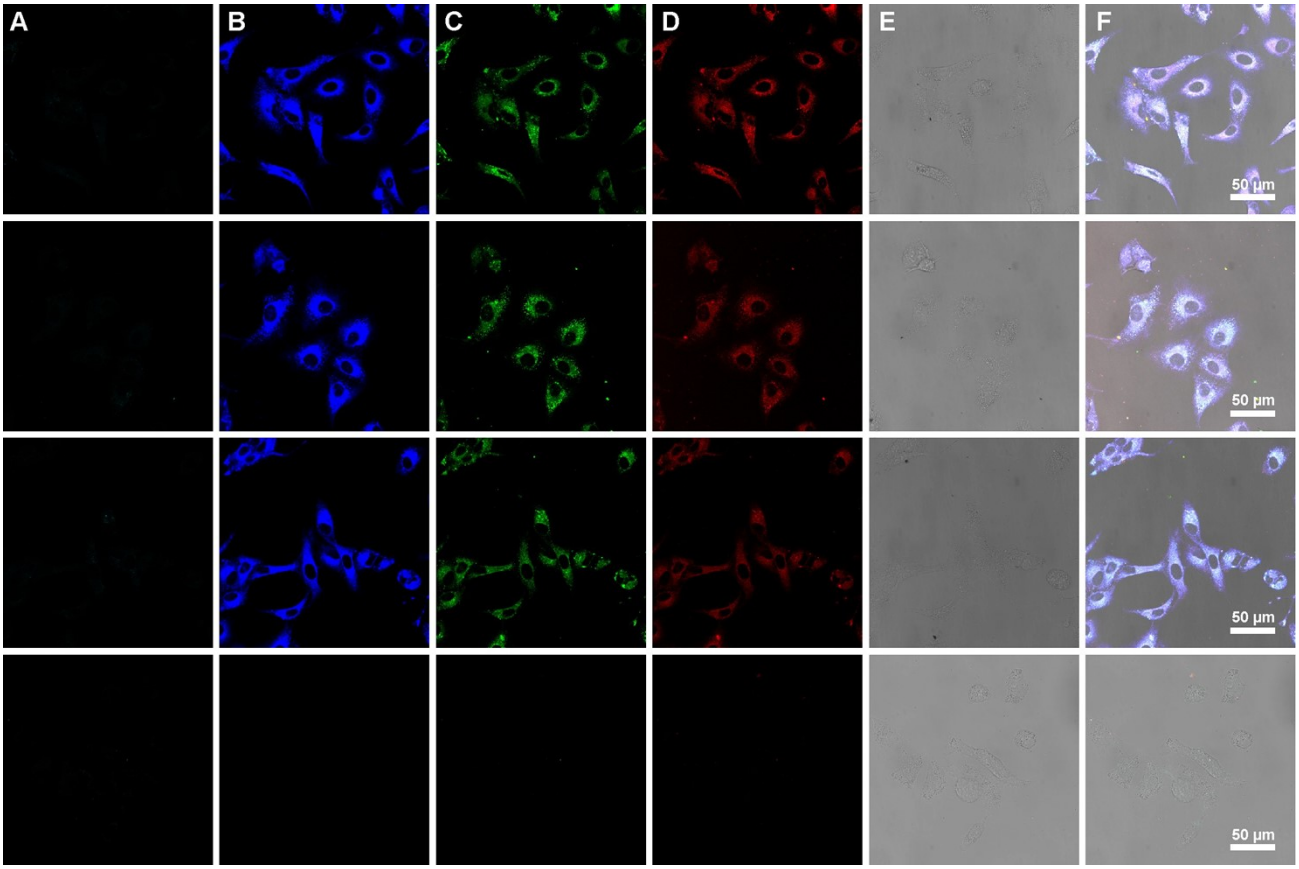

Figure S93. Live cell confocal microscopy image of A549 cells incubated for 4 hours with **3** (top three row) and without dye (bottom row, control), scale bar 50 µm (A) 405 nm, (B) 488 nm, (C) 552 nm, (D) 638 nm, (E) DIC, (F) Merged.

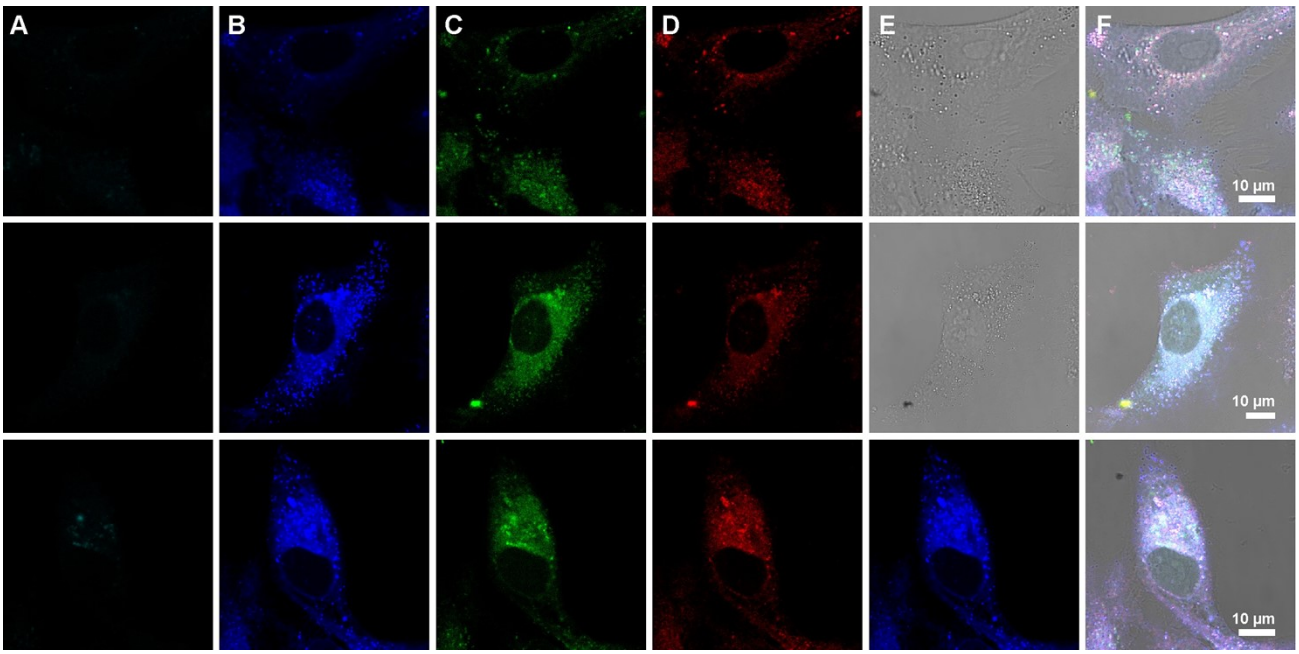

Figure S94. Live cell confocal microscopy image of A549 cells incubated for 4 hours with **3**, scale bar 10 μm (A) 405 nm, (B) 488 nm, (C) 552 nm, (D) 638 nm, (E) DIC, (F) Merged.

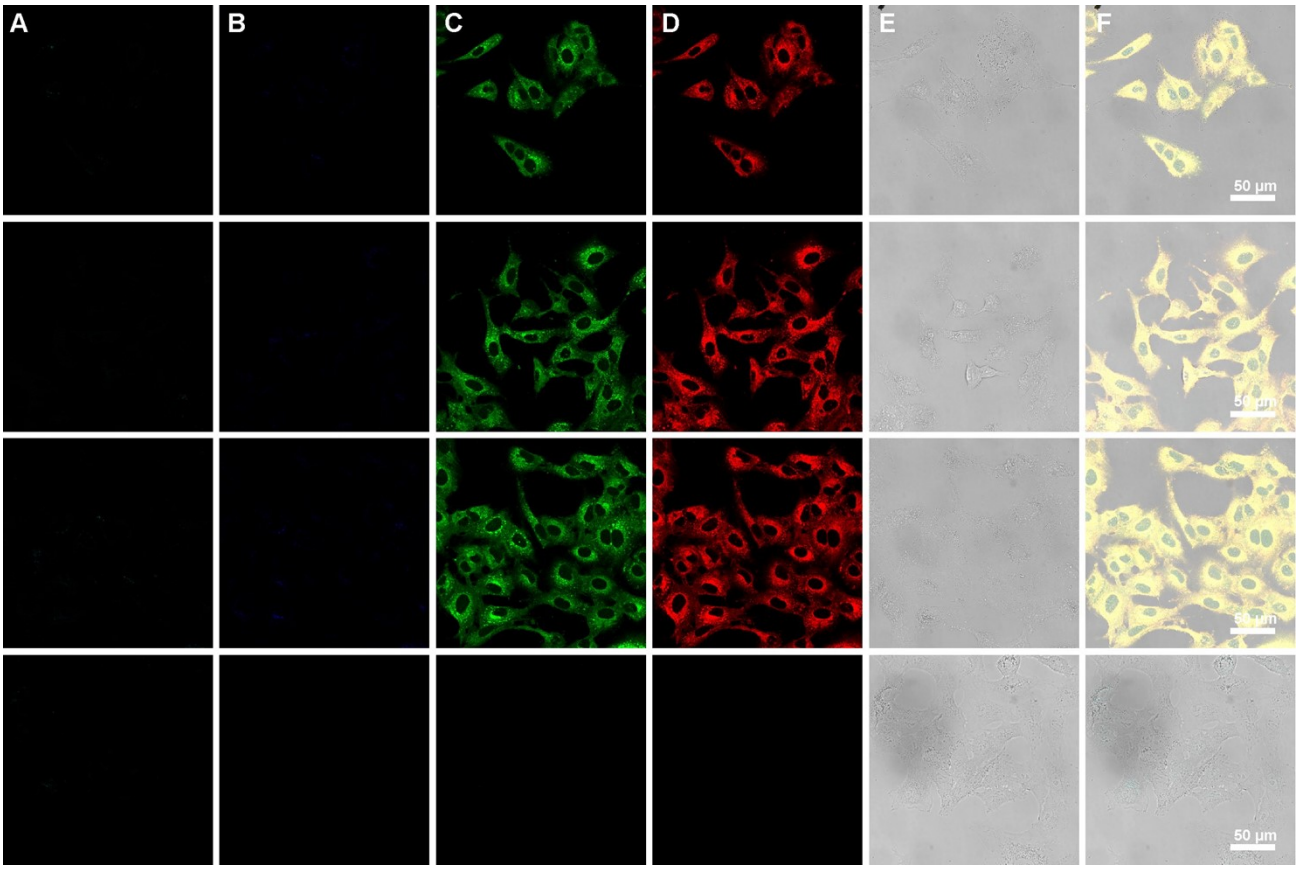

Figure S95. Live cell confocal microscopy image of A549 cells incubated for 4 hours with **5** (top three row) and without dye (bottom row, control), scale bar 50 μm (A) 405 nm, (B) 488 nm, (C) 552 nm, (D) 638 nm, (E) DIC, (F) Merged.

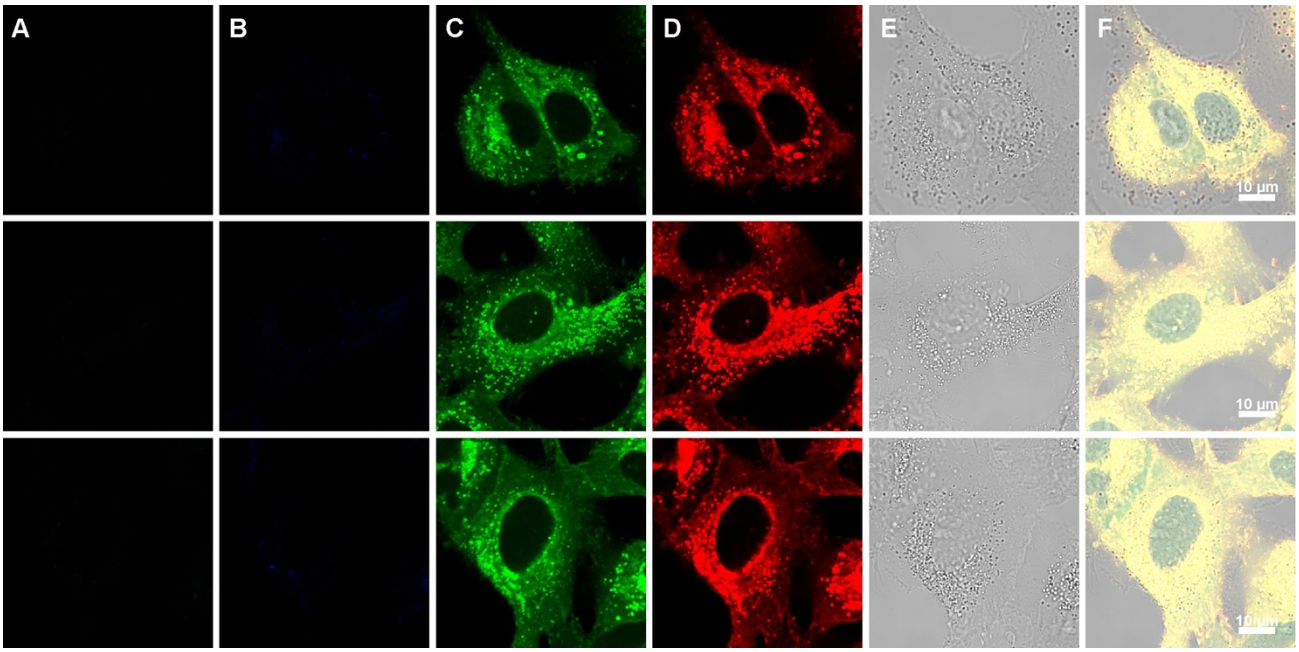

Figure S96. Live cell confocal microscopy image of A549 cells incubated for 4 hours with **5**, scale bar 10 μm (A) 405 nm, (B) 488 nm, (C) 552 nm, (D) 638 nm, (E) DIC, (F) Merged.

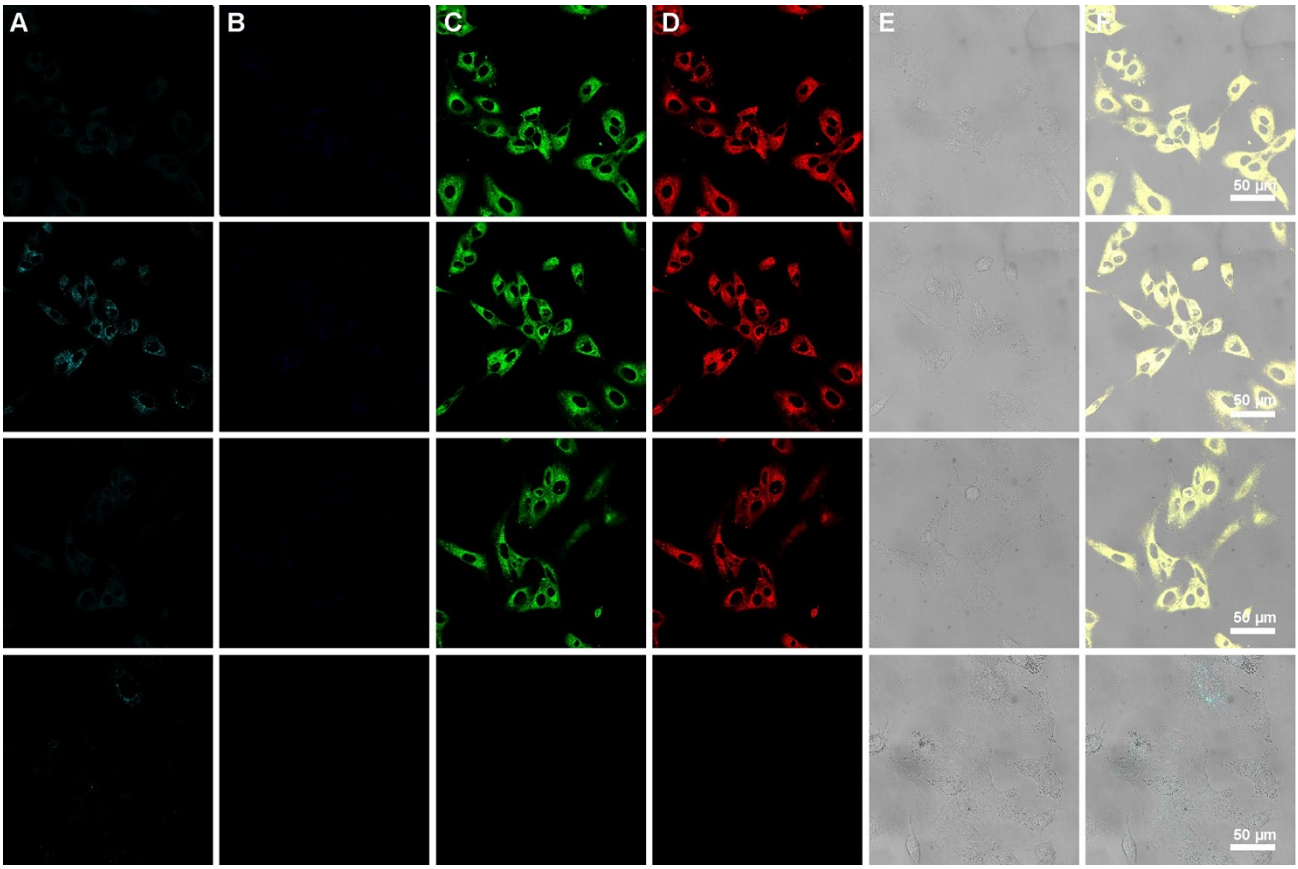

Figure S97. Live cell confocal microscopy image of A549 cells incubated for 4 hours with **7** (top three row) and without dye (bottom row, control), scale bar 50 μm (A) 405 nm, (B) 488 nm, (C) 552 nm, (D) 638 nm, (E) DIC, (F) Merged.

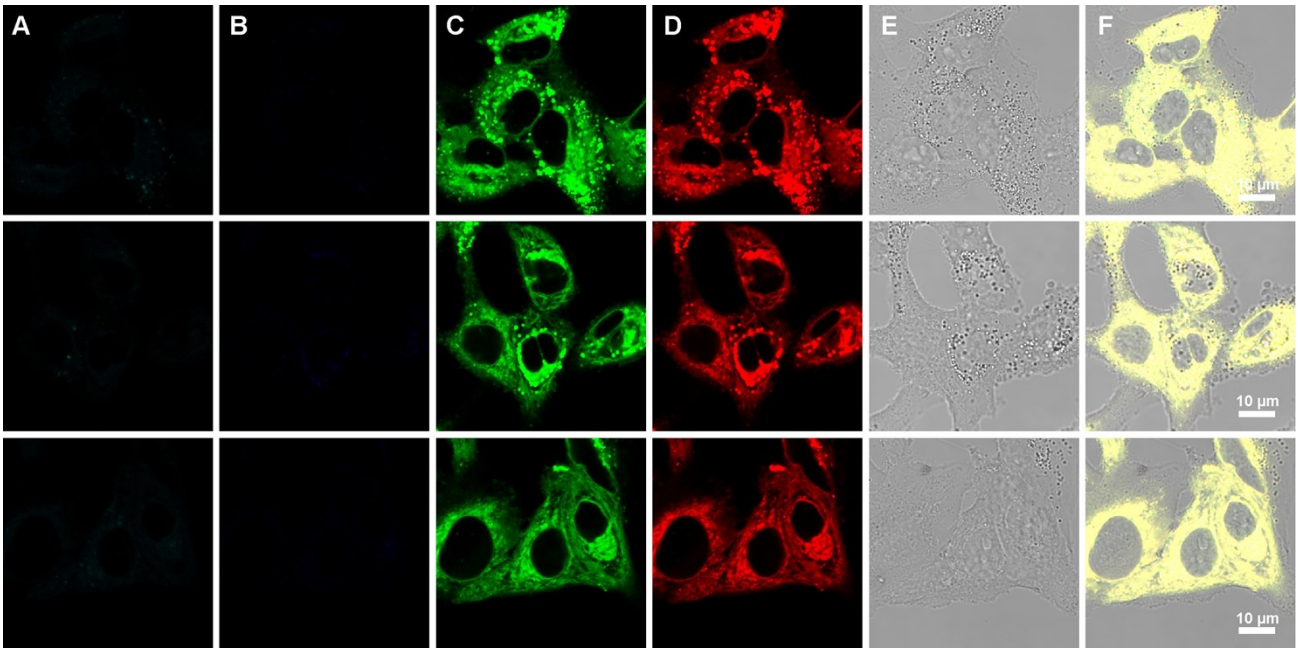

Figure S98. Live cell confocal microscopy image of A549 cells incubated for 4 hours with **7**, scale bar 10 μm (A) 405 nm, (B) 488 nm, (C) 552 nm, (D) 638 nm, (E) DIC, (F) Merged.

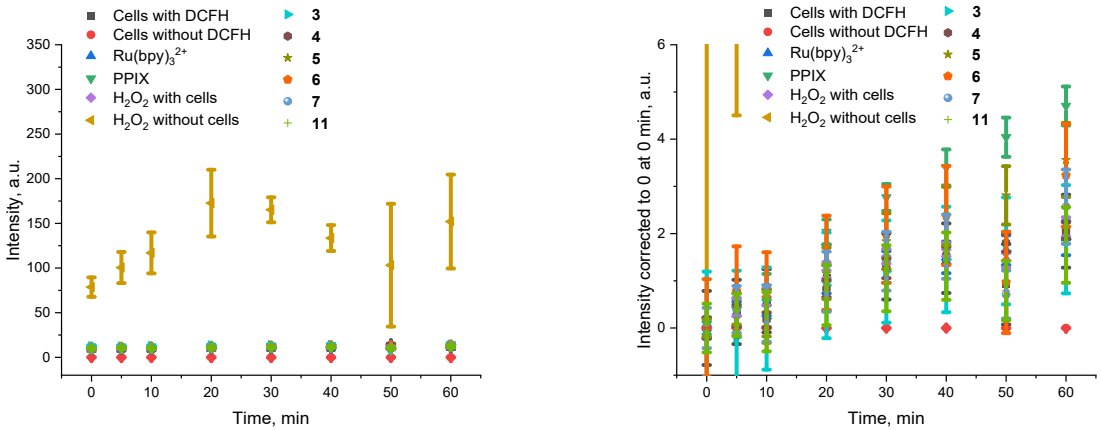

Figure S99. ROS generation study using DCFH (20 μM) as a total ROS trap *in vitro* in A549 cells (left) and normalized with intensity set to zero at the start of irradiation with 645 nm (right).

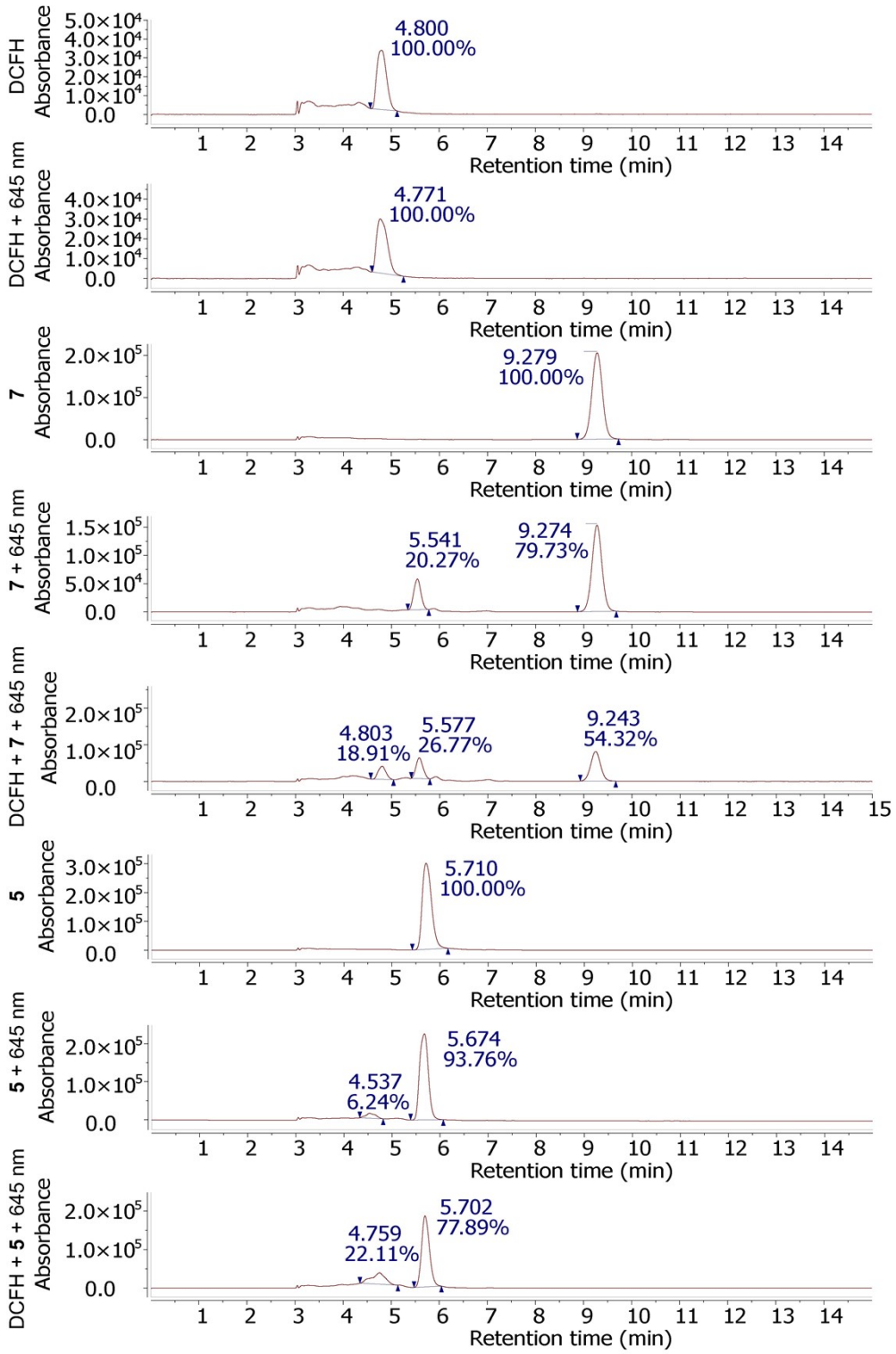

Figure S100. HPLC chromatograms before and after irradiation (30 min, 645 nm) of the ROS trap (dichlorodihydrofluorescein, DCFH) and compounds **5**, **7** and their mixtures. Isocratic 5% water in methanol.

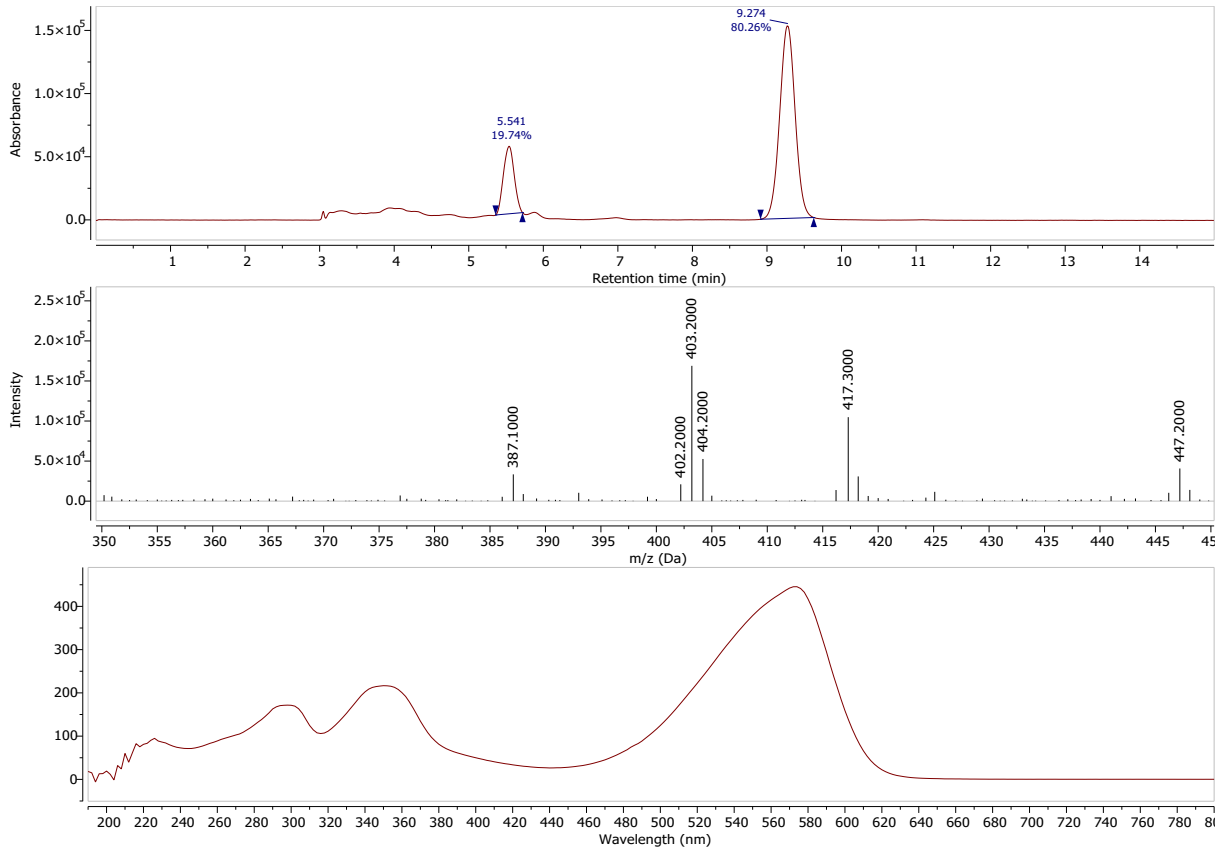

Figure S101. LC-MS of compound **7** after 30 min of 645 nm irradiation in MeOH/DMSO (v/v, 1/1) with mass and absorption spectra of the photoproduct at 5.541 min. Theoretical exact mass of the aldehyde as double bond cleavage product: $[M+H]^+$ 403.2187. Isocratic 5% water in methanol.

References

(1) Gottlieb, H. E.; Kotlyar, V.; Nudelman, A. NMR Chemical Shifts of Common Laboratory Solvents as Trace Impurities. *J. Org. Chem.* **1997**, *62* (21), 7512–7515. https://doi.org/10.1021/jo971176v.

(2) Clark, R. C.; Reid, J. S. The Analytical Calculation of Absorption in Multifaceted Crystals. *Acta Crystallogr. A Found. Crystallogr.* **1995**, *51* (6), 887–897. https://doi.org/10.1107/S0108767395007367.

(3) Dolomanov, O. V.; Bourhis, L. J.; Gildea, R. J.; Howard, J. A. K.; Puschmann, H. *OLEX2*: A Complete Structure Solution, Refinement and Analysis Program. *J. Appl. Crystallogr.* **2009**, *42* (2), 339–341. https://doi.org/10.1107/S0021889808042726.

(4) Sheldrick, G. M. Crystal Structure Refinement with *SHELXL*. *Acta Crystallogr. C Struct. Chem.* **2015**, *71* (1), 3–8. https://doi.org/10.1107/S2053229614024218.

(5) Spek, A. L. Structure Validation in Chemical Crystallography. *Acta Crystallogr. D Biol. Crystallogr.* **2009**, *65* (2), 148–155. https://doi.org/10.1107/S090744490804362X.

(6) Williams, A. T. R.; Winfield, S. A.; Miller, J. N. Relative Fluorescence Quantum Yields Using a Computer-Controlled Luminescence Spectrometer. *Analyst* **1983**, *108* (1290), 1067. https://doi.org/10.1039/an9830801067.

(7) Brouwer, A. M. Standards for Photoluminescence Quantum Yield Measurements in Solution (IUPAC Technical Report). *Pure Appl. Chem.* **2011**, *83* (12), 2213–2228. https://doi.org/10.1351/PAC-REP-10-09-31.

(8) Suzuki, K.; Kobayashi, A.; Kaneko, S.; Takehira, K.; Yoshihara, T.; Ishida, H.; Shiina, Y.; Oishi, S.; Tobita, S. Reevaluation of Absolute Luminescence Quantum Yields of Standard Solutions Using a Spectrometer with an Integrating Sphere and a Back-Thinned CCD Detector. *Phys. Chem. Chem. Phys.* **2009**, *11* (42), 9850. https://doi.org/10.1039/b912178a.

(9) Wu, J.; Mou, H.; Xue, C.; Leung, A. W.; Xu, C.; Tang, Q.-J. Photodynamic Effect of Curcumin on Vibrio Parahaemolyticus. *Photodiagnosis Photodyn.* **2016**, *15*, 34–39. https://doi.org/10.1016/j.pdpdt.2016.05.004.

(10) Sitkowska, K.; Hoes, M. F.; Lerch, M. M.; Lameijer, L. N.; Van Der Meer, P.; Szymański, W.; Feringa, B. L. Red-Light-Sensitive BODIPY Photoprotecting Groups for Amines and Their Biological Application in Controlling Heart Rhythm. *Chem. Commun.* **2020**, *56* (41), 5480–5483. https://doi.org/10.1039/D0CC02178D.

(11) Slanina, T.; Shrestha, P.; Palao, E.; Kand, D.; Peterson, J. A.; Dutton, A. S.; Rubinstein, N.; Weinstain, R.; Winter, A. H.; Klán, P. In Search of the Perfect Photocage: Structure–Reactivity Relationships in *Meso* -Methyl BODIPY Photoremovable Protecting Groups. *J. Am. Chem. Soc.* **2017**, *139* (42), 15168–15175. https://doi.org/10.1021/jacs.7b08532.